Eldholm, O., Thiede, J., Taylor, E., et al., 1989
Proceedings of the Ocean Drilling Program, Scientific Results, Vol. 104

30. CENOZOIC SILICOFLAGELLATES, EBRIDIANS, AND ACTINISCIDIANS FROM THE VØRING PLATEAU (ODP LEG 104)[1]

Sigurd Locker[2,3] and Erlend Martini[2]

ABSTRACT

The lower Miocene to Pleistocene at Sites 642 and 644 is subdivided into eight silicoflagellate zones and nine ebridian-actiniscidian zones. Due to the bioevents selected, the silicoflagellate zonation may be recognized in high northern and southern latitudes. A sequence of 24 diagnostic silicoflagellate, ebridian and actiniscidian events tied to absolute ages is established, and both the biozonations and the event sequence are correlated with standard nannoplankton zones and paleomagnetic anomalies.

Based on fluctuations of cool and warm water-preferring silicoflagellate taxa, more than ten cooling phases of sea-surface waters are recognized for the early Miocene to late Pliocene at Site 642. A relative paleotemperature curve derived from same data indicates that sea-surface temperatures were relatively high from 21.7 to nearly 13.4 Ma. Temperatures decreased progressively during the late Miocene until a distinct warm peak around 5.45 Ma. During the Pliocene sea-surface temperatures were generally low and dropped drastically at about 3.2 Ma, just before the final disappearance of silicoflagellates at Site 642 around 3.1 Ma, probably corresponding to a brief glacial phase. At Site 644, silicoflagellates, ebridians, and actiniscidians persisted from 2.8 until 2.57 Ma, when abundances suddenly decreased with the onset of a substantial Northern Hemisphere glaciation. After an interval of disappearance from about 2.5 to 2.1 Ma, siliceous flagellates reappeared at Site 644 during several phases of warm-temperate water incursions from the North Atlantic. At about 1.9 Ma ebridians disappeared at Site 644, and at 0.74 Ma silicoflagellates and actiniscidians also disappeared. Abundance drops and disappearances of silicoflagellate and ebridian species from the early Miocene to late Pliocene proceeded during cooling phases. The most prominent events were the abundance drops in *Corbisema* and *Foliactiniscus* species and the disappearance of all *Naviculopsis* species in the early Miocene, and the successive disappearances of many silicoflagellate and ebridian species during the late Miocene and Pliocene.

Seven new silicoflagellate taxa (*Cannopilus hemisphaericus* f. *heptagonus, Dictyocha fibula* subsp. *tenuis, Distephanus paraspeculum* f. *paraspeculum* and f. *hexagonalis, D. quinarius, D. speculum* subsp. *constrictus, D. sulcatus* f. *maximus*), six new ebridian species (*Falsebria arborea, Haplohermesinum hovassei, Hermesinella primitiva, Pseudammodochium fenestratum, Spongebria curta, S. miocenica*), and two new actiniscidian species (*Actiniscus planatus, Foliactiniscus pulvinus*) are described from Sites 642 and 644.

INTRODUCTION

During Leg 104 of the Ocean Drilling Program, eight holes were drilled at three sites on the Vøring Plateau, a prominent marginal high of the Norwegian–Greenland Sea (Fig. 1). The sites were arranged in a NW–SE transect to investigate structural and paleoenvironmental features of the plateau. Of special interest was the Neogene and Quaternary evolution of the Norwegian Current, which overflowed this area in the past. To provide data for the history of the Vøring Plateau and the Norwegian Current, three holes (642C, 642D, 644A) with a nearly complete Miocene to Quaternary sequence were selected for studies of siliceous plankton organisms.

In the present paper silicoflagellates, ebridians, and actiniscidians, i.e., three groups of siliceous flagellates, are treated. First the time ranges of species found in Miocene to Pleistocene strata at Sites 642 and 644 are discussed. The results are summarized in range charts of species recorded (Tables 1 to 3), range charts of stratigraphically important taxa (Figs. 3 and 4), and a list of diagnostic bioevents (Table 4). From these stratigraphic data a silicoflagellate and an ebridian-actiniscidian zonation are established (Fig. 2). After the time scale is fixed and calibrated to absolute ages, changes in the silicoflagellate and ebridian-actiniscidian assemblages are investigated to describe paleobiocoenotical and paleoenvironmental developments during the Neogene and Quaternary. The results are displayed in variation diagrams (Figs. 5, 7, and 8) and a paleotemperature curve (Fig. 6).

METHODS

The investigations are based on smear and strewn slides. Smear slides were made to estimate the general content of siliceous microfossils in all samples and to determine numerical relations between the different groups of siliceous microplankton. In total, 342 samples covering the Neogene to Quaternary core-sections of Holes 642C/D and 644A were investigated.

Resulting from smear slide investigations, 99 samples (49 belonging to Holes 642C and 642D, and 50 to Hole 644A) were selected for strewn-slide investigations on silicoflagellates, ebridians, and actiniscidians. To get higher concentrations of siliceous skeletons, the samples were processed with hydrogen peroxide, hydrochloric acid and sodium pyrophosphate. The unsieved particles were embedded in Canada-balsam (Hole 644A) and Hyrax, respectively (Holes 642C/D). The strewn slides were used to determine the frequencies of silicoflagellate, ebridian, and actiniscidian species, and to choose biostratigraphic time markers.

Concerning counting procedures, it should be noted that smear-slide data refer to microscopical view fields. They are given in classes that indicate percentage coverage by specimens: t = traces $<1\%$, not found in every field of view; R = rare $<5\%$, present in every field of view; C = common $<25\%$; A = abundant $<50\%$; D = dominant $>50\%$. Strewn-slide data are related to counting traverses across slides; they are usually cited as percentages of totally counted specimens. Only in the case of low specimen density, i.e., less than 50 specimens, are absolute numbers listed. Generally, 8 to 9 rows per slide (22 × 22 mm in size) were counted with a bright-field ocular (magnifications of 390× and 625×) to obtain 300 specimens of silicoflagellates and 300 specimens of

[1] Eldholm, O., Thiede, J., Taylor, E., et al., 1989. *Proc. ODP, Sci. Results*, 104: College Station, TX (Ocean Drilling Program).

[2] Geologisch-Paläontologisches Institut der Universität, Senckenberg-Anlage 32-34, D-6000 Frankfurt am Main, Federal Republic of Germany.

[3] Present address: Geologisch-Paläontologisches Institut der Universität, Olshausenstr. 40, D-2300 Kiel, Federal Republic of Germany.

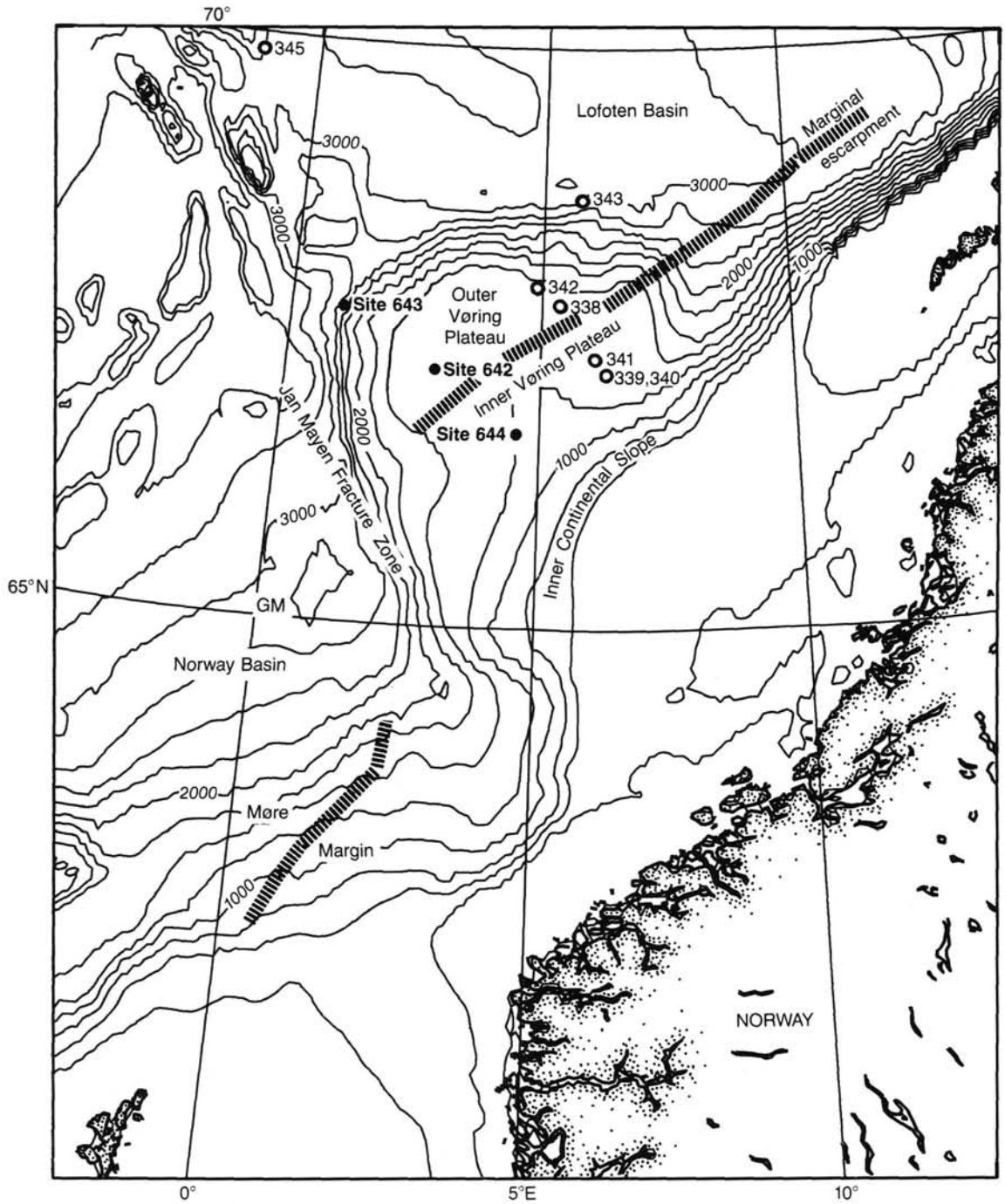

Figure 1. Location of ODP Leg 104 sites (solid circles) and DSDP Leg 38 sites (open circles) drilled on the Vøring Plateau. Contour intervals are 250 m.

ebridians and actiniscidians. Values below 300 therefore, indicate that the final number could not be reached within these rows.

Regarding taxonomy, some general units are introduced to record skeletons of uncertain taxonomic position or single specimens of known affinity. In silicoflagellates, the terms species diversae and formae diversae are used to register different taxa within a certain genus or a species and subspecies, respectively. In ebridians, the group ammodochioid skeletons describes uncertain skeletons of *Ammodochium*, *Ditripodium*, *Parathranium*, and *Thranium*, the group ebriopsoid skeletons comprises skeletons of *Ebriopsis* and *Haplohermesinum*, and the group hermesinoid skeletons contains skeletons of *Hermesinella* and *Hermesinum*. *Falsebrioid skeletons* refers to undifferentiated larger triaenes. The formula species diversae lists single specimens of different taxa within a genus. In actiniscidians, juvenile, poorly silicified, corroded or hypersilicified skeletons are summarized under *Actiniscus* sp. Due to their uncertain taxonomic affinities, skeletons of *Calicipedinium* and *Carduifolia* are excluded from the countings.

Based on primary strewn-slide data, assemblage abundances, species diversities and species abundances are calculated for paleoenvironmental interpretations. As used here, species diversities and abundances may be regarded as appropriate biocoenotic parameters, as they are applied to relations between the members of assemblages. Assemblage abundances, however, may be influenced by preservational conditions and represent, thus, sometimes merely a taphocoenotic parameter, which

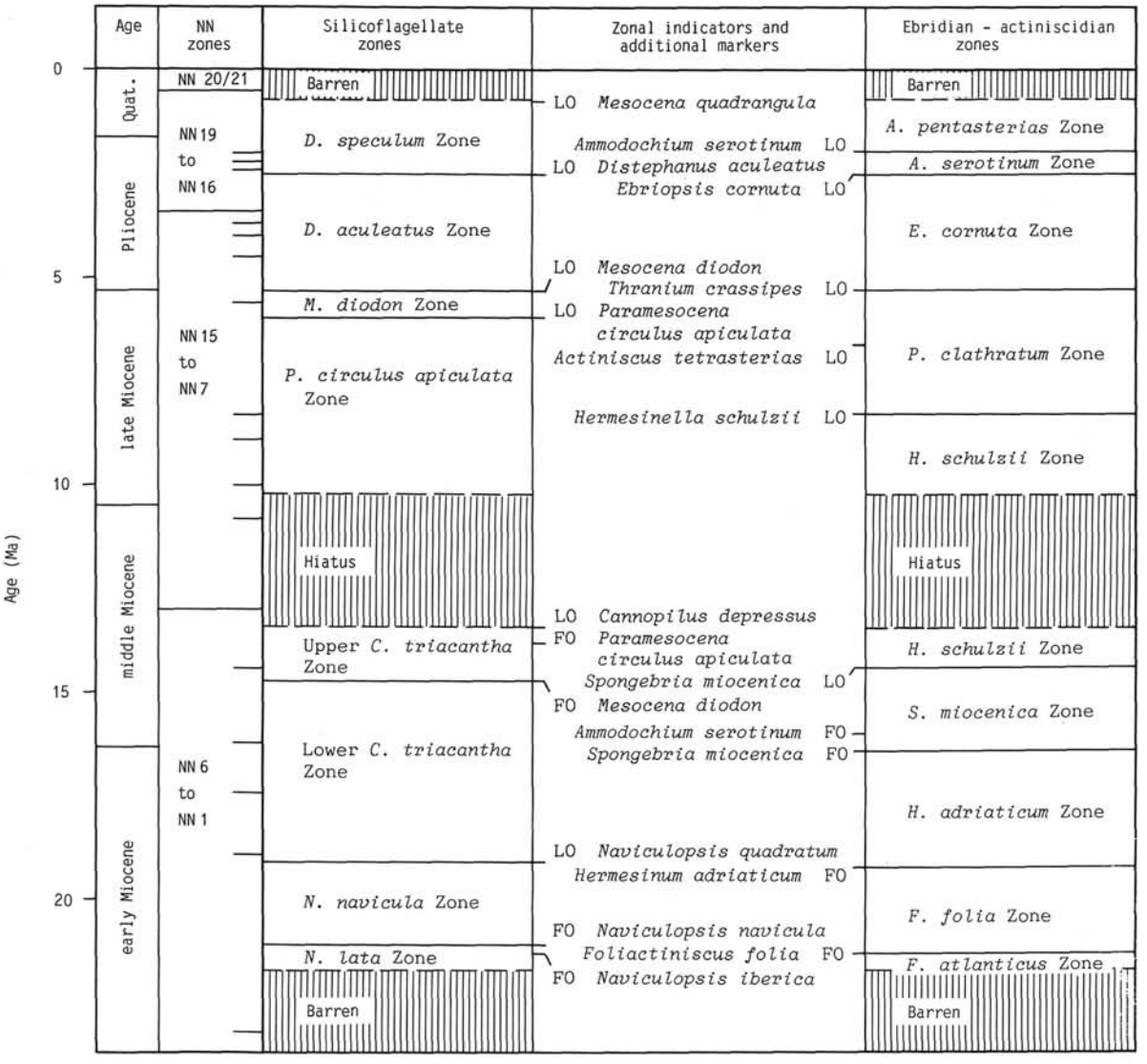

Figure 2. Silicoflagellate and ebridian-actiniscidian zones used for Sites 642 and 644, first and last occurrences (FO, LO) of diagnostic species, and correlation to standard nannoplankton zones (based on paleomagnetic data of Bleil, this volume). Because only sets of nannoplankton zones could be proved (Donnally, this volume), positions of particular zones are calculated and indicated by bars.

nevertheless provides important paleoenvironmental information. Abundances of silicoflagellate and ebridian-actiniscidian assemblages are generally referred to an area of 80 mm^2 on a slide, which corresponds to the eight traverses regularly counted. Simple species diversities are enumerated only for autochthonous taxa of specific or subspecific rank, thus including infraspecific taxa of lower rank. Species abundances are summarized for certain genera and genus groups, according to the phylogenetic concepts explained below.

Age determinations are related to the paleomagnetic time scale of Bleil (this volume) in which the ages of Berggren et al. (1985) are used. From the paleomagnetic interpretations given in Bleil, only the lowermost part of Hole 642C is excluded, because from 183.11 to 196.58 mbsf we assume a correspondence to Chron C5B just below Subchrons C5A-N8 and C5A-R8 from ca. 175.00 to 182.41 mbsf. This interpretation seems to be more in accordance to calcareous nannoplankton and silicoflagellate stratigraphies at Site 642 and correlations to other regions. Concerning age assignments, calculations are made for single samples which are related to the nearest reversal. As samples from all core sections were used, the possible error of Miocene to early Pliocene paleobiological and paleoenvironmental events amounts to between 120 and 400 k.y. and of late Pliocene to Pleistocene events to between 13 and 40 k.y.

According to the *Instructions for Contributors to the Proceedings of the Ocean Drilling Program* (ODP, November 1985), strong distinction is made between chronostratigraphic and chronological indications. The terminus first/last occurrence (FO, LO) and first/last occurrence level (FOL, LOL) are related to the time-space scale, and the terminus first/last appearance (FA, LA) and first/last appearance datum (FAD, LAD) to the time scale. Bioevents are treated as features that happened in time.

PLANKTON STRATIGRAPHY

Silicoflagellate Zonation

Beginning with the Miocene a pronounced differentiation can be observed between the silicoflagellate assemblages of low- to mid- and higher latitudes (Bukry, 1975a; Ciesielski, 1975; Busen and Wise, 1977; Bukry, 1981a; Perch-Nielsen, 1985), which requires different biozonations for tropical to temperate and subpolar regions. The present investigations show, however, that similar successions of bioevents may be selected to subdivide subpolar sediments of both hemispheres.

In general, the silicoflagellate zonation used for Leg 104 (Fig. 2) resembles the subdivision applied during Leg 38 (Martini and Müller, 1976). But with the addition of the *Mesocena diodon* Zone, the *Distephanus stauracanthus* and *Mesocena quadrangula* Subzones, and the distinction of a Lower and Upper *Corbisema triacantha* Zone this zonation is extended and more specified. By restricting the taxon *Mesocena circulus* s.l. to its ancestral part *Mesocena/Paramesocena circulus apiculata*, the zonation used in this paper definitely approximates that one employed at Site 594 in the subpolar southwestern Pacific (Locker and Martini, 1986a). Comparable correspondences are indicated to sites in the Southern Ocean and in the southern Atlantic (Ciesielski, 1975; Shaw and Ciesielski, 1983). The remarkable and relatively strong parallelism seen in some late Miocene to Quaternary subdivisions obviously reflects concurrent developments in high northern and southern silicoflagellate assemblages during Neogene time.

The silicoflagellate zones used are described and occurrences in the studied holes are indicated. Remarks on Holes 338 and 348, which are well documented for Leg 38 (Martini and Müller, 1976), are included. References to some representative holes that contain these zones outside the investigation area are added. However, the silicoflagellate zonation of Leg 104 sites presented by Ciesielski (in Eldholm, Thiede, Taylor, et al., 1987) is not dealt with, as results were preliminary. Correlations with nannoplankton zones and paleomagnetic anomalies are also discussed.

Naviculopsis lata Zone

Definition: Interval from the first occurrence of *Naviculopsis lata* to the first occurrence of *Naviculopsis navicula*. Upper Oligocene (?) to lower Miocene.

Reference: Martini (1972).

Occurrence: Found in Hole 642D, Samples 104-642D-9X-5, 70–71 cm to 104-642D-11X-1, 55–56 cm (264.20–277.35 mbsf). From Core 104-642D-12X to 104-642D-14X only three out of 13 samples yielded a few silicoflagellates and ebridians. The discovery of a *Paramesocena* skeleton in Sample 104-642D-13X-3, 48-49 cm may indicate, however, that the sedimentary sequence above the basalt represents a mixed interval. The zone is known also from Hole 338, Sections 38-338-18R-1 to 38-338-19R-2.

Content: The assemblages are characterized by *Cannopilus hemisphaericus*, *Corbisema flexuosa*, *C. triacantha*, *Distephanus crux* s.l., *D. crux darwinii*, *D. speculum haliomma*, *Naviculopsis lata*, and *Septamesocena apiculata*. *Naviculopsis lacrima* may also have stratigraphical value. The zone contains the FOL of *N. iberica*.

Naviculopsis navicula Zone

Definition: Interval from the first occurrence of *Naviculopsis navicula* to the last occurrence of *Naviculopsis quadratum* (synonym *N. rectangularis*). Lower Miocene.

Reference: Martini (1972).

Occurrence: Found in Hole 642D, Samples 104-642D-6X-3, 66–67 cm to 104-642D-9X-4, 70–71 cm (232.16-262.70 mbsf). Present also in Hole 338, Sections 38-338-12R-2 to 38-338-17R-4.

Content: The assemblages are determined by *Cannopilus hemisphaericus*, *Distephanus crux* s.l., *D. crux parvus*, *D. speculum haliomma*, *Naviculopsis iberica*, *N. navicula*, *N. quadratum* and *Septamesocena apiculata*. *Corbisema triacantha* distinctly diminishes towards the top of the zone.

Remarks: The upper boundary of the *Naviculopsis navicula* Zone is placed at the LO of *N. quadratum*, which corresponds to the last occurrences of *N. iberica* and *N. navicula navicula* in Hole 642D. The synchronous disappearance of all *Naviculopsis* species may indicate a sudden change of paleoenvironmental conditions or a small hiatus, as these species disappear in other areas at different time levels.

Lower Corbisema triacantha Zone

Definition: Interval from the last occurrence of *Naviculopsis quadratum* to the first occurrence of *Mesocena diodon*. Lower to middle Miocene.

Reference: Martini (1971, 1972) defined the *Corbisema triacantha* Zone as an interval that ranges from the LO of *N. quadratum* to the LO of *C. triacantha*. But because the FAD of *M. diodon* represents an event within this zone that may be recognized in low and high latitudes, it is used here to subdivide the interval into a lower and an upper part.

Occurrence: Found in Holes 642C and 642D, Samples 104-642C-22H-3, 66–67 cm to 104-642C-24H-5, 70–71 cm and 104-642D-3X-1, 60–61 cm to 104-642D-6X-2, 66–67 cm (181.16–230.66 mbsf). Present also in Hole 338, Sections 38-338-10R-2 to 38-338-11R-4.

Content: The assemblages are characterized by *Cannopilus hemisphaericus*, *Distephanus crux* s.l., *D. crux parvus*, *D. crux stradneri*, *D. speculum haliomma*, and *Septamesocena apiculata*. *Cannopilus schulzii*, is of special interest because its main distribution is in this zone. *Corbisema triacantha* generally remains rare throughout the interval. The zone includes the FO levels of *Cannopilus depressus* and *C. ernestinae*. *Distephanus speculum haliomma* suddenly disappears at or just above the upper boundary.

Upper Corbisema triacantha Zone

Definition: Interval from the first occurrence of *Mesocena diodon* to the last occurrence of *Corbisema triacantha*. Middle Miocene.

Reference: See discussion under Lower *Corbisema triacantha* Zone.

Occurrence: Found in Hole 642C, Samples 104-642C-19H-5, 50–51 cm to 104-642C-22H-2, 66–67 cm (155.50–179.66 mbsf). Present in Hole 338, Sections 38-338-8R-3 to 38-338-10R-1, but, possibly, also in Hole 348, Sections 38-348-14R-1 to 38-348-17R, CC (included in the *Mesocena circulus* Zone).

In Hole 338 (Martini and Müller, 1976) the onset of *Mesocena/Paramesocena circulus apiculata* and the persistence of *Mesocena/Septamesocena apiculata* above Sample 38-338-8R-3, 2–3 cm may indicate that the Upper *Corbisema triacantha* Zone still continues to the top of the section in the figure. In Hole 348 (Martini and Müller, 1976) the zone may be expressed by the co-occurrence of *Cannopilus depressus*, *C. ernestinae*, *Mesocena diodon*, and *Septamesocena apiculata*; the upper boundary could be drawn above Sample 38-348-14R-1, 90–91 cm, i.e., just above the last occurrences of *S. apiculata* and *C. depressus*.

Content: The assemblages are determined by *Cannopilus depressus*, *Distephanus crux* s.l., *D. speculum* s.l., and *Mesocena diodon*. *Corbisema triacantha* occurs scattered throughout the interval, and *Distephanus stauracanthus* is restricted to a single occurrence. The zone includes the FOL of *Paramesocena circulus apiculata* and the LO levels of *Cannopilus hemisphaericus* and *Septamesocena apiculata*.

Remarks: Because *C. triacantha* occurrence is rare and scattered throughout the zone, the peak occurrence of *D. stauracanthus* in conjunction with the LO of *C. depressus* is used here to identify the upper boundary.

Distephanus stauracanthus Subzone

Definition: Interval in the Upper *Corbisema triacantha* Zone that ranges from the first to the last occurrence of *Distephanus stauracanthus* (synonym *D. crux* var. *octacanthus*). Middle Miocene.

Reference: Introduced by Martini (1971) as *Dictyocha octacantha* horizon; treated by Ling (1972) as *Dictyocha fibula* var. *octagona* assemblage; but formally defined as *Distephanus stauracanthus* Subzone with the boundaries indicated by Dumitrică

(1973c). Occurrence: Present in Hole 642C, Sample 104-642C-19H-5, 50–51 cm (155.50 mbsf). Not found in Leg 38 holes.

Remarks: This subzone is known from many regions, but in higher latitudes its recognition may be difficult due to sparce occurrences of the nominate species.

Paramesocena circulus apiculata Zone

Definition: Interval from the last occurrence of *Corbisema triacantha* to the last occurrence of *Paramesocena circulus apiculata* (synonym *Mesocena circulus* var. *apiculata*, but cited also as *M. circulus*). Middle to upper Miocene.

Reference: Introduced by Ling (1973) as *Mesocena circulus* var. *apiculata* Zone with the top as indicated above; used by Bukry (1975a) as *Mesocena circulus* Subzone of his *Distephanus speculum speculum* Zone; and cited by Martini and Müller (1976) as *Mesocena circulus* Zone with the same base as noted above. According to taxonomic decisions, the name was changed to *Paramesocena apiculata* Zone in Locker and Martini (1986a).

Occurrence: Found in Hole 642C, Samples 104-642C-15H-4, 66–67 cm to 104-642C-19H-4, 50–51 cm (116.16–154.00 mbsf). Originally indicated also from Holes 338 and 348, but present, probably, only in Hole 348, Sections 38-348-11R-1 to 38-348-13R, CC (see explanations under Upper *Corbisema triacantha* Zone).

Content: The poor asemblages are characterized by *Distephanus aculeatus*, *D. crux* s.l., *D. speculum* s.l., and *Paramesocena circulus apiculata*. Towards the end of the zone *D. crux* s.l. drastically drops in frequency, and *D. speculum* s.l. first appears with coronate members.

Remarks: The *Paramesocena circulus apiculata* Zone is based on the ancestor of *P. circulus circulus*. A reinvestigation of the *Mesocena circulus* specimens found in Hole 338 (Martini and Müller, 1976) has shown that they belong to *P. circulus apiculata*, as assumed by Locker and Martini (1986a). Thus we confirm the stratigraphic value of *P. circulus apiculata* as an indicator for the middle to late Miocene in high latitudes.

Mesocena diodon Zone

Definition: Interval from the last occurrence of *Paramesocena circulus apiculata* to the last occurrence of *Mesocena diodon*. Upper Miocene to lower Pliocene.

Reference: Introduced by Perch-Nielsen (1975a) as *Mesocena diodon* Subzone of her *Paradictyocha dumitricae* Zone with the top as noted above; treated by Ciesielski (1975) as a zone that includes the base given above; and cited by Locker and Martini (1986a) as a zone that combines the restricted base indicated by Ciesielski and the top mentioned by Perch-Nielsen.

Occurrence: Found in Hole 642C, Samples 104-642C-13H-3, 30–31 cm to 104-642C-15H-3, 66–67 cm (95.30–114.66 mbsf). Present also in Hole 348, Sections 38-348-9R-3 to 38-348-10R, CC (included in the *Distephanus boliviensis* Zone).

Content: The poor assemblages are characterized by *Distephanus aculeatus*, *Mesocena diodon*, and *Distephanus speculum* s.l., the last one showing many coronate specimens.

Remarks: According to paleomagnetic interpretations (Bleil, this volume) the *Mesocena diodon* Zone does not cross the Miocene/Pliocene boundary in Hole 642C.

Distephanus aculeatus Zone

Definition: Interval from the last occurrence of *Mesocena diodon* to the last occurrence of *Distephanus aculeatus* (synonym *D. boliviensis*). Lower to upper Pliocene.

Reference: Introduced by Bukry and Foster (1973) as *Distephanus boliviensis* Zone with the top as indicated above, but base redefined in this paper.

Occurrence: Found in Hole 642C, Samples 104-642C-9H-1, 64–65 cm to 104-642C-13H-2, 66–67 cm (61.34–94.16 mbsf), and Hole 644A, Samples 104-644A-30H-2, 56–57 cm to 104-644A-34H-5, 66–67 cm (228.16–252.66 mbsf). Present also in Hole 348, but restricted here to Sections 38-348-6R-1 to 38-348-8R-3 (see remarks under *Mesocena diodon* Zone).

Content: The impoverished assemblages are constituted of *Distephanus aculeatus* and *D. speculum* s.l., the last one including many coronate specimens. Special stratigraphic value can be assigned to *D. speculum constrictus* and *D. sulcatus* which are restricted to this zone.

Distephanus speculum Zone

Definition: Interval above the last occurrence of *Distephanus aculeatus*. Upper Pliocene to Holocene, Recent.

Reference: Introduced by Ciesielski (1975) as a zone that was subdivided by two subgroups of *D. speculum*, but treated here without splitting the taxon.

Occurrence: Found in Hole 644A, Samples 104-644A-10H-2, 74–75 cm to 104-644A-23H-2, 55–56 cm (84.94–196.15 mbsf). Present also in Hole 348, Sections 38-348-5R-5 to 38-348-5R, CC.

Content: The only consistent but rare species in the investigated area remains *D. speculum* s.l., which contains relatively high numbers of coronate specimens. The zone includes the total range of *D. speculum octonarius* and the acme interval of *Mesocena quadrangula*.

Mesocena quadrangula Subzone

Definition: Interval in the *Distephanus speculum* Zone that ranges from the base of acme to the last occurrence of *Mesocena quadrangula* (cited also as *M. elliptica*). Pleistocene.

Reference: Introduced by Martini (1971) as *Mesocena quadrangula* Zone with a different base; treated by Bukry and Foster (1973) as *Mesocena elliptica* Zone with the base indicated above; but, although not formally cited as zone, most accurately placed in the Pleistocene by Dumitrică (1973a).

Occurrence: Found in Hole 644A, Samples 104-644A-10H-3, 74–75 cm to 104-644A-12H-5, 66–67 cm (86.44–108.36 mbsf). Unknown from Leg 38 holes.

Remarks: This subzone is preferably known from low- to mid- latitude sites. Although its base has a somewhat doubtful starting point, it can be easily recognized in many sections.

Up to the middle Miocene Upper *Corbisema triacantha* Zone the zonation described may be recognized in low and high latitudes, especially with reference to the FA dates of *M. diodon* and *P. circulus apiculata*, and the LA dates of *S. apiculata* and *C. depressus*. In the eastern tropical Pacific the *Naviculopsis lata, Naviculopsis ponticulus*, and *Corbisema triacantha* Zones found at Site 575 (Bukry, 1985b) generally correspond to the zonation shown above. Although not indicated with the names used here, the full sequence is recovered also at Site 278 in the southwestern Pacific (Bukry, 1975a: *D. speculum pentagonus* + *N. quadratum* + *C. triacantha* Zones) and at Site 266 in the Southern Ocean (Ciesielski, 1975: *N. robusta/N. regularis* + *N. navicula* + *C. triacantha* Zones). From the central and northern Pacific only the *Corbisema triacantha* Zone including the *Distephanus stauracanthus* Subzone is known, at Sites 66 (Martini, 1971) and 173 (Ling, 1977), for instance. In the North Atlantic the *Naviculopsis navicula* and *Corbisema triacantha* Zones are recorded from Site 415 off northwest Africa (Bukry, 1980), but the most comprehensive data on the succession is found at Site 407 southwest of Iceland (Martini, 1979: *N. lata* + *N. navicula* + *C. triacantha* Zones).

Above the middle Miocene Upper *Corbisema triacantha* Zone the zonation used in this paper is representative only for higher latitudes. In the North Pacific the *Paramesocena circulus apiculata*, *Mesocena diodon*, *Distephanus aculeatus*, and *Distephanus speculum* Zones are present in the upper Miocene to Pleistocene sequence of Site 192 (Ling, 1973: *M. circulus* var. *apiculata* + *D. speculum* var. *pentagonus* + *C. hemisphaericus* Zones, and following units). In the southwestern Pacific Site

594 provides an appropriate sequence (Locker and Martini, 1986a: *P. apiculata* + *M. diodon* + *D. speculum* Zones), and in the Southern Ocean Site 266 (Ciesielski, 1975: *Mesocena circulus* + *Mesocena diodon* + *Dictyocha aspera* var. *pygmaea/ Dictyocha fibula* var. *pumila* + *Distephanus boliviensis* + *Distephanus speculum* Zones). For the South Atlantic Site 513 may be cited (Shaw and Ciesielski, 1983: *M. circulus/M. diodon* + *M. diodon* Zones, but above, not discriminated), and for the North Atlantic Site 407 (Martini, 1979: *M. diodon* Zone not designated + *D. boliviensis* + *D. speculum* Zones).

Regarding series and subseries boundaries in the zonation described (Fig. 2), it must be taken into account that silicoflagellates enable only approximate determinations. As no microfossil group used for Leg 104 investigations yielded time markers for all boundaries, indicators have been taken from different plankton groups (Eldholm, Thiede, Taylor, et al., 1987). In general, the boundaries designated by this means are adopted here, but due to our plankton investigations and paleomagnetic interpretations (Bleil, this volume) some minor changes are introduced. Thus the lower/middle Miocene boundary is placed at the top of Subchron C5C-N1 in the Lower *Corbisema triacantha* Zone, which lies below the FO of *Denticulopsis lauta* in Core 104-642C-23H (Ciesielski, unpublished data). The middle/upper Miocene boundary is drawn at the LO of *Cannopilus depressus* and *Distephanus stauracanthus* (Locker and Martini, this paper), which meets the upper boundary of the Upper *Corbisema triacantha* Zone and approximates the top of nannoplankton Zone NN6. Above, a hiatus may be present because the horizon with *C. depressus* and *D. stauracanthus* (NN6) is directly overlain by strata with *Globorotalia mayeri* and *Neogloboquadrina acostaensis* (N14/16 = NN 8/9) (Spiegler and Jansen, this volume; compare also Goll, this volume). The Miocene/ Pliocene boundary is placed at the top of Subchron C3A-N1, which coincides with the top of the *Mesocena diodon* Zone. According to paleomagnetic interpretations, the lower/upper Pliocene boundary occurs in the *Distephanus aculeatus* Zone. The Pliocene/Pleistocene boundary tied with the top of the Olduvai Event is in the *Distephanus speculum* Zone.

Ebridian-Actiniscidian Zonation

Comparisons between the Norwegian-Greenland Sea and the southwestern Pacific (Locker and Martini, 1986b) indicate that also the assemblages of Neogene ebridians and actiniscidians are differentiated from low to high latitudes. Because the Norwegian Sea assemblages are very diversified, an independent zonation is established for the Miocene of these high northern latitudes. Only the uppermost part of the subdivision covering the Pliocene to Pleistocene interval exhibits similarities to other regions, thus enabling some correlations.

Foliactiniscus atlanticus Zone

Definition: Interval from the first occurrence of *Foliactiniscus atlanticus* to the first occurrence of *Foliactiniscus folia*. Oligocene (?) to lower Miocene.

Reference: New zone.

Occurrence: Found in Hole 642D, Samples 104-642D-10X-3, 70–71 cm to 104-642D-11X-1, 55–56 cm (270.80–277.35 mbsf).

Content: The assemblages are characterized by *Ammodochium pyramidale*, *Haplohermesinum hovassei*, *Hermesinella conata*, *H. schulzii*, *Parathranium bispinum*, *Actiniscus flosculus* and *Foliactiniscus atlanticus*. Higher frequencies are provided only by *F. atlanticus*. Comparable to younger zones, numerous skeletons of *Falsebria* and *Actiniscus* occur which are difficult to determine on the species level.

Remarks: The FAD of *F. atlanticus* is unknown at present, but may be expected in the Oligocene.

Foliactiniscus folia Zone

Definition: Interval from the first occurrence of *Foliactiniscus folia* to the first occurrence of *Hermesinum adriaticum*. Lower Miocene.

Reference: New zone.

Occurrence: Found in Hole 642D, Samples 104-642D-6X-5, 66–67 cm to 104-642D-10X-2, 70–71 cm (235.16–269.30 mbsf).

Content: The assemblages are constituted of *Ammodochium pyramidale*, *Haplohermesinum hovassei*, *Hermesinella conata*, and other *Hermesinella* species, *Parathranium bispinum*, *P.* cf. *clathratum*, *Actiniscus flosculus*, *Foliactiniscus atlanticus*, and *F. folia*. Frequency relations are comparable to those of the underlying zone.

Hermesinum adriaticum Zone

Definition: Interval from the first occurrence of *Hermesinum adriaticum* to the first occurrence of *Spongebria miocenica*. Lower Miocene.

Reference: New zone.

Occurrence: Found in Hole 642D, Samples 104-642D 3X-1, 60–61 cm to 104-642D-6X-4, 66–67 cm (200.20–233.66 mbsf).

Content: The rich assemblages are characterized by *Ammodochium pyramidale*, *Ditripodium amphora* and *D.* cf. *amphora*, *Falsebria* cf. *arborea*, *Haplohermesinum hovassei*, *Hermesinum adriaticum*, *H. obliquum*, *Actiniscus flosculus*, *Foliactiniscus folia*, and some *Hermesinella* and *Parathranium* species. *Parathranium curvipes* may also have stratigraphic value, although it occurs rarely. Within this zone *Hermesinella primitiva*, the simplest Neogene member of the genus, disappears.

Spongebria miocenica Zone

Definition: Interval from the first to the last occurrence of *Spongebria miocenica*. Lower to middle Miocene.

Reference: New zone.

Occurrence: Found in Hole 642C, Samples 104-642C-21H-6, 60–61 cm to 104-642C-24H-5, 70–71 cm (176.10–199.10 mbsf).

Content: This zone shows a drastic change in the composition of assemblages. *Spongebria curta*, *S. miocenica*, *Parathranium clathratum*, and *Thranium crassipes* appear, and *Ammodochium serotinum* replaces *A. pyramidale*. Other taxa continously present are *Ditripodium latum*, *Falsebria* aff. *arborea*, *Haplohermesinum hovassei*, *Hermesinella conata*, *Hermesinum obliquum*, *Parathranium* cf. *clathratum*, *Actiniscus flosculus*, and *A. pentasterias*. Toward the top of the zone *Foliactiniscus atlanticus* and *F. folia* disappear.

Hermesinella schulzii Zone

Definition: Interval from the last occurrence of *Spongebria miocenica* to the last occurrence of *Hermesinella schulzii*. Middle to upper Miocene.

Reference: New zone.

Occurrence: Found in Hole 642C, Samples 104-642C-17H-5, 50–51 cm to 104-642C-21H-5, 60–61 cm (136.50–174.60 mbsf).

Content: The assemblages are characterized by *Ammodochium iserotinum*, *Ditripodium elephantinum* and *D.* cf. *elephantinum*, *Falsebria* cf. *arborea*, *Hermesinella conata*, *H. schulzii*, *Thranium crassipes*, and some *Parathranium* and *Actiniscus* species. Of special interest are the occurrences of *Podamphora elgeri* and *Actiniscus tetrasterias*.

The zone includes the LO levels of *Hermesinella conata* and *H. schulzii* which are probably close to their phylogenetic LA dates. In contrast, the last occurrences of *Hermesinum adriaticum* and *H.* obliquum obviously reflect only biogeographic changes or restrictions, because these species are known from low- to mid- latitude Pliocene strata (Locker and Martini, 1986b),

from Pleistocene sediments (Dumitrică, 1973b), and from Holocene tropical to temperate oceans (Tappan, 1980).

Parathranium clathratum Zone

Definition: Interval from the last occurence of *Hermesinella schulzii* to the last occurrence of *Thranium crassipes*. Upper Miocene to lowermost Pliocene.

Reference: New zone.

Occurence: Found in Hole 642C, Samples 104-642C-13H-1, 66–67 cm to 104-642C-17H-4, 15–16 cm (92.66–134.65 mbsf).

Content: The assemblages are characterized by *Ammodochium serotinum*, *Falsebria* cf. *arborea*, *Parathranium bispinum*, *P. clathratum* and *P.* cf. *clathratum*, *Thranium crassipes* and *T.* cf. *crassipes*, *Actiniscus flosculus* and *A. pentasterias*. Ebridian frequencies are usually on the level of older zones, and only *A. serotinum* may attain higher numbers. Within the zone *Ebriopsis cornuta* seems to have its first occurrence, whereas the range of *Actiniscus tetrasterias* ends just above the base.

Remarks: At Site 642 the LO of *Thranium crassipes* lies above that one recognized in the southwestern Pacific (Locker and Martini, 1986b). Therefore, the *Thranium crassipes* Zone in the southwestern Pacific represents only a local range zone. Since *T. crassipes* was used already as zonal indicator, *Parathranium clathratum* was selected as substitute nominator for the interval defined above. The LO of true *P. clathratum* specimens possessing long opisthoclades seems roughly to coincide with the LO of *T. crassipes* at Site 642.

Ebriopsis cornuta Zone

Definition: Interval from the last occurrence of *Parathranium clathratum* to the last occurrence of *Ebriopsis cornuta* (cited also as *E. antiqua*). Lower to upper Pliocene.

Reference: Introduced by Ling (1973) as *Ebriopsis antiqua* Zone; cited by Locker and Martini (1986b) as *Ebriopsis cornuta* Zone; but base modified in this paper.

Occurrence: Found in Hole 642C, Samples 104-642C-9H-1, 64–65 cm, to 104-642C-12H-6, 65–66 cm (61.34–90.65 mbsf), and in Hole 644A, Samples 104-644A-30H-2, 56–57 cm to 104-644A-34H-5, 66–67 cm (228.16–252.66 mbsf).

Content: The impoverished assemblages include *Ammodochium serotinum*, *Ebriopsis cornuta*, *Falsebria arborea* and *F.* cf. *arborea*, *Actiniscus flosculus* and *A. pentasterias*. High frequencies are provided only by *Falsebria* cf. *arborea* and *Actiniscus* sp. A most important event represents the sudden appearance of *Pseudammodochium robustum* just above the base of the zone.

Ammodochium serotinum Zone

Definition: Interval from the last occurrence of *Ebriopsis cornuta* to the last occurrence of *Ammodochium serotinum* (cited also as *A. rectangulare*). Upper Pliocene.

Reference: Introduced by Ling (1973) as *Ammodochium rectangulare* Zone; and used by Locker and Martini (1986b) as *Ammodochium serotinum* Zone with the boundaries given originally.

Occurrence: Found in Hole 644A, Samples 104-644A-21H-1, 66–67 cm to 104-644A-23H-2, 55–56 cm (185.46–196.15 mbsf).

Content: The very poor assemblages contain only a few specimens of *Ammodochium serotinum* and *Actiniscus* sp., indicating that a level above the *Ebriopsis cornuta* Zone is reached.

Actiniscus pentasterias Zone

Definition: Interval above the last occurrence of *Ammodochium serotinum*. Upper Pliocene to Holocene.

Reference: New zone.

Occurrence: Found in Hole 644A, Samples 104-644A-10H-2, 74–75 cm to 104-644A-17H-2, 66–67 cm (84.94–151.36 mbsf).

Content: The zone is described by the presence of *Actiniscus pentasterias* and undifferentiated *Actiniscus* specimens. Single occurrences of ebridian skeletons obviously are allochthoneous.

At present only the Pliocene portion of the described zonation can be traced into other regions, as no other sections are adequately investigated for comparisons. The *Ebriopsis cornuta* and *Ammodochium serotinum* Zones are found at Sites 173, 184, and 192 in the northern Pacific (Ling, 1973, 1977: *E. antiqua* + *A. rectangulare* Zones). In the southwestern Pacific both zones were identified at Site 591 (Locker and Martini, 1986b). Despite some species in common, the lower part of the Norwegian Sea zonation cannot be correlated to the southwest Pacific, because different paleoecological conditions have caused a quite different succession of stratigraphically important events in both regions.

CORRELATION OF BIOEVENTS

Correlations of strata are usually accomplished with biozones, i.e., stratigraphic intervals that are defined by bioevents being first or last appearance data of selected species. But such intervals may include additional events that are important for biostratigraphy. Hence, a sequence of bioevents may have more stratigraphic potential than a sequence of biozones, which provokes stratigraphic discussions based solely on events. In summary, the stacking of bioevents may provide both a data set for high-resolution stratigraphy and for high-precision correlation. Furthermore, a well-calibrated sequence of events may help future correlating of biozones that are founded on different events.

Because the present investigations yielded several events beside those indicating boundaries of zones, a sequence of events was established for stratigraphical discussions. For this reason from Tables 1 to 3, displaying stratigraphic data of Holes 642C/D and 644A, 17 silicoflagellate taxa and 11 ebridian and actiniscidian taxa are selected. Their vertical ranges are studied in relation to the paleomagnetic time scale (Bleil, this volume) and the Neogene standard nannoplankton zonation (Martini, 1971; Martini and Müller, 1986), both of which are tied to absolute ages (Berggren et al., 1985). The results are shown in Figures 3 and 4, and Table 4. Regarding the data base for age comparisons, the following DSDP Sites were used: Site 66, central Pacific (silicoflagellates = S, and coccolithophorids = C: Martini 1971); Site 157, eastern equatorial Pacific (S: Bukry and Foster 1973, C: Bukry 1973, paleomagnetic data = P: Kaneps 1973); Site 173, northeastern Pacific (ebridians = E: Ling 1977, C: Wise 1973); Sites 184 and 192, North Pacific (E: Ling 1973, diatoms = D: Koizumi 1973); Site 206, southwestern Pacific (S: Dumitrică 1973d, C: Edwards 1973); Site 266, Southern Ocean (S: Ciesielski 1975, C: Burns 1975); Site 278, southwestern Pacific (S: Bukry 1975a, C: Edwards and Perch- Nielsen 1975); Sites 338 and 348, Norwegian-Greenland Sea (S: Martini and Müller 1976, C: Martini and Müller 1976, Müller 1976); Sites 369 and 370, eastern North Atlantic (S and C: Bukry 1978a); Site 407, North Atlantic (S and C: Martini 1979); Site 408, North Atlantic (S and C: Bukry 1979); Sites 470 and 472, northeastern Pacific (S and C: Bukry 1981b); Site 513, South Atlantic (S: Shaw and Ciesielski 1983, P: Ciesielski 1983); Site 575, central Pacific (S: Bukry 1985b, C: Pujot 1985, P: Weinreich and Theyer 1985); Sites 577, 579, and 580, northwestern Pacific (S: Bukry and Monechi 1985, P: Bleil 1985); Site 591, southwestern Pacific (S and E: Locker and Martini 1986a, b, C: Lohmann 1986); Site 594, southwestern Pacific (S: Locker and Martini 1986a, C: Lohmann 1986, P: Barton and Bloemendal 1986).

The first silicoflagellate event that could be used to fix the early Neogene at the sites studied is the FAD of *Naviculopsis lata*. But because *N. lata* appears just at the base of the fossiliferous sequence of Hole 642D, this species remains inappro-

Table 1. Holes 642C and 642D. Stratigraphic distribution of silicoflagellates in lower Miocene to upper Pliocene sediments. Numbers below taxa indicate percent or absolute frequencies, last ones are marked by an asterisk in the column "specimens counted." Definition of assemblage abundances and species diversities: See text. Note: Samples 104-642C-9H-1, 64–65 cm to 104-642D-11X-1, 55–56 cm represent strewn-slide data, all others are smear-slide observations.

Holes 642C/D		*Cannopilus depressus*	*C. ernestinae*	*C. hemisphaericus* f. *hemisphaericus*	*C. hemisphaericus* f. *heptagonus*	*C. schulzii*	*Corbisema flexuosa*	*C. triacantha*	*C. species diversae*	*Dictyocha epiodon*	*D. messanensis aspinosa*	*D. messanensis messanensis*	*D. perlaevis*	*D. species diversae* (messanensoid)	*Dictyocha clinata*	*D. fibula* s.l.	*D. fibula tenuis*	*D. varia*	*D. species diversae* (asperoid)	*Distephanus aculeatus* f. *aculeatus*	*D. aculeatus* f. *binoculus*	*D. crux* s.l.	*D. crux bispinosus*	*D. crux darwinii*	*D. crux longispinus*	*D. crux parvus*	*D. crux siradneri*	*D. paraspeculum* f. *hexagonalis*	*D. paraspeculum* f. *paraspeculum*	*D. polyactis*	*D. quinarius*	*D. speculum* s.l. f. *cann.-hexacanthus*
Series	Samples (Intervals in cm)																														
Quaternary to Pliocene	1H-1, 80–81 to 8H-3, 30–31													Barren																	
														Barren																	
Upper Pliocene	9H-1, 64–65											<1		<1						9	60	<1									
	10H-2, 71–72													Barren																	
Lower Pliocene	10H-4, 71–72																			6	57	<1									
	11H-2, 52–53												<1							P	<1					P					<1
	11H-5, 65–66							<1	<1							2					25	3							2		
	12H-2, 70–71																					1									
	12H-5, 65–66																		<1	4										<1	
	13H-1, 66–67							<1	P											39	2	<1								<1	
Upper Miocene	13H-3, 30–31																			12	14	P									
	14H-2, 66–67																			6	1	<1								1	<1
	14H-5, 55–56																2			37	3	P									
	15H-1, 66–67						P													17	<1	<1	P							36	
	15H-4, 66–67															12				22											
	16H-1, 50–51																			6	P	1					P				1
	16H-4, 50–51																			6		2				1					
	17H-2, 60–61													2						4	P	13					1				1
	17H-5, 50–51																	2		6	6	31								1	
	18H-2, 65–66	P					P				3				1							33									
	18H-5, 60–61								1					2					1			11									
	19H-2, 50–51			3							<1							<1	1			20				<1					
Middle Miocene	19H-5, 50–51	<1	2							P								7		<1		59									
	20H-1, 56–57	2						<1		<1	P					3	3	2	3	2		9									<1
	20H-4, 55–56	6	24													4			4			42					2			2	
	21H-1, 50–51	4		2				P												8		46					10			10	
	21H-4, 60–61	1	1	3							P							<1				73			4	5	4				
	22H-1, 66–67	4		4				P												4		73				4	1				
	22H-4, 60–61			8																cf.1		69				2	1				
	23H-2, 54–55	<1		4													2			<1		81				3	<1				
	23H-5, 70–71	<1	<1	2				P								<1	<1		P	4		72				3	<1				
	24H-2, 70–71			7		1											2		<1			58				12					
Lower Miocene	24H-5, 70–71			10	<1	1		<1												<1		53			1	5	4				
	3X-2, 60–61		1	15	<1	2																41				1	2				
	3X-5, 66–67			12	<1	<1																46				5	1				
	4X-2, 66–67			13																		54				<1	<1				
	4X-5, 62–63			12		<1		<1												<1		50			3	5					
	5X-2, 47–48			6				<1							<1							53			4	7					
	5X-5, 60–61			7	1																	47		<1	2	12	1				
	6X-2, 66–67			23	<1																	25		1	2	6					
	6X-4, 66–67			7											<1					2		44		<1	4	11					
	7X-2, 66–67			8				1	4						1							61		1	3	2					
	7X-5, 66–67			19																2		46			1	4	18				
	8X-2, 66–67			16			<1	<1			<1								<1			43			<1	12	3				
	8X-5, 66–67			10			1	2			P											51				1		1			
	9X-2, 66–67			9			<1	6												<1		43		3		<1	5	2	8		
	9X-5, 70–71			4				2			aff<1											62		3		1		<1	<1		
	10X-2, 70–71			4			3	54			aff<1							<1	<1			23		4	<1		1		<1		
	10X-4, 70–71			8			9	52	P		<1									<1		17		1	2		P				
	10X-6, 70–71			4			18	26														23					13				
	11X-1, 55–56			1			7	12														6									
	11X-2, 55–56	Barren																													

priate for specific comparisons. Disregarding its unrepresentative occurrence in Hole 642D, the appearance of *N. lata* generally requires discussion, because it is found at different time levels. At DSDP Sites 278, 338, and 369 the FAD of *N. lata* lies in nannoplankton Zone NP25. But at Sites 407 and 575 the event is determined in Zone NN1.

The FAD of *Naviculopsis iberica* is also indicated at different positions. At Site 338 it falls into Zone NP25 or NN1, but at Site 407 it is in the upper part of Zone NN1. At Site 642 the event is placed in Zone NN2 according to paleomagnetic data.

The FAD of *Naviculopsis navicula* is determined rather uniformly. At Site 407 it is indicated in the uppermost part of Zone NN1, and at Sites 266, 338, and 642 in Zone NN2.

The LAD of *Naviculopsis quadratum* (synonym *N. rectangulare*) is proved in the upper or uppermost part of Zone NN3 at Sites 338 and 370. At Site 575 the nearly equivalent LAD of *N. navicula ponticulus* is found in Zone NN3 or at the termination of paleomagnetic Chron C5D. At Site 266 the LAD of *N. navicula* may be assumed between the upper part of Zone NN3 or lowermost part of Zone NN4. At Site 642 both the species *N. quadratum* and *N. navicula* disappear around the lower boundary of Zone NN3 according to the paleomagnetic interpretations of Bleil (this volume), but this may be due to a change in paleoenvironmental conditions or a small hiatus.

The FAD of *Mesocena diodon* is recorded in the lower part of Zone NN5 at Site 338, and in the upper part at Sites 591,

Table 1 (continued).

D. speculum s.l. f. *pentagonus*	*D. speculum* s.l. f. *speculum*	*D. speculum* s.l. f. *speculum* (coronoid)	*D. speculum* s.l. f. formae diversae	*D. speculum constrictus* f. *constrictus*	*D. speculum constrictus* formae diversae	*D. speculum giganteus* f. *cann.-hexacanthus*	*D. speculum giganteus* f. *giganteus*	*D. speculum haliomma* f. *haliomma*	*D. speculum haliomma* f. *speculum*	*D. speculum haliomma* formae diversae	*D. stauracanthus* f. *octagonus*	*D. sulcatus* f. *maximus*	*D. sulcatus* formae diversae	*Mesocena diodon*	*M. elliptica*	*M. quadrangula*	*M. triangula*	*Naviculopsis iberica*	*N. lacrima*	*N. lata*	*N. navicula navicula*	*N. navicula obtusarca*	*N. quadratum*	*N.* species diversae	*Paramesocena circulus apiculata*	*P. circulus circulus*	*Septamesocena apiculata* f. *apiculata*	*S. apiculata* f. *curvata*	*Macrora stella* (Synuraceae)	Specimens counted	Assemblage abundances	Species diversities	Silicoflagellate zones
								Barren																						0	0	0	
								Barren																						0	0	0	Barren
1	19	7	<1	2								<1																		300	540	5	
								Barren																						0	0	0	
	25	9		<1								1	1																	300	700	4	
<1	5	2		90	1																						<1			300	930	5	*Distephanus aculeatus*
	2	64		<1									P			<1													120	110	8	Zone
	2						1																							4•	4	3	
	67	5				<1	22																							220	220	4	
<1	25	11					21											<1												270	270	5	
4	32	10					cf.2							26			P													50	50	6	
	36	3				<1	cf.18							30		2	2				P									300	300	8	*Mesocena diodon*
	19	30					9							P																110	110	7	Zone
<1	30	15						1						<1																230	210	6	
4	18	34												8			P				P									50	50	6	
	43	36												10												2				70	60	5	
	21													P												2		P		32•	32	5	*Paramesocena circulus apiculata*
	2																									2				25•	25	5	
	49													3												2				100	100	7	Zone
	60													1												3				110	110	6	
1	74																									10				100	100	3	
	68																									7				210	210	7	
<1	18										<1			<1						P						11				120	120	10	*D. stauracanthus*
<1	68													1												3				180	180	13	Upper
2														14																50	50	9	*Corbisema triacantha*
	16													2														2		P	50	40	10	
								1	<1					4	1													2			160	160	12	Zone
	6													P														1	1	70	70	10	
	9							2	7																				1	90	90	8	
								1	3	<1																		1	<1	140	140	9	
								5	10	<1															<1			<1	<1	250	240	13	
								8	10																<1			<1	1	210	210	8	
								20	2																<1			<1	2	300	320	10	Lower
								31	4																				1	210	210	8	*Corbisema triacantha*
								32	2	<1																			<1	300	400	7	
								30																				1	<1	300	300	6	Zone
								26	2																				<1	300	350	9	
								24	<1	P															<1			1	3	230	230	8	
								26	1																			1	1	220	220	8	
								38	5																			<1	1	300	320	7	
								10	<1									18				<1		cf.1				<1	<1	300	590	12	
								11										4				2		cf.P						90	80	11	
								6										1										2	1	100	100	9	*Naviculopsis navicula*
								4	<1							1		3				<1		9				4	<1	160	160	15	Zone
								10										P			3	2	7		1			4	6	P	90	90	13	
								17	3									1				<1	<1		<1			2			200	200	14	
								19	4	<1								<1				<1			<1				<1	300	270	11	
								5								<1		<1				1		aff. <1				<1	<1	300	420	17	*Naviculopsis lata*
								4												<1	1	1						<1	4	P	300	890	13	Zone
								3												3	5							5	3		110	110	9	
																					2							2			30•	30	6	
								Barren																						0	0	0	Barren

594, and 642. At Site 206 the species appears in the lower part of Zone NN6.

The LAD of *Septamesocena apiculata* can be assigned to the upper part of Zone NN5 at Site 594. The FAD of *Paramesocena circulus apiculata* is known mainly from the lower to middle part of Zone NN6, which can be demonstrated at Sites 206, 408, 470, and 594. At Site 642 both events may be expected in the lower part of Zone NN6, if the paleomagnetic data of Table 4 are extrapolated.

The LAD of *Distephanus stauracanthus* (synonym *D. crux* var. *octacanthus*) is repeatedly recorded from the upper part of Zone NN6, in which the variant *D. stauracanthus* f. *octagonus* seems to be most diagnostic (Bukry, 1981b, 1985b). The upper part of Zone NN6 is determined at Sites 66, 472, and 591, for instance. The LAD of *Corbisema triacantha* which usually follows the LAD of *D. stauracanthus* is unrepresentatively developed at Site 642, due to ecological restrictions in these high northern latitudes. As secondary indicator, therefore, *Cannopilus depressus* was selected. But the real LAD of this species may be depressed at Site 642 by a hiatus above the single occurrence of *D. stauracanthus*.

The LAD of *Paramesocena circulus apiculata* is described both by nannoplankton and paleomagnetic data. At Site 348 the top of nannoplankton Zone NN11 is indicated, whereas at

Table 2. Holes 642C and 642D. Stratigraphic distribution of ebridians and actiniscidians in lower Miocene to upper Pliocene sediments. Numbers below taxa indicate percent or absolute frequencies, last ones are marked by an asterisk in the column "specimens counted." Definition of assemblage abundances and species diversities: See text. Note: Samples 104-642C-9H-1, 64–65 cm to 104-642D-11X-1, 55–56 cm represent strewn-slide data, all others are smear-slide observations.

Holes 642C/D		*Ammodochium pyramidale*	*A. serotinum*	*A. species diversae*	ammodochioid skeletons	*Craniopsis* sp.	*Ditripodium amphora*	*D.* cf. *amphora*	*D. elephantinum*	*D. japonicum*	*D. latum*	*Ebria inornata*	*Ebriopsis cornuta*	*E. crenulata*	ebriopsoid skeletons	*Falsebria ambigua* s.l.	*F. arborea*	*F.* cf. *arborea*	*F.* sp.	falsebrioid skeletons	*Haplohermesinum hovassei*	*H. narbonensis*	*Hermesinella conata*	*H. fenestrata*	*H. primitiva*	*H. schulzii*	*Hermesinum adriaticum*	*H. mirabile*
Series	Samples (Intervals in cm)																											
Quaternary to Pliocene	1H-1, 80–81 to 8H-3, 30–31												Barren		Barren													
Upper Pliocene	9H-1, 64–65		1		<1								8				5	35		13								
	10H-2, 71–72														Barren													
Lower Pliocene	10H-4, 71–72		2										6				3	36		20								
	11H-2, 52–53												3				12	37		12								
	11H-5, 65–66		<1	<1	<1					<1			4					10		3								
	12H-2, 70–71																											
	12H-5, 65–66				9															1								
	13H-1, 66–67				1				cf.P				P			<1		<1	4	11								
Upper Miocene	13H-3, 30–31		68		2	<1												<1	4	8								
	14H-2, 66–67		47		6	<1												3	9	10	<1							
	14H-5, 55–56		30		18								P					<1	10	4								
	15H-1, 66–67	P	38	2	15									cf.P				1	9	4								
	15H-4, 66–67		16		2														2	1								
	16H-1, 50–51		5		2											<1		1	8	5								
	16H-4, 50–51		13		4													1	13	8								
	17H-2, 60–61		9		2				<1									9	13	9								
	17H-5, 50–51		5		2				cf.<1							<1		7	9	14	1		1			<1		
	18H-2, 65–66		5		3	<1						<1							1	10			1			P		
	18H-5, 60–61		12		2				cf.<1							<1		3	4	8			<1					
	19H-2, 50–51		12		4				cf.2					P		<1		1	4	9			2				2	
Middle Miocene	19H-5, 50–51		23		3											<1		3	16	15						P	<1	
	20H-1, 56–57		29		4				cf.<1							<1			1	7			<1			P	4	
	20H-4, 55–56		34		3				<1		<1					1		<1	1	5	2		<1				<1	
	21H-1, 50–51	<1	28		4											<1				2			1			<1	3	P
	21H-4, 60–61	<1	25		2				<1		<1					2			2	8	<1		2			<1	1	
	22H-1, 66–67	<1	18	P	2											2		cf.<1	<1	24			2	cf.<1		1		
	22H-4, 60–61	2	20		3				<1		2					<1		aff.5	1	28	2		<1					
	23H-2, 54–55	<1	17	<1	6				cf.<1		2							aff.3		36	1						<1	
	23H-5, 70–71	P	22		6						3							aff.3	3	34	<1		P				<1	
	24H-2, 70–71		29		1						2					2		aff.4	1	28	2			P			1	
Lower Miocene	24H-5, 70–71	2			1						1	cf.<1				1		aff.1	1	16	1		9			5	2	
	3X-2, 60–61	7			4											1		1	3	10	1		6	2		7	2	
	3X-5, 66–67	6			2		1										1	2	3	9	1		4			1	2	
	4X-2, 66–67	5			5						<1					3		2	2	5	6		<1			1	1	
	4X-5, 62–63	4			4		<1	<1								1		2		8	7		<1	<1		P	2	
	5X-2, 47–48	10			2												1	5	1	8	1		2	1			1	
	5X-5, 60–61	2			6			P								<1	<1	3		6	4		2	cf.2		<1	2	
	6X-2, 66–67	13			3			<1								1	2		5	8	4		3	3	2		1	
	6X-4, 66–67	5			6			2				cf.<1				2	<1	1		3	7	<1	2		1	<1	P	
	7X-2, 66–67	8			5			<1								2			<1	3	7		<1	3	2			
	7X-5, 66–67	7			6											1	<1			2	7		<1	cf.1				
	8X-2, 66–67	6			9	<1										2	1		2	5	9		1	3	<1			
	8X-5, 66–67	6										cf.1					1			6	9		3	2	1			
	9X-2, 66–67	1			1											2		1	7	6	4	2	1	1				
	9X-5, 70–71	14			11											1	1		1	5	5					1		
	10X-2, 70–71	2			1											<1	2		6	4	2	<1			<1	<1		
	10X-4, 70–71	4			2											<1			5	11	2		1	cf.<1		1		
	10X-6, 70–71	3			3			3								3	2		4	3	7		2	cf.2	4	2		
	11X-1, 55–56	<1			<1											1	2		<1	3	1							
	11X-2, 55–56														Barren													

Sites 513 and 594 magnetic Subchron C3A-R2 corresponding to the upper part of Zone NN11 is shown. These data coincide well with Site 642.

The LAD of *Mesocena diodon*, in contrast, must be placed in Subchron C3A-Nl or the lower part of Zone NN12 at Site 642 according to paleomagnetic data (Bleil, this volume), which is not in accordance with other data. In other regions the event appears somewhat later at the top of nannoplankton Zone NN12 or in Subchron C3-N3/4. So the top of Zone NN12 is evidenced at Sites 348 and 394, and magnetic anomalies C3-N3/4 at Sites 513 and 594.

Depending on the latitude of sites, the LAD of *Distephanus aculeatus* (synonym *D. boliviensis*) ranges from Zone NN15 to NN18. The earliest datum is found at Site 642 in Subchron C2A-R2, which corresponds to nannoplankton Zone NN15. Subchrons C2A-N1/3 or Zone NN16 are indicated at Sites 513, 594, and 644. The latest datum is known from Site 157, being in Subchron C2-R or nannoplankton Zone NN18.

The last silicoflagellate event to be discussed is the LAD of *Mesocena quadrangula* (cited also as *M. elliptica*). It is found just below the Brunhes Epoch at Site 644, and thus corresponds well with many other sites. In particular, the magnetic interval

Table 2 (continued).

H. obliquum	hermesinoid skeletons	*Parathranium bispinum*	*P.* cf. *californicum*	*P. clathratum*	*P.* cf. *clathratum*	*P. curvipes*	*Podamphora elgeri*	*Pseudammodochium robustum*	*P.* species diversae	*Spongebria curta*	*S. miocenica*	*Thranium crassipes*	*T.* cf. *crassipes*	*T. patulum*	*Actiniscus elongatus*	*A. flosculus*	*A. laciniatus*	*A. pentasterias*	*A. planatus*	*A. tetrasterias*	*A.* sp.	*Foliactiniscus atlanticus*	*F. folia*	*F. mirabilis*	*F. pulvinus*	Specimens counted	Assemblage abundances	Species diversities (ebridians)	Species diversities (actiniscidians)	Ebridian-actiniscidian zones
												Barren														0	0	0	0	Barren
												Barren														0	0	0	0	
								16								<1		<1			20					300	600	4	2	
												Barren														0	0	0	0	
					cff.P			8										1			24					300	740	5	1	*Ebriopsis cornuta* Zone
					cff.P			1								1					34					300	940	4	2	
		<1		cf.<1	12			39							3	1		1			24					300	1000	7	3	
																1					2					3*	3	0	2	
		57			6										4	6		3			14					70	70	3	3	
		23		9	36							2				<1		1			11					300	360	6	2	
		4		<1								3				<1		<1			8					180	180	5	2	
		10			2				<1			7	2					<1			2					300	460	6	1	
		25		<1	2							9	<1								<1					300	1190	6	1	*Parathranium clathratum* Zone
		16			2							10	2	1							P					300	1440	6	1	
	<1	<1			<1		2					3	<1		1	2		41			27					300	300	6	3	
													<1		5	2		48		3	19	<1				170	150	4	4	
		33	2	1	1							1				1		6		2	13					200	200	6	3	
<1				5	2							<1			<1	2		12		2	32					130	130	6	4	
	<1	<1	<1	<1	<1							2			<1	5		5		7	40					300	600	9	4	
		<1	<1	2	2							2			P	6	<1	8		20	38					210	190	9	5	
		4	1				<1					<1			<1	4		14		9	36	<1				300	320	9	4	
3		10	2	1	<1							2			2	2	<1	7		5	29					300	460	11	5	*Hermesinella schulzii* Zone
<1		<1	<1	2	1		<1					5			<1	1		4		2	22					300	790	11	4	
3		3	2	3	4		<1				<1	2			1	4		5		4	21					300	390	13	4	
1				2	1							2				8		7		3	26	<1				300	360	10	3	
1		3		2	4							4				9		4			33					300	380	11	2	
1		<1	<1	3	5							3			<1	6		4	<1		32					300	740	13	4	
1	<1	1		4	4						4	4				2		<1	1		27					170	170	11	3	
<1	1			2	<1						9	2				5		1			14	1				300	350	10	3	
<1		<1	1	1	8						8	cf.<1				2		1			8	1	1			300	510	12	4	*Spongebria miocenica* Zone
1		1	1	1	12					1	2	cf.<1				1					5	2	<1			300	900	13	3	
2	<1		1	1	4					3	2	cf.<1				3		1		aff.<1	10	<1	<1			300	750	12	5	
1	5	2	2	<1	11					<1	1					3		<1			32	<1				260	260	14	3	
3	5	2	3		8											4		1			29	1				200	200	11	3	
2	1	6	3		15											2					25	14				300	330	11	2	
2	<1	10	6		17											<1					18	15				300	320	11	2	
3	1	10	3		7	<1										3					25	17		<1		280	280	13	3	*Hermesinum adriaticum* Zone
1	1	10	3		3											2					31	17				240	240	10	2	
2	2	26	7			P										<1					24	10				300	360	12	2	
1	2	14	4		3	<1										<1					14	15				220	220	13	2	
2	2	12	6		<1	<1										2					25	13	6			300	360	15	3	
	<1	7	2		3											2					29	16	9			200	200	10	3	
1	1	8	<1		2											2				aff.1	32	16	9		2	210	210	9	5	
	2	7	4		3											1					36	6	2			180	180	9	3	*Foliactiniscus folia* Zone
		4			3											6					54	3	1			70	70	9	3	
		5			3											3					39	23	1			200	200	8	3	
		6			4											3					32	16				100	100	6	2	
	<1	6	<1		2											3					26	42	<1			270	270	9	3	
		15	5		9	<1										4					21	18				200	200	10	2	*Foliactiniscus atlanticus* Zone
	1	2	4		1	3										3					27	21				180	180	12	2	
		P														9					59	23				170	170	4	2	
												Barren														0	0	0	0	Barren

C1-R1 is known from some piston cores in the Pacific and Indian Oceans (Ling, 1970. Dumitrică, 1973a), and from DSDP Sites 157 and 580. At Sites 577 and 579, and in piston cores of the northwestern Pacific (Ling, 1976) the disappearance event is present in the lower part of the Brunhes Epoch.

The ebridian and actiniscidian events cited in Table 4 can be compared only for the Pliocene time interval with other regions, as appropriate data for older epochs are missing in the literature. The LAD of *Ebriopsis cornuta* (cited also as *E. antiqua*) generally corresponds to the LAD of *Distephanus aculeatus* at both the Sites 642 and 644, thus being present in Subchron C2A-N1 at Site 644. It is amazing that the same time level is indicated at Sites 184 and 192 in the northernmost Pacific, if new correlation data are used. So the LAD of the diatom *Denticulopsis kamtschatica*, found just below the LAD of *E. cornuta* at Sites 184 and 192 (Koizumi, 1973), is placed nowadays directly at the top of paleomagnetic Chron C2A (Barron, 1980).

The LAD of *Ammodochium serotinum* (cited also as *A. rectangulare*) is found in the upper part of Subchron C2-R or below the Pliocene/Pleistocene boundary at Site 644. And again the records of northern Pacific sites are close to this date. At Site 173 the LAD of *A. serotinum* lies in the upper part of

Table 3. Hole 644A. Stratigraphic distribution of silicoflagellates, ebridians, and actiniscidians in upper Pliocene to Pleistocene sediments. Numbers below taxa indicate percent or absolute frequencies, last ones are marked by an asterisk in the column "specimens counted." Definition of assemblage abundances and species diversities: See text. Note: Samples 104-644A-10H-2, 74–75 cm to 104-644A-34H-5, 66–67 cm represent strewn-slide data, all others are smear-slide observations.

Hole 644A		*Cannopilus hemisphaericus* f. *hemisphaericus*	*Corbisema triacantha*	*C.* species diversae	*Dictyocha messanensis messanensis*	*D. perlaevis*	*D. varia*	*D.* species diversae	*Distephanus aculeatus* f. *aculeatus*	*D. aculeatus* f. *binoculus*	*D. crux* s.l.	*D. speculum* s.l. f. *cannopileus-hexacanthus*	*D. speculum* s.l. f. *pentagonus*	*D. speculum* s.l. f. *speculum*	*D. speculum* s.l. f. *speculum* (coronoid)	*D. speculum* s.l. formae diversae	*D. speculum constrictus* f. *constrictus*	*D. speculum constrictus* formae diversae	*D. speculum octonarius* f. *octonarius*	*D. speculum octonarius* f. *septenarius*	*Mesocena quadrangula*	*Naviculopsis* species diversae	Specimens counted	Assemblage abundances	Species diversities	Silicoflagellate zones
Series	Samples (Intervals in cm)																								
Holocene to Pleistocene	1H-1, 68–69 to 10H-1, 63–64											Barren / Barren										0 / 0	0 / 0	0 / 0	Barren
Pleistocene	10H-2, 74–75													P								P	P	1	
	10H-3, 74–75																				3	3*	3	1	
	11H-2, 67–68											Barren										0	0	0	*Mesocena quadrangula* Subzone
	11H-6, 66–67					P								P						2		2*	2	3	
	12H-4, 66–67												1							1	1	3*	3	3	
	12H-5, 66–67													P							1	1*	1	2	
	13H-1, 55–56													3					1			4*	4	2	
	13H-3, 53–54											Barren										0	0	0	
	14H-2, 78–79													1	1							2*	2	1	
	14H-4, 65–66											No silicoflagellates										0	0	0	
	15H-3. 66–67											No silicoflagellates										0	0	0	
	15H-5, 66–67					P	cf.1															1*	1	1	
	16H-1, 66–67													P								P	P	1	*Distephanus speculum* Zone
	16H-4, 65–66					cf.P					P		1	3	P						1	5*	5	2	
	17H-2, 66–67													2								2*	2	1	
	17H-4, 66–67					cf.1								1								2*	2	2	
	18H-1, 48–49													P								P	P	1	
	18H-6, 67–68							P														P	P	0	
	19H-3, 66–67											Barren										0	0	0	
	19H-5, 65–66														P							P	P	1	
	20H-1, 65–66			P																	1	1*	1	0	
	20H-4, 66–67				1									1								2*	2	2	
	21H-1, 66–67					1			P					P								1*	1	2	
	22H-1, 66–67										P											P	P	0	
	22H-4, 66–67											Barren										0	0	0	
	23H-1, 55–56					cf.1		1														2*	2	1	
	23H-2, 55–56				1								1									2*	2	2	
Upper Pliocene	24H-3, 66–67			1																		1*	1	0	Barren/ unzoned
	25H-1, 66–67																				P	P	P	0	
	25H-3, 48–49											Barren										0	0	0	
	26H-2, 48–49		P																			P	P	0	
	28H-3, 48–49											Barren										0	0	0	
	29H-1, 48–49											Barren										0	0	0	
	30H-1, 57–58										1											1*	1	0	
	30H-2, 56–57							1	P	1			P	1	1							4*	4	2	*Distephanus aculeatus* Zone
	31H-2, 66–67							P		1	P		P	P								1*	1	2	
	31H-3, 66–67									13	P	1	3	4	5							26*	26	2	
	31H-4, 66–67				1	5			1	5	2		P	6	10							30*	30	4	
	32H-2, 66–67						cf.1	1	1	3	3		1	8	13							31*	31	2	
	32H-4, 20–21		2							6	1	1		1	11							22*	22	2	
	33H-1, 66–67	1							P	2	P		P	1	7	P					1	12*	12	2	
	34H-2, 68–69	1				P			1	2	2			1	3							10*	10	3	
	34H-4, 66–67							1		2	P			1	4		1					9*	9	3	
	34H-5, 66–67		<1						P	<1	1		<1	3	3		91	1				300	470	3	

planktonic foraminifer Zone N21, which correlates with magnetic Subchron C2-R or the top of nannoplankton Zone NN17. At Sites 184 and 192 this datum is more indistinct but surely in the late or very late Pliocene according to diatoms (Koizumi 1973).

SITE SUMMARIES

Site 642

Silicoflagellates

Holes 642C and 642D (67°13.2′N, 02°55.8′E, water depth 1277 m) are located at the outer Vøring Plateau. The composite section comprises a sequence of hemipelagic and pelagic sediments (0 to 277.6 mbsf), an intermediate interval of volcaniclastic sediments (277.6–315.2 mbsf), and a series of basalts interlayered with volcaniclastic sediments (315.2–1229.4 mbsf). The upper sedimentary sequence is determined as Miocene to Quaternary, the intermediate interval is considered to be Eocene mixed with some displaced Neogene, and the lower volcanic series is placed in the Eocene (Eldholm, Thiede, Taylor, et al., 1987).

The Miocene to Quaternary sequence was differentiated by shipboard scientists into three lithologic units and some subunits. Lithologic Unit 1, from 0 to 59.7 mbsf (Cores 104-642C-1H to 104-642C-8H), consists of glacial and interglacial muds

Table 3 (continued).

Ammodochium pyramidale	*A. serotinum*	*Ditripodium latum*	*Ebriopsis cornuta*	*E. crenulata*	Ebriopsoid skeletons	*Falsebria arborea*	*Falsebria* cf. *arborea*	falsebrioid skeletons	*Haplohermesinum hovassei*	*Hermesinella conata*	*H. fenestrata*	*Hermesinum obliquum*	*Parathranium bispinum*	*P.* cf. *clathratum*	*Pseudammodochium fenestratum*	*P. robustum*	*P.* species diversae	*Thranium* cf. *crassipes*	*Actiniscus atlanticus*	*A.* cf. *flosculus*	*A. pentasterias*	*A. tetrasterias*	*A.* sp.	Specimens counted	Assemblage abundances	Species diversities (ebridians)	Species diversities (actiniscidians)	Ebridian-actiniscidian zones
										Barren														0	0	0	0	Barren
										Barren														0	0	0	0	
																					4		4	8*	8	0	1	
																							1	1*	1	0	1	
											Barren													0	0	0	0	
																				1	P		4	5*	5	0	2	
																					1		2	3*	3	0	1	
																							18	18*	18	0	1	*Actiniscus pentasterias* Zone
																					2		47	49*	49	0	1	
											Barren													0	0	0	0	
																							8	8*	8	0	1	
																							1	1*	1	0	1	
																					P		1	1*	1	0	1	
																2							2	4*	4	0	1	
																1					P		3	4*	4	0	1	
		1																		1			15	17*	17	0	2	
																					1		12	13*	13	0	1	
								1															3	4*	4	0	1	
																							3	3*	3	0	1	
																1								1*	1	0	0	
											Barren													0	0	0	0	Unzoned
																							P	P	P	0	1	
																							2	2*	2	0	1	
																							1	1*	1	0	1	
	4																						3	7*	7	1	1	
										No ebridians and actiniscidians														0	0	0	0	*Ammodochium serotinum* Zone
										Barren														0	0	0	0	
																				1			2	3*	3	0	2	
	1																						1	2*	2	1	1	
										No ebridians and actiniscidians														0	0	0	0	
										No ebridians and actiniscidians														0	0	0	0	
										Barren														0	0	0	0	
																1								1*	1	0	0	Barren/ unzoned
										Barren														0	0	0	0	
										Barren														0	0	0	0	
					P																			P	P	0	0	
	3		2			4	75	13															3	230	230	3	1	
			10	2		4	60	12									2	2					8	50	30	3	1	
	<1		8			4	59	13			<1			<1			<1						13	230	230	4	1	
	<1		8			1	38	11			P			<1		<1	<1			<1	<1	<1	38	270	270	5	2	
<1	25		7				33	12									P			<1	3		19	170	170	4	2	*Ebriopsis cornuta* Zone
	1		2			2	41	13	1	P							P			1	3		36	180	180	4	2	
	1		8				28	11				2	1				3		P		5		41	80	80	5	1	
	3		8			P	41	7												1	3		37	80	80	3	2	
			2				67	7		1								1			2		20	70	70	2	1	
	2		30	P		1	36	6					<1	<1							<1		23	300	500	5	1	

that are late Pliocene to Quaternary in age. This unit is almost barren of siliceous microfossils. Only three samples yielded a few remnants of corroded diatoms and sponge spicules.

Lithologic Unit 2, between 59.7 and 156.6 mbsf (Cores 104-642C-8H to 104-642C-19H), represents an interbedded sequence of calcareous and siliceous pelagic muds and oozes that are Miocene to Pliocene in age. The uppermost part of this unit still belongs to the overlying barren interval; but from Sample 104-642C-9H-1, 64–65 cm (61.34 mbsf), downward-rich assemblages of siliceous plankton are present, including chrysomonades, silicoflagellates, ebridians, actiniscidians, diatoms, and radiolarians. Also, rare sponge spicules and phytoliths are known. The silicoflagellate assemblages between Samples 104-642C-9H-1, 64–65 cm and 104-642C-13H-2, 66–67 cm (61.34–94.16 mbsf) are dominated by *Distephanus aculeatus* and *D. speculum*, and can be placed in the lower to upper Pliocene *Distephanus aculeatus* Zone (Table 1). Most common taxa are *D. aculeatus* f. *aculeatus*, f. *binoculus,* and *D. speculum* s.1. f. *speculum*, but in certain intervals *D. speculum constrictus* and *D. speculum giganteus* may be rather common. Stratigraphically important are some true *Paramesocena circulus circulus* specimens in Sample 104-642C-llH-2, 52–53 cm, which confirm a Pliocene age. The interval between Samples 104-642C-13H-3, 30–31 cm and 104-642C-15H-3, 66–67 cm (95.30–114.66 mbsf), belongs to the *Me-*

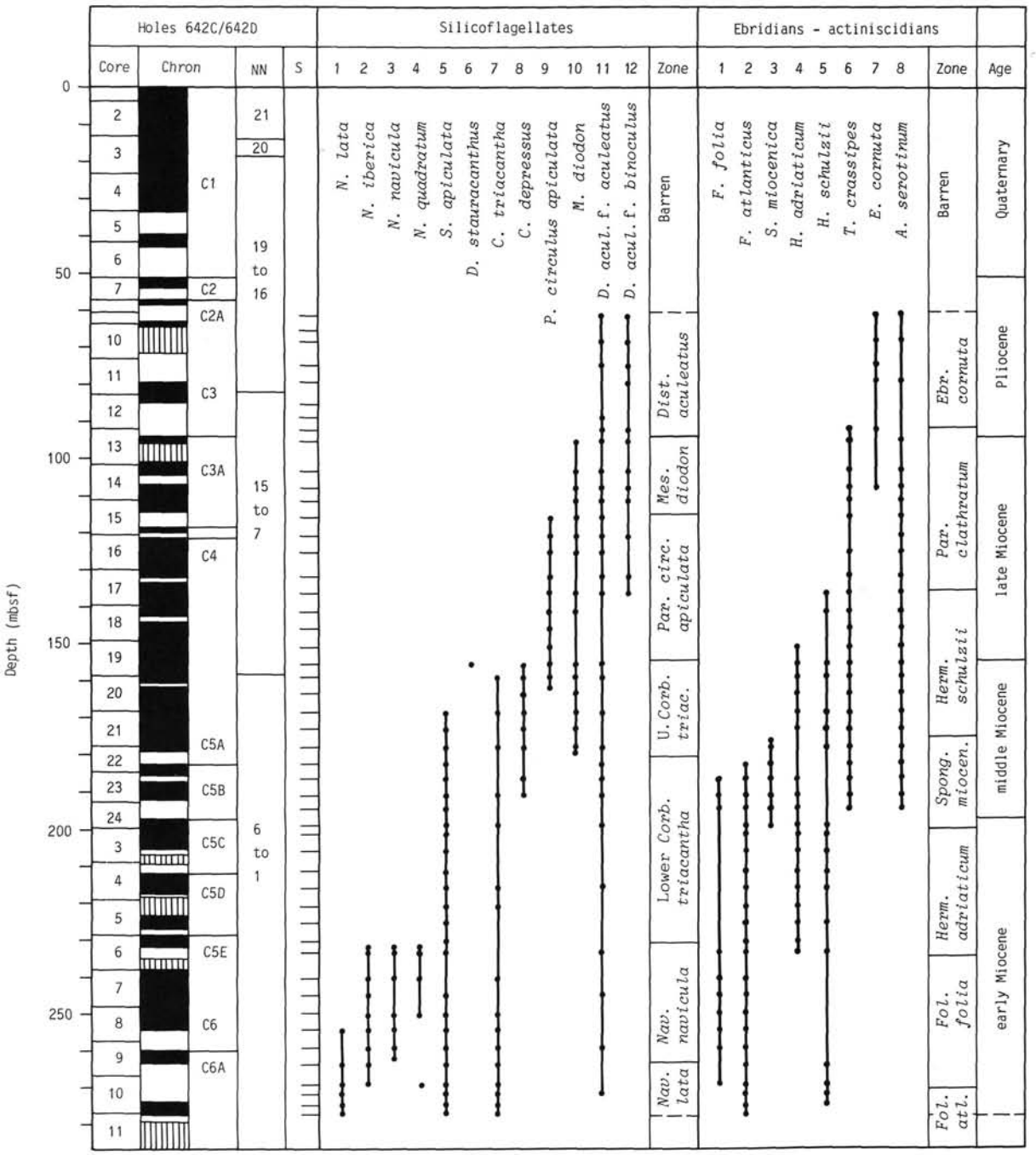

Figure 3. Holes 642C and 642D. Stratigraphic ranges of selected silicoflagellate, ebridian and actiniscidian species, related biozonations, and correlation with paleomagnetic anomalies (Bleil, this volume), and standard nannoplankton zones (Donnally, this volume). S signifies sample position.

socena diodon Zone as determined by common to abundant. *D. aculeatus*, *D. speculum* s.l., and *M. diodon*. Noticeable is the presence of *Distephanus crux bispinosus* in Sample 104-642C-15H-1, 66–67 cm because its stratigraphic position coincides with the lowest occurrence of the subspecies in Hole 594 in the southwestern Pacific (Locker and Martini, 1986a). In other regions the Miocene/Pliocene boundary lies within the *Mesocena diodon* Zone, but in Hole 642C it must be placed at the top of the zone according to paleomagnetic interpretations (Bleil, this volume). Thus at Site 642 the *Mesocena diodon* Zone represents only the upper Miocene. From Sample 104-642C-15H-4, 66–67 cm to 104-642C-19H-4, 50–51 cm (116.16–154.00 mbsf), the middle to upper Miocene *Paramesocena circulus apiculata* Zone is present. *Distephanus aculeatus* f. *aculeatus* and *D. crux* s.l. are common to abundant, whereas *D. speculum* s.l. f. *speculum* may be dominant. *Paramesocena circulus apiculata* generally occurs rare to common. Sample 104-642C-19H-5, 50–51 cm (155.50 mbsf), in the lowermost Unit 2 represents the middle Miocene *Distephanus stauracanthus* Subzone of the Upper *Corbisema triacantha* Zone, proved by the last consistent occurrence of *Cannopilus depressus* and the presence of *Distephanus stauracanthus* f. *octagonus*.

Lithologic Unit 3, from 156.5 to 277.6 mbsf (Cores 104-642C-19H to 104-642C-24H, and 104-642D-3X to 104-642D-11X), con-

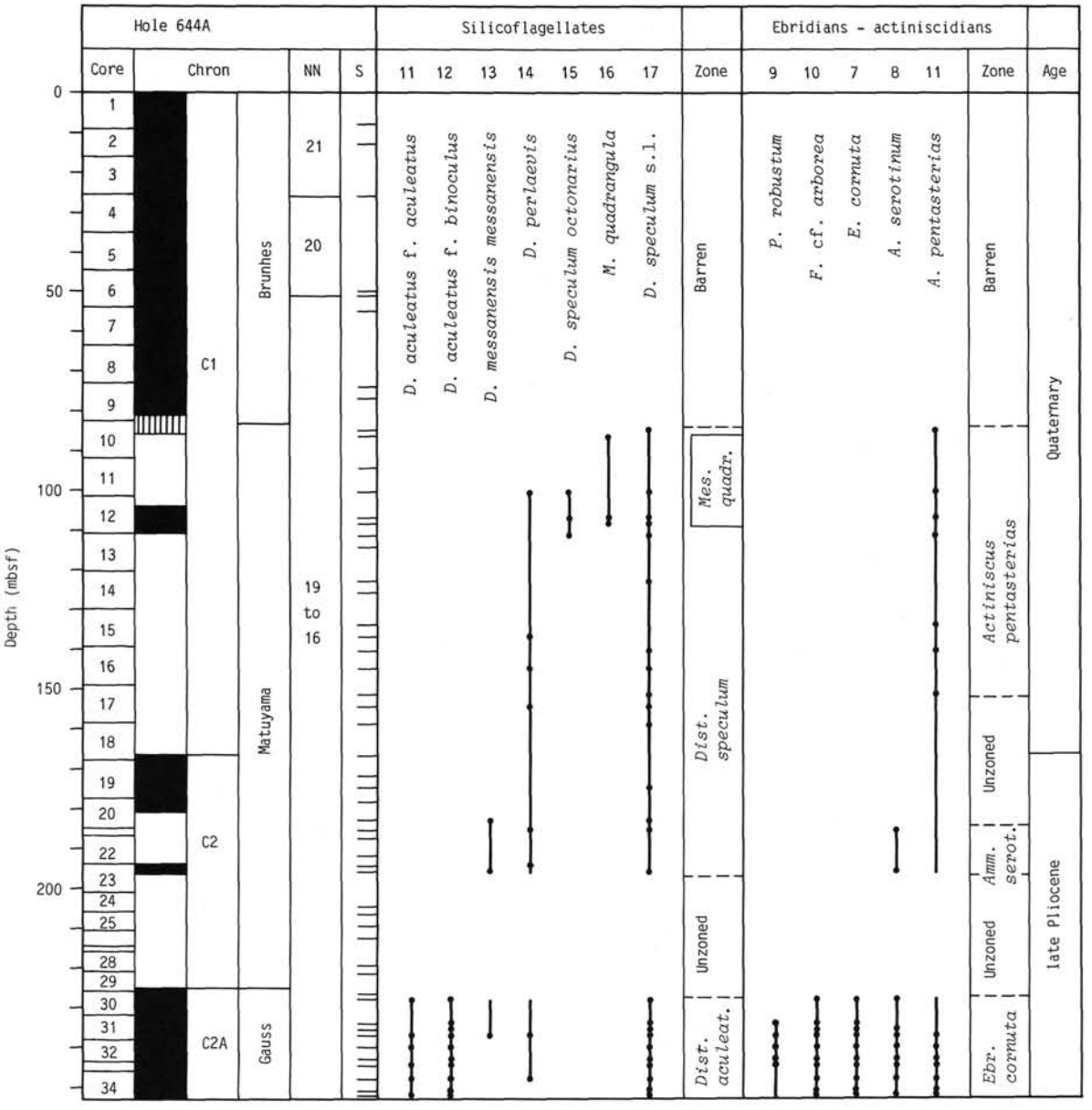

Figure 4. Hole 644A. Stratigraphic ranges of selected silicoflagellate, ebridian and actiniscidian species, related biozonations, and correlation with paleomagnetic anomalies (Bleil, this volume) and standard nannoplankton zones (Donnally, this volume). S signifies sample position.

sists of pelagic siliceous muds and oozes that are Miocene in age. The interval between Samples 104-642C-20H-1, 56–57 cm and 104-642C-22H-2, 66–67 cm (159.06-179.66 mbsf), belongs to the middle Miocene Upper *Corbisema triacantha* Zone. This latter interval is characterized by high species densities, including different members of the genera *Cannopilus* and *Dictyocha*. But in general, the assemblages are dominated by specimens of *Distephanus crux* s.l. The Upper *Corbisema triacantha* Zone contains several important levels: the FOL of *Paramesocena circulus apiculata* and the LO levels of *Cannopilus hemisphaericus*, *Distephanus speculum haliomma* and *Septamesocena apiculata*. Samples 104-642C-22H-3, 66–67 cm to 104-642C-24H-5, 70–71 cm and 104-642D-3X-1, 60–61 cm to 104-642D-6X-2, 66–67 cm (181.16–230.66 mbsf), are placed in the lower to middle Miocene Lower *Corbisema triacantha* Zone. Dominant constituents of the assemblages are *C. hemisphaericus*, *D. crux* s.l. and *D. speculum haliomma*, the last one showing a distinct downhole shift in frequency from f. *speculum* to f. *haliomma*. *Cannopilus schulzii* which occurs in this interval may have special stratigraphic value. Comparable to the Upper *Corbisema triacantha* Zone, the nominate species still has scattered occurrences. The interval between Samples 104-642D-6X-3, 66–67 cm and 104-642D-9X-4, 70–71 cm (232.16–262.70 mbsf) is distinguished by various *Naviculopsis* species, and can be referred to the lower Miocene *Naviculopsis navicula* Zone. The assemblages are characterized again by *C. hemisphaericus*, *D. crux* s.l. and *D. speculum haliomma*. The lowermost part of Unit 3, from Sample 104-642D-9X-5, 70–71 cm to 104-642D-11X-1, 55–56 cm (264.20–277.35 mbsf), is assigned to the *Naviculopsis lata* Zone. *Corbisema triacantha*, *D. crux* s.l. and *D. speculum haliomma* dominate, whereas *Naviculopsis lata* and *N. lacrima* are rare but most diagnostic for stratigraphy. Regarding the Oligocene/Miocene boundary drawn by coccoliths in Hole 643 (Donally, this volume) and diatom correlations to Hole 642D (Ciesielski, un-

Table 4. Holes 642C/D and 644A. Bioevents in relation to paleomagnetic anomalies (after Bleil, this volume) and Neogene standard nannoplankton zones (deduced from paleomagnetic anomalies). Zones within brackets indicate position of events outside the investigation area. Letters refer to actiniscidian species (A), ebridian species (E), and silicoflagellate species (S). Occ signifies a single occurrence of the species. Note: Paleomagnetic data with an asterisk are not in accordance with Bleil (this volume). Explanations: See "Methods" section.

Epoch	Biovent	Age (Ma)	Hole, sample (cm)	Depth (mbsf)	Subchron	NN-Zone
Pleistocene	LAD *M. quadrangula* (S)	0.76	644A-10H-3, 74–75	86.44	C1-R1	upper NN19
Late Pliocene	LAD *A. serotinum* (E)	1.93	644A-21H-1, 66–67	185.46	upper C2-R	lowermost NN19
	LAD *E. cornuta* (E) and LAD *D. aculeatus* (S)	2.50 / 3.10	644A-30H-2, 56–57 / 642C-9H-1, 64–65	228.16 / 61.34	uppermost C2A-N1 / C2A-R2	upper NN16 / lower NN16
E. Pliocene	LAD *T. crassipes* (E)	5.26	642C-13H-1, 66–67	92.66	lower C3-R4	NN12
Late Miocene	LAD *M. diodon* (S)	5.41	642C-13H-3, 30–31	95.30	C3A-N1	lower NN12
	LAD *P. circ. apiculata* (S)	5.96	642C-15H-4, 66–67	116.16	C3A-R2	upper NN11
	LAD *A. tetrasterias* (A)	6.55	642C-16H-1, 50–51	121.00	C3B-R	NN11
	LAD *H. schulzii* (E)	—	642C-17H-5, 50–51	136.50	unresolved C4/C4A	(~top NN10)
Middle Miocene	LAD *C. triacantha* (S)	—	not representative in Hole 642C			
	LAD *C. depressus* (S) and Occ *D. stauracanthus* (S)	—	642C-19H-5, 50–51	155.50	unresolved C5A*	(upper NN6)
	FAD *P. circ. apiculata* (S)	—	642C-20H-3, 56–57	162.06	unresolved C5A*	(NN6)
	LAD *S. apiculata* (S)	—	642C-21H-1, 50–51	168.50	unresolved C5A*	(lowermost NN6)
	LAD *S. miocenica* (E)	14.42	642C-21H-6, 60–61	176.10	C5A-N8*	uppermost NN5
	FAD *M. diodon* (S)	14.71	642C-22H-2, 66–67	179.66	C5A-R8*	upper NN5
	FAD *A. serotinum* (E)	16.03	642C-24H-2, 70–71	194.60	C5B-R2*	NN5
Early Miocene	FAD *S. miocenica* (E) and LAD *A. pyramidale* (E)	16.40	642C-24H-5, 70–71	199.10	C5C-N1	upper NN4
	LAD *N. quadratum* (S)	19.08	642D-6X-3, 66–67	232.16	lower C5E-N	around NN2/3
	FAD *H. adriaticum* (E)	19.21	642D-6X-4, 66–67	233.66	C5E-R	uppermost NN2
	FAD *N. nav. navicula* (S)	21.12	642D-9X-4, 70–71	262.70	C6A-N1	NN2
	FAD *F. folia* (A) and FAD *N. iberica* (S)	21.32	642D-10X-2, 70–71	269.30	C6A-R1	NN2
	FAD *N. lata* (S)	—	not observed in Hole 642D			

published data), the interval down to Sample 104-642D-llX-1, 55–56 cm can be placed entirely into the lower Miocene.

Ebridians and Actiniscidians

Lithologic Unit 1, from 0 to 59.7 mbsf, is barren of ebridians and actiniscidians. This is true also for the uppermost part of lithologic Unit 2, which occurs between 59.7 and 156.6 mbsf. But commencing with Sample 104-642C-9H-1, 64–65 cm (61.34 mbsf), impoverished assemblages of ebridians and actiniscidians are recorded from the lower part of Unit 2. As the assemblages between Samples 104-642C-9H-1, 64–65 cm and 104-642C-12H-6, 65–66 cm (61.34–90.65 mbsf), contain *Ammodochium serotinum* and *Ebriopsis cornuta*, this interval is assigned to the lower to upper Pliocene *Ebriopsis cornuta* Zone (Table 2). Besides the species cited, *Falsebria arborea* and *Pseudammodochium robustum* are characteristic members. Of some interest also is the single occurrence of *Ditripodium japonicum*, because this taxon was first described from the upper Miocene of Japan (Deflandre, 1951). The interval between Samples 104-642C-13H-1, 66- 67 cm, and 104-642C-17H-4, 15–16 cm (92.66–134.65 mbsf), is determined by *Parathranium bispinum*, *P. clathratum* and *Thranium crassipes*, and placed in the predominantly upper Miocene *Parathranium clathratum* Zone. At the base *Actiniscus tetrasterias* has its distinct last occurrence. But most conspicous are the high frequencies of *A. serotinum* which range from abundant to dominant toward the top of the zone. The lower part of lithologic Unit 2 belongs to the middle to upper Miocene *Hermesinella schulzii* Zone which is developed in total between Samples 104-642C-17H-5, 50–51 cm and 104-642C-21H-5, 60–61 cm (136.50–174.60 mbsf). This zone contains a great variety of ebridian and actiniscidian species, among which *Hermesinella conata*, *H. schulzii* and *Actiniscus tetrasterias* are most characteristic. High frequencies are provided again by *A. serotinum*. Within this zone the last occurrences of *Hermesinum adriaticum* and *H. obliquum*, and the first continuous occurrence of *Actiniscus tetrasterias* are found. As indicated above, the disappearance of both the *Hermesinum* species must be explained ecologically.

The *Hermesinella schulzii* Zone continues into the upper part of lithologic Unit 3, which is present from 156.5 to 277.6 mbsf. But below this zone, between Samples 104-642C-21H-6, 60–61 cm and 104- 642C-24H-5, 70–71 cm (176.10–199.10 mbsf), the lower to middle Miocene *Spongebria miocenica* Zone is discriminated, based on the total range of its nominate species. Diagnostic other taxa are *Ditripodium latum*, *Haplohermesinum hovassei*, and *Spongebria curta*. Besides *A. serotinum* falsebrioid and actiniscoid skeletons are most common. Toward the top of the zone *Foliactiniscus atlanticus* disappears after being consistently present in older strata. At the lower boundary the first appearances of *Thranium crassipes* and *Ammodochium serotinum* provide important events. The interval from Sample 104-642D-3X-1, 60–61 cm to 104-642D-6X-4, 66–67 cm (200.20–233.66 mbsf), is placed in the lower Miocene *Hermesinum adriaticum* Zone which is determined also by *Ammodochium pyramidale*, *Parathranium bispinum* and *Foliactiniscus atlanticus*. The range of *Paranthranium curvipes* in the lower part of the zone is notable. Between Samples 104-642D-6X-5, 66–67 cm and 104-642D-10X-2, 70–71 cm (235.16–269.30 mbsf), the lower Miocene *Foliactiniscus folia* Zone is present; it contains *Ammodochium pyramidale*, *Haplohermesinum hovassei* and *Foliactiniscus atlanticus* besides other taxa. As in the over- and underlying zones, small numbers of thick *Falsebria ambigua* skeletons may indicate that minor reworking occurred during the deposition of the lower Miocene. The lowermost part of the section, between Samples 104-642D-l0X-3, 70–71 cm and 104-642D-11X-1, 55–56 cm (270.80–277.35 mbsf), belongs to the *Foliactiniscus atlanticus* Zone that exhibits the nominate species as rather common. Diagnostically important are the sporadic but distinct occurrences of *Hermesinella primitiva* and *Parathranium curvipes*.

Site 644

Silicoflagellates

Hole 644A (66°40.7'N, 04°34.6'E, water depth 1227 m) is situated in the Vøring Basin close to the inner continental slope at the southeastern margin of the Vøring Plateau. The section cored consists of hemipelagic and pelagic sediments (0–252.8 mbsf), and can be placed in the upper Pliocene to Quaternary (Eldholm, Thiede, Taylor, et al., 1987). The sedimentary sequence was subdivided by shipboard scientists into two lithologic units and three subunits.

Lithologic Unit 1, from 0 to 230.9 mbsf (Cores 104-644A-1H to 104-644A-30H), represents an interbedded series of carbonate-poor glacial muds with calcareous but sometimes siliceous interglacial muds and oozes that range from Pliocene to Holocene in age. With the exclusion of a few samples containing strongly corroded diatoms and sponge spicules, this unit remains barren of siliceous microfossils down to Core 104-644A-9H. Commencing with Sample 104-644A-10H-2, 74–75 cm (84.94 mbsf), sparse occurrences of silicoplankton including chrysomonades, silicoflagellates, ebridians, actiniscidians, diatoms, and radiolarians may be observed. Of particular note are higher numbers of siliceous sponge spicules in Subunit 1C and scattered phytoliths throughout the section. Regarding silicoflagellates, the interval between Samples 104-644A-10H-2, 74–75 cm and 104-644A-23H-2, 55–56 cm (84.94-196.15 mbsf) can be placed in the long-ranging upper Pliocene to Holocene *Distephanus speculum* Zone (Table 3). This zone is characterized by the permanent occurrence of *Distephanus speculum* s.l. f. *speculum*. Other taxa, including the warm-water representatives *Dictyocha messanensis messanensis* and *D. perlaevis*, are dispersely distributed. Although rarely found, the occurrences of *D. speculum octonarius* and *Mesocena quadrangula* are most important for stratigraphic reasons, because both species are used to define biostratigraphic units in some regions. In the present case the more distinct range of *M. quadrangula* is selected to circumscribe the *Mesocena quadrangula* Subzone between Samples 104- 644A-10H-3, 74–75 cm and 104-644A-12H-5, 66–67 cm (86.44–108.35 mbsf). From Sample 104-644A-23H-3, 55–56 cm to 104-644A-30H-1, 57- 58 cm (197.65–226.67 mbsf), an unzoned interval is designated due to the very scarce occurrence of silicoflagellates. The lowermost Sample 104-644A-30H-2, 56–57 cm (228.16 mbsf), of Unit 1 belongs to the underlying *Distephanus aculeatus* Zone.

Lithologic Unit 2, between 230.7 and 252.8 mbsf (Cores 104-644A- 30H to 104-644A-34H), comprises siliceous and siliceous-calcareous oozes that are of late Pliocene age. The silicoflagellate assemblages are dominated by *Distephanus aculeatus* and *D. speculum* s.l., and can be assigned to the lower to upper Pliocene *Distephanus aculeatus* Zone. In *D. speculum* s.l. the high number of coronoid specimens is remarkable.

Ebridians and Actiniscidians

The upper part of lithologic Unit 1 down to Core 104-644A-9H, between 0 and 230.9 mbsf, is barren of ebridians and actiniscidians. Commencing with Sample 104-644A-10H-2, 74–75 cm (84.94 mbsf), some actiniscidians and allochthonous ebridians are observed (Table 3). As *Actiniscus pentasterias* is found among predominantly juvenile or weakly silicified skeletons, the upper Pliocene to Holocene *Actiniscus pentasterias* Zone can be determined between Samples 104-644A-10H-2, 74–75 cm and 104-644A-17H-2, 66–67 cm (84.94–151.36 mbsf). Due to the undiagnostic habitus of *Actiniscus* skeletons, below this an unzoned interval is distinguished from Sample 104-644A-17H-3, 66–67 cm to 104-644A-20H-5, 66–67 cm (152.86–184.36 mbsf). Although rarely found, the occurrence of *Ammodochium serotinum* enables the identification of the upper Pliocene *Ammodochium serotinum* Zone between Samples 104-644A-21H-1, 66–67 cm and 104-644A-23H-2, 55–56 cm (185.46–196.15 mbsf). An unzoned interval follows from Sample 104-644A-23H-3, 55–56 cm, to 104-644A-30H-1, 57–58 cm (197.65-226.67 mbsf). The lowermost Sample 104-644A-30H-2, 56–57 cm (228.16 mbsf), of Unit 1 is placed in the *Ebriopsis cornuta* Zone which continues in lithologic Unit 2 down to the terminal depth of the hole.

Lithologic Unit 2, between 230.7 and 252.8 mbsf, is assigned to the lower to upper Pliocene *Ebriopsis cornuta* Zone. This zone is characterized by various ebridian and actiniscidian taxa, among which *Actiniscus* sp. and *Falsebria* cf. *arborea* are most common. Special interest surrounds *Pseudammodochium robustum* because it is found also in the upper Pliocene of Hole 642C.

PLANKTON HISTORY

Silicoflagellate Evolution

Early Miocene to Late Pliocene Developments at Site 642

Plankton data derived from long sedimentary sequences provide both information on the history of the plankton itself and on the oceanic region concerned. Therefore, the present investigations may contribute to some of the topics designated for Leg 104 (see Chapter 1, this volume and Eldholm, Thiede, Taylor, et al., 1987), especially the discussions on Neogene to Quaternary developments in plankton assemblages and related paleoenvironmental changes on the Vøring Plateau.

From the spectrum of biocoenotic terms (Schwerdtfeger, 1975) the parameters of assemblage abundance, species abundance, and species diversity are selected to describe developments in Neogene to Quaternary plankton assemblages of the Vøring Plateau. According to Table 1, silicoflagellate abundances at Site 642 were usually high from the early Miocene to early Pliocene, i.e., from 21.5 to 5.0 Ma (*N. lata* Zone to lower *D. aculeatus* Zone: Sample 104-642D-10X-6, 70–71 cm to 104-642C-12H-5, 65–66 cm), with the exclusion of a hiatus from about 13.4 to about 10.2 Ma (above Sample 104-642C-19H-5, 50–51 cm) and some minor intervals having values below 100. After about 10.2 Ma, frequencies distinctly dropped in the early Pliocene at 4.8 Ma, and in the late Pliocene at about 3.2 Ma (*D. aculeatus* Zone: Samples 104-642C-12H-2, 70–71 cm, and 104-642C-10H-2, 71–72 cm, to 104-642C-10H-1, 64–65 cm), which was followed by the disappearance of all silicoflagellates at about 3.1 Ma (above Sample 104-642C-9H-1, 64–65 cm) far before the Matuyama/Gauss reversal. The noted abundance depressions probably correspond to cooling phases of sea-surface waters, which are explained below.

As shown in Table 1, species diversities attained an average value of 12 during the early Miocene until 19.2 Ma (*N. lata* Zone to uppermost *N. navicula* Zone: Sample 104-642D-10X-6, 70–71 cm to 104- 642D-6X-4, 66–67 cm). During the late early Miocene, from 18.7 to 16.6 Ma, diversities were depressed to values around 8 (Lower *C. triacantha* Zone: Sample 104-642D-6X-2, 66–67 cm to 104-642D-3X-2, 60–61 cm), but before the middle middle Miocene at about 13.4 Ma higher values around 10 were reached once more (upper Lower *C. triacantha* Zone to upper Upper *C. triacantha* Zone: Sample 104-642C-24H-5, 70–71 cm to 104-642C-19H-5, 50–51 cm). From the late Miocene to late Pliocene, silicoflagellate diversities were distinctly lower and around 6 (*P. circulus apiculata* Zone to *D. aculeatus* Zone: Sample 104-642C-19H-2, 50–51 cm to 104-642C-9H-1, 64–65 cm). The indicated diversity depressions obviously reflect periods with lower sea-surface temperatures, as discussed below.

Species abundances are shown in Figure 5, which summarizes single species data in genera groups for better recognition. The data were prepared in the following manner: According to

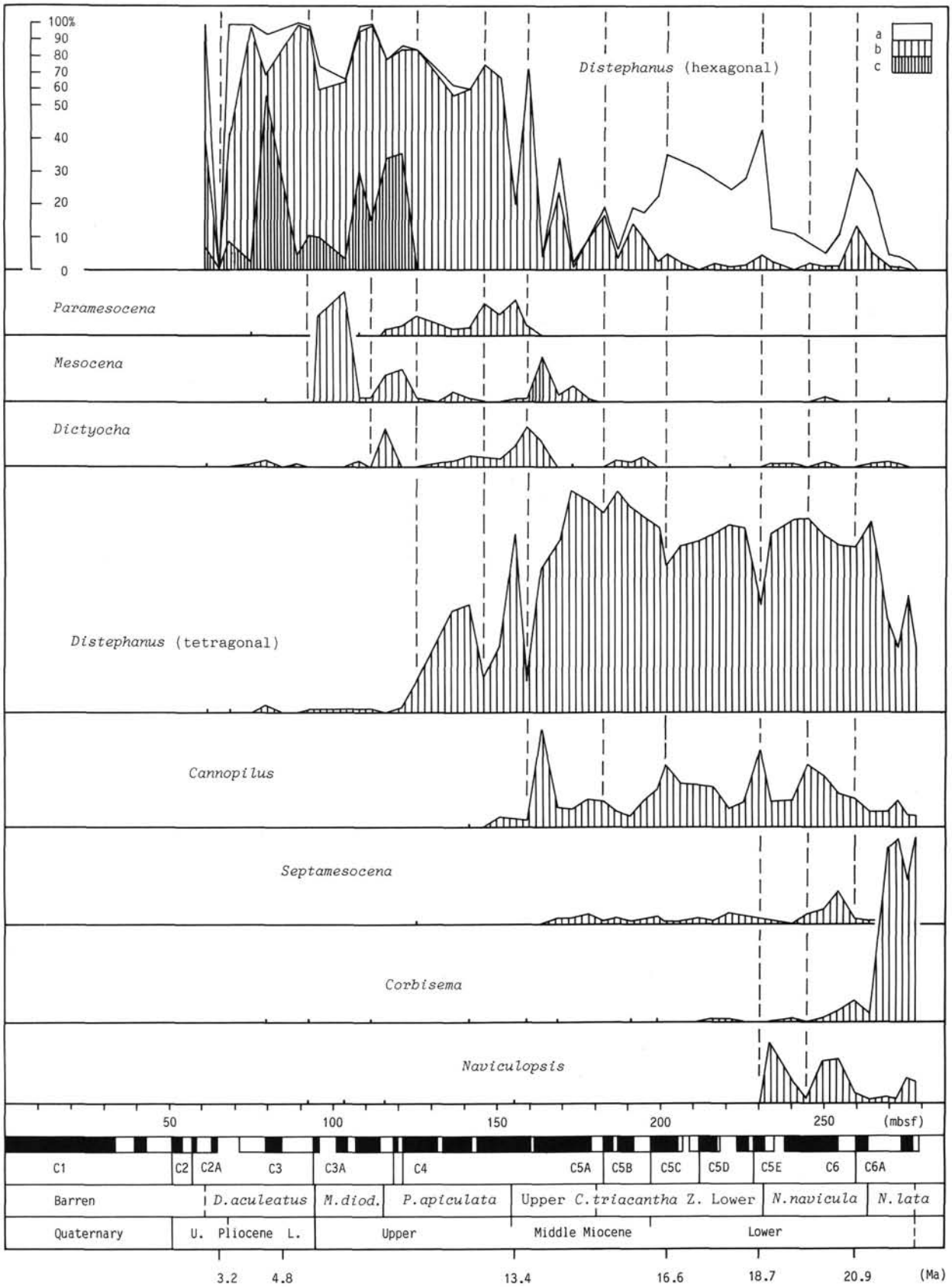

Figure 5. Site 642. Fluctuation of silicoflagellate abundances from the early Miocene to late Pliocene. Cooling phases (dashed lines) are deduced from relations between cool- and warm-water-preferring taxa (designation of preferences: see text). Ages are calculated from paleomagnetics (Bleil, this volume). Variant groups of *Distephanus speculum* refer to cannopiloid (a), normal distephanoid (b), and coronoid members (c).

the phylogenetic concept of Locker and Martini (1986a), all species with an apical apparatus were placed in the genera *Corbisema* (trigonal with apical bar), *Dictyocha* (tetragonal with apical bar), *Distephanus* (penta- to polygonal with apical ring) and *Cannopilus* (penta- to polygonal with apical windows). Infraspecific taxa with mutated features were referred to their normal relatives. From this grouping only *Distephanus crux* (tetragonal with apical ring) was excluded, as its symmetry is close to the ancestral genus *Dictyocha*. Species with a reduced apical apparatus were assigned to the genera *Septamesocena* (derived from *Corbisema*), *Naviculopsis* and *Mesocena* (both derived from *Dictyocha*), and *Paramesocena* (derived from *Distephanus*).

The data prepared for Figure 5 indicate that species abundances fluctuated during the Neogene. This was obviously in response to temperature changes in sea-surface waters, because the antagonistic ecologies of Holocene *Dictyocha* species/subspecies (warm-adapted) and *Distephanus* species/subspecies (cool-adapted) (Yanagisawa, 1943; Poelchau, 1976) are reflected also by their fossil members and other taxa. Referred to corresponding peaks in *Distephanus* and *Cannopilus* and related depressions in warm to warm-temperate species, more than 10 cooling phases of different intensity developed during the Neogene at Site 642. The cooling phases effected significant changes both in species abundances and assemblage structure: At 21.2 Ma in early Miocene time frequencies of *Corbisema triacantha* were drastically reduced by an increase of hexagonal *Distephanus* specimens, which was in response to a temperature decline (uppermost *N. lata* Zone: Sample 104-642D-9X-5, 70–71 cm). During a cooling phase around 19.0 Ma the genus *Naviculopsis* disappeared (top event of *N. navicula* Zone: above Sample 104-642D-6X-3, 66–67 cm). Above about 13.4 Ma abundances of tetragonal *Distephanus* taxa decreased parallel to an increase of hexagonal *Distephanus* specimens (*P. circulus apiculata* Zone: above Sample 104-642C-19H-5, 50–51 cm), which reflects a proceeding cooling of sea-surface waters toward the end of the Miocene. However, during the latest Miocene from 5.5 to 5.4 Ma a prominent warming phase marked by high *Mesocena* abundances interrupted the general cooling trend (*M. diodon* Zone: Samples 104-642C-14H-2, 66–67 cm and 104-642C-13H-3, 30–31 cm). After this interval only hexagonal *Distephanus* taxa persisted in high frequency until the early Gauss Epoch, indicating that a low temperature level was reached.

To describe the general course of sea-surface temperatures in high northern latitudes during Neogene time, the data included in Figure 5 were transformed to a paleotemperature curve. As a basis the formula of Kanaya and Koizumi (1966) was used and modified to $T_s = 100\,X_w/(X_w + X_c)$. In this formula X_w and X_c represent frequencies of warm and cool adapted species, and T_s the resulting relative paleotemperature value for silicoflagellates. According to their behavior in Figure 5 and known paleobiogeographic data, species groups were treated as follows: *Distephanus* (hexagonal) and *Cannopilus* were regarded as cool-adapted, *Paramesocena* as cool-temperate, *Distephanus* (tetragonal), *Mesocena* and *Naviculopsis* as warm-temperate, and *Corbisema*, *Dictyocha*, and *Septamesocena* as warm-adapted. This is in contrast to some other investigations (Ciesielski, 1975; Busen and Wise, 1977; Bukry, 1981b, 1985b), where frequencies of *Naviculopsis* and/or Mesocenoid taxa are otherwise distributed over the parameters X_w and X_c.

Resulting Figure 6 demonstrates that relative sea-surface temperatures turned out to be high during the early to middle Miocene from 21.5 to about 13.4 Ma (*N. lata* to Upper *C. triacantha* Zone: Sample 104-642D-10X-6, 70–71 cm to 104-642C-19H-5, 50–51 cm). However, at 18.7 and 16.6 Ma distinct temperature depressions developed (Lower *C. triacantha* Zone: Samples 104-642D-6X-2, 66–67 cm and 104-642D-3X-2, 60–61 cm), and at about 14.2 Ma a temperature high was reached (Upper *C. triacantha* Zone: Sample 104-642C-21H-4, 60–61 cm). During the late Miocene, temperatures permanently declined until a brief warming phase around 5.45 Ma (*M. diodon* Zone: Samples 104-642C-14H-2, 66–67 cm, and 104-642C-13H-3, 30–31 cm). After 5.4 Ma relative temperatures were generally at a very low level.

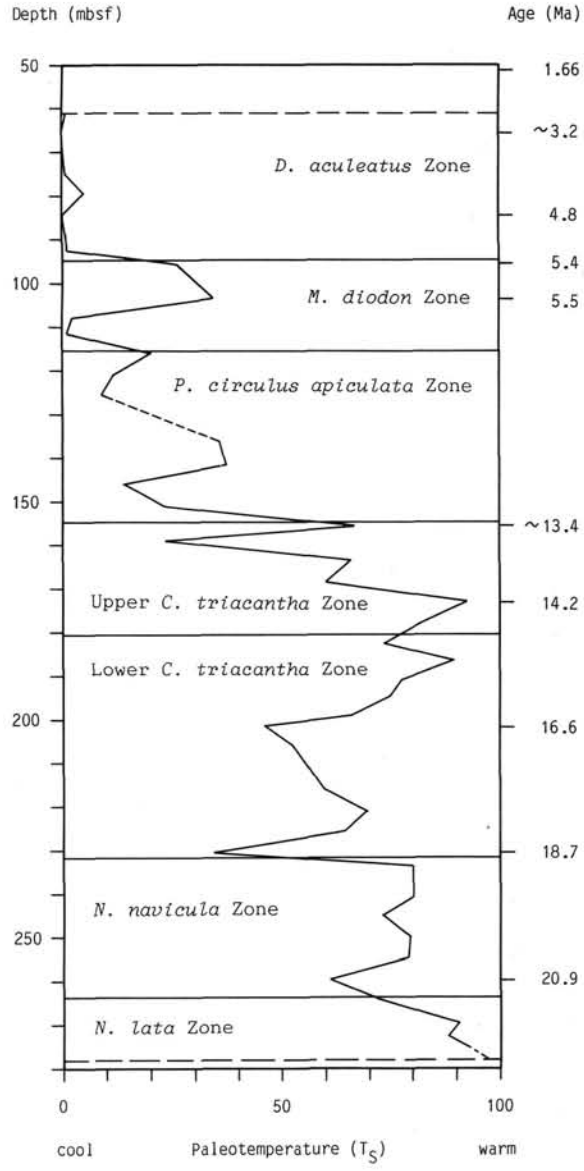

Figure 6. Paleotemperature trend during the early Miocene to late Pliocene time interval, based on warm-and cool-water-preferring silicoflagellate taxa at Site 642 (designation of preferences: see text). Ages are calculated from paleomagnetics (Bleil, this volume).

Late Pliocene to Pleistocene Developments at Site 644

According to Table 3, silicoflagellate abundances at Site 644 were high only at 2.8 Ma (*D. aculeatus* Zone: Sample 104-644A-34H-5, 66–67 cm). Above that time level, abundances were moderate, but dropped once more at 2.57 Ma (*D. aculeatus* Zone: Sample 104-644A-31H-2, 66–67 cm). From about 2.5 to 2.1 Ma (unzoned interval: Sample 104-644A-30H-1, 57–58 cm to 104-644A-23H-3, 55–56 cm) silicoflagellates disappeared, indicating that life or preservational conditions were unfavorable. However, above the 0.4- m.y barren interval, silicoflagellates re-

appeared temporarily and in very low frequencies. After 0.74 Ma (above Sample 104-644A-10H-2, 74–75 cm) silicoflagellates disappeared also at Site 644.

As shown in Table 3, species diversities of 2 and 3 were usually attained during the late Pliocene until 2.5 Ma (upper *D. aculeatus* Zone: Sample 104-644A-34H-5, 66–67 cm, to 104-644A-30H-2, 56–57 cm). In Pleistocene time only one or two species/subspecies were present at Site 644, but around 0.9 Ma three *M. quadrangula* Subzone: Samples 104-644A-12H-4, 66–67 cm, and 104-644A-11H-6, 66–67 cm).

Although species abundances were very low during the latest Pliocene and Pleistocene, silicoflagellates provide some important oceanographic data. As shown in Figure 7, repeated appearances of *Dictyocha messanensis*, *D. perlaevis*, and *Mesocena quadrangula* indicate that, until the middle Pleistocene, warm-temperate surface-waters reached the area of Site 644 several times. The incursions proceeded at 2.0 and 1.9 Ma, from 1.5 to 1.3 Ma, and from 0.95 to 0.88 Ma (all *D. speculum* Zone: Sample 104-644A-23H-2, 55–56 cm to 104-644A-20H-4, 66–67 cm, Sample 104-644A-17H-4, 66–67 cm to 104-644A-15H-5, 66–67 cm, and 104-644A-12H-5, 66–67 cm to 104-644A-11H-6, 66–67 cm). The last *Mesocena* ingression was at 0.76 Ma (top of *M. quadrangula* Subzone: Sample 104-644A-10H-3, 74–75 cm).

Ebridian and Actiniscidian Evolution

Early Miocene to Late Pliocene Developments at Site 642

Developments in ebridians and actiniscidians may also be described by variations in assemblage abundance, species abundance, and species diversity. According to Table 2, ebridian-actiniscidian abundances at Site 642 were generally high from the early Miocene to early Pliocene, i.e. from 21.7 to 5.0 Ma (*F. atlanticus* Zone to lower *E. cornuta* Zone: Sample 104-642D-11X-1, 55–56 cm to 104-642C-12H-5, 65–66 cm), the hiatus between about 13.4 and about 10.2 Ma excluded (within the *H. schulzii* Zone: above Sample 104-642C-19H-5, 50–51 cm). During the early and late Pliocene, ebridian-actiniscidian abundances followed the trend in silicoflagellates, including the lows and the disappearance at about 3.1 Ma.

As shown in Table 2, species diversities of ebridians were usually high from the early Miocene to early late Miocene (*F. atlanticus* Zone to upper *H. schulzii* Zone: Sample 104-642D-10X-6, 70–71 cm to 104-642C-19H-2, 50–51 cm), reaching maximum values between 13 and 15. After that time, diversities decreased to an average value of six. Species diversities of actiniscidians were strikingly low during the whole Neogene, attaining values between one and five.

Species abundances are shown in Figure 8, which summarizes species data as follows: According to their phylogenetic relationship (Deflandre, 1951), all species with a triode were grouped in the genera *Ammodochium* (having proclades, opisthoclades, and both syncladian rings), *Pseudammodochium* (with a globular skeleton) and *Ditripodium* + *Parathranium* + *Thranium* (having proclades, opisthoclades, and an upper syncladian ring but a reduced lower one). Species with a triaene were placed in the groups *Hermesinella* + *Hermesinum* (having proclades, a syncladian ring and an opisthocladian basket), *Ebriopsis* + *Haplohermesinum* (with one actinian triplet flattened), and in the genera *Podamphora* (with large skeletons similar to *Hermesinella*), *Falsebria* (consisting only of triaenes) and *Spongebria* (with reduced triaenes). Actiniscidian species were allotted to the genera *Actiniscus* (with a central depression) and *Foliactiniscus* (with central crests).

The data presented in Figure 8 indicate that species abundances fluctuated during the Neogene. As Holocene *Actiniscus* species advance well into subpolar regions (Tappan, 1980), related peaks apparently explain periods of cooler sea-surface waters. This is confirmed in some intervals by the cool peaks of silicoflagellates which were transferred from Figure 5 to the diagram for better comparison. Referred to the peaks of *Actiniscus* and *Cannopilus* + *Distephanus* (hexagonal) species, the groups *Ditripodium* + *Parathranium* + *Thranium* and *Hermesinella* + *Hermesinum* may be interpreted as cool-temperate adapted, whereas most other species seem to reflect warm or warm- temperate preferences. This is especially true for the common taxa *Ammodochium*, *Falsebria*, and *Foliactiniscus*, the last of which implies a remarkable ecological antagonism to *Actiniscus*. Comparable to silicoflagellates, the cooling phases induced significant changes in species abundances and assemblage structure: At about 16.6 Ma during a prominent cooling phase *Foliactiniscus* taxa distinctly decreased in frequency (uppermost *H. adriaticum* Zone: Sample 104-642D-3X-2, 60–61 cm). During the late Miocene and early Pliocene around 5.8 and 5.3 Ma (*P. clathratum* Zone: Samples 104-642C-15H-1, 66–67 cm, and 104-642C-13H-1, 66–67 cm) species of *Parathranium* developed excessively, thus confirming the cool phases of silicoflagellates. The abundance peaks of *Pseudammodochium* after the 4.8-Ma temperature depression certainly were caused by warming phases. However, in summary there is a trend that the main cool peaks of ebridian and actiniscidian species often appear delayed with respect to cool peaks of silicoflagellates, a phenomenon that remains unexplained at present.

Late Pliocene to Pleistocene Developments at Site 644

According to Table 3, ebridian and actiniscidian abundances were rather high during the late Pliocene until 2.5 Ma, with the exception of a sharp drop at 2.57 Ma (*E. cornuta* Zone: Sample 104-644A-34H-5, 66–67 cm to 104-644A-31H-3, 66–67 cm, drop-in Sample 104-644A-30H-2, 56–57 cm). But in latest Pliocene and Pleistocene times abundances were drastically lowered. At about 1.9 Ma (above Sample 104-644A-21H-1, 66–67 cm) ebridians disappeared, and at 0.74 Ma (above Sample 104-644A-10H-2, 74–75 cm) actiniscidians did also.

As shown in Table 3, until the Matuyama/Gauss reversal at about 2.5 Ma, ebridian and actiniscidian diversities were similar to those at Site 642. However, subsequently only three taxa persisted into the Pleistocene.

Summary and Comparisons

The present plankton investigations of Neogene to Quaternary sediments at Sites 642 and 644 provide data for a 20-m.y. period of paleoenvironmental history on the Vøring Plateau. Distinct changes in assemblage abundance, species abundance, and species diversity are used to describe paleoceanographic and paleoclimatologic developments.

During early and middle Miocene times, i.e., from 21.7 to about 13.4 Ma, silicoflagellate, ebridian, and actiniscidian abundances were usually high at Site 642 (Tables 1, 2), indicating that open ocean conditions with increased productivity prevailed for more than 8 m.y. over the central part of the Vøring Plateau. The high nutrient and silica concentrations necessary for extensive plankton growth may have been supplied by intensified weathering on nearby land-masses and high river input under warm-humid climates (Henrich et al., this volume). High diversities of silicoflagellate and ebridian species (Tables 1, 2) and abundance relations between warm and cool adapted silicoflagellate taxa (Fig. 6) confirm in general the high temperature level assumed. Silicoflagellate species abundances (Fig. 5) and relations between temperature-sensitive silicoflagellate taxa (Fig. 6) demonstrate, however, that sea-surface temperatures fluctuated in a large scale, including more than 10 distinct cooling phases. Two of the most prominent cooling phases were at 18.7 and 16.6 Ma, just at the beginning and at the end of a longer but weak cooling period during the early Miocene that is indicated

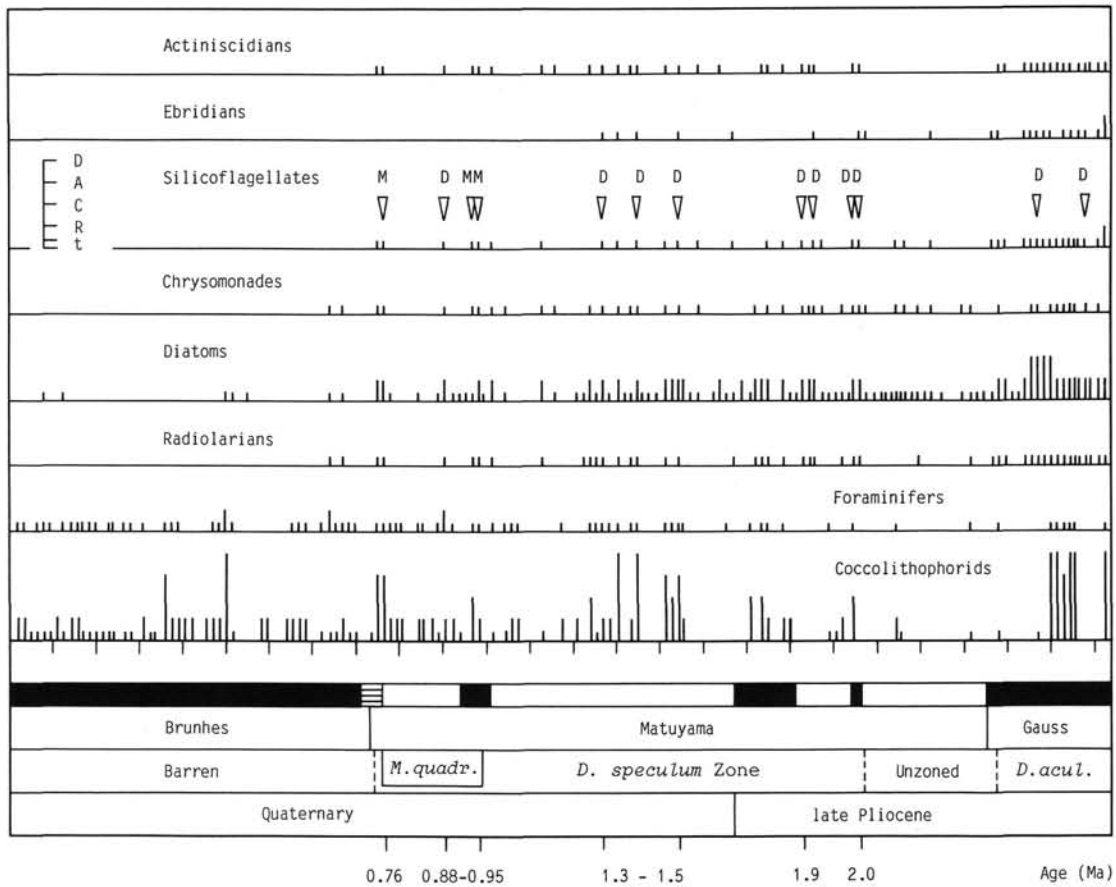

Figure 7. Site 644. Fluctuation of siliceous and calcareous plankton from the late Pliocene to Holocene. Frequencies derived from smear-slide estimates include t = traces, <1% of coverage; R = rare <5%; C = common <25%; A = abundant <50%; D = dominant >50%. Warm- to temperate-indicating taxa are marked by D = *Dictyocha perlaevis* and *D. messanensis*, and M = *Mesocena quadrangula*. Ages are calculated from paleomagnetics (Bleil, this volume).

also by lower silicoflagellate diversities (Table 1). After that period temperatures rose again and reached a maximum at about 14.2 Ma.

Siliceous plankton assemblages associated with the cooling phases underwent important changes: Within the cooling phase around 21 Ma, frequencies of *Corbisema* species decreased abruptly. During the prominent temperature depression at about 19 Ma all species of *Naviculopsis* disappeared at Site 642. At 16.6 Ma abundances of *Foliactiniscus* species dropped with the end of the cooling period between 18.7 and 16.6 Ma. However, several first appearance events (*Spongebria miocenica, Ammodochium serotinum, Mesocena diodon*, and *Paramesocena circulus apiculata*) indicate that the evolutionary potential of siliceous flagellates was high until about 13.4 Ma.

During late Miocene to late Pliocene times, i.e., from about 10.2 to about 3.1 Ma (above the hiatus assumed between about 13.4 and 10.2 Ma), silicoflagellate and ebridian abundances were high (if partial enrichment of siliceous particles by chemical processing of the samples is neglected). But in contrast to the period prior the hiatus, plankton productivity was probably controlled by different effects of the Norwegian Current or its precursor that was first established in middle Miocene time (Henrich et al., this volume). Abundance variations of silicoflagellate taxa (Fig. 5) demonstrate that sea-surface temperatures fluctuated during the late Miocene. Relations between different silicoflagellate taxa (Fig. 6) indicate, however, that these fluctuations followed a general cooling trend toward the Pliocene, which is underlined also by lower silicoflagellate and ebridian diversities (Tables 1, 2). Evidenced by high *Mesocena* densities, the permanent cooling trend was interrupted by a short warming phase around 5.45 Ma (Figs. 5, 6). After that episode the temperature decline continued until all siliceous flagellates disappeared around 3.1 Ma at Site 642. Two sharp drops in silicoflagellate and ebridian abundances at 4.8 and about 3.2 Ma (Tables 1, 2; Fig. 6) may be related to cooling phases during which dissolution of siliceous skeletons prevailed over production or during which production may have totally ceased.

Important changes in siliceous plankton assemblages are associated with the late Miocene temperature decline. The frequencies of hexagonal *Distephanus* specimens permanently increased while tetragonal specimens gradually disappeared. The most conspicuous phenomena are the nearly exclusive disappearances in silicoflagellate and ebridian species from the late Miocene to late Pliocene (*Hermesinum adriaticum, H. obliquum, Hermesinella schulzii, Paramesocena circulus apiculata, Mesocena diodon, Thranium crassipes, Parathranium clathratum, P. bispinum, Distephanus aculeatus, Ebriopsis cornuta* and *Ammodochium serotinum*). These disappearances obviously parallel the permanent deterioration of paleoenvironmental conditions.

While siliceous flagellates disappeared at Site 642 around 3.1 Ma, they persisted in low density at Site 644 until 2.5 Ma (Table 3, Fig. 7), which may be due to better preservational conditions under higher accumulation rates at this near-shore site. A strong reduction in silicoflagellate and ebridian-actiniscidian abundances is recognized at 2.57 Ma, which can be related to the first major

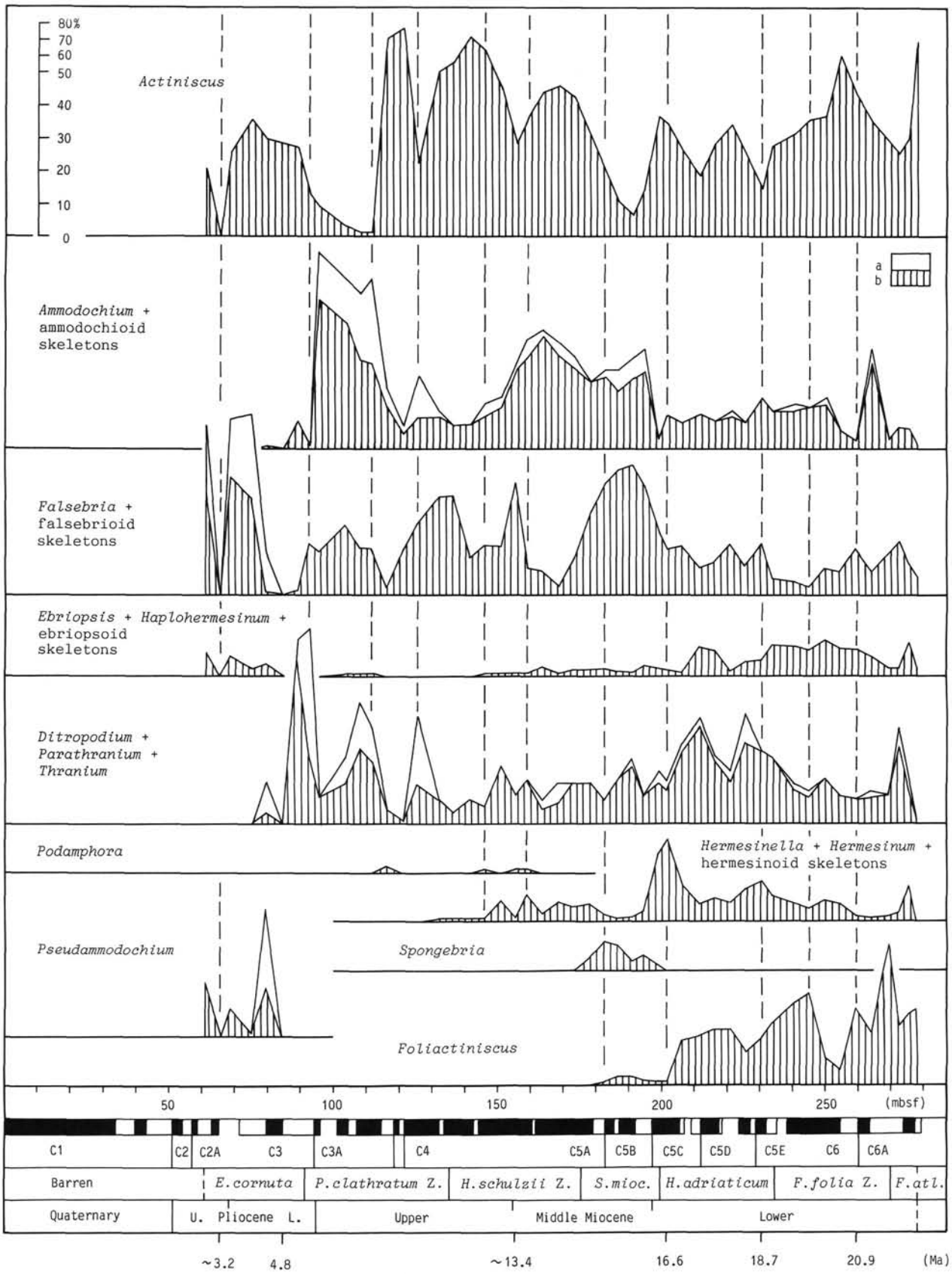

Figure 8. Site 642. Fluctuation of ebridian and actiniscidian abundances from the early Miocene to late Pliocene. Cooling phases (dashed lines) are transferred from Fig. 5. Ages are calculated from paleomagnetics (Bleil, this volume). Letters refer to normal skeletons (a) and double skeletons (b).

expansion of the Scandinavian ice sheet (Henrich, this volume; Jansen et al., this volume). The glaciation surely caused a decrease of plankton production and an increase of opal dissolution in highly oxygenated deep waters. After 2.5 Ma, siliceous flagellates disappeared for about 0.4 m.y. at Site 644, but reappeared in diminished number to persist until different time levels. Distinct occurrences of *Dictyocha messanensis, D. perlaevis*, and *Mesocena quadrangula* indicate that during this last period of existence, warm-temperate surface waters from the northern Atlantic entered the Vøring Plateau region several times. The ingressions were at 2.0 and 1.9 Ma, from 1.5 to 1.3 Ma, and from 0.95 to 0.88 Ma. The last *Mesocena* incursion proceeded at 0.76 Ma. Prior this date ebridians disappeared at 1.9 Ma, while silicoflagellates and actiniscidians were deposited until 0.74 Ma. The final disappearance of siliceous flagellates at Site 644 obviously was in response to the development of a predominantly glacial regime on the Vøring Plateau (Eldholm, Thiede, Taylor, et al., 1987).

The middle to late Miocene temperature decline was primarily related to sea-surface temperatures at Site 642, but may be regarded as a general expression of high northern latitude climate during the indicated time interval. This is evidenced, in particular, by oxygen isotope studies at several oceanic sites in middle to high latitudes that revealed a similar temperature trend. Thus, a middle to late Miocene cooling of sea-surface and bottom waters is shown at Site 408 in the northern Atlantic (Keigwin, et al., 1987) and at Sites 279 and 281 in the southwestern Pacific (Shackleton and Kennett, 1975). A long-term cooling of bottom waters was also described at Site 525 in the southern Atlantic (Shackleton, et al. 1984). The concurrent cooling of surface and bottom waters in both hemispheres obviously reflects the global impact of antarctic ice-sheet expansion that commenced in middle Miocene time (Kennett, 1982). The conspicuous warming phase indicated around 5.45 Ma at Site 642 seems to contradict the distinct drop of seafloor temperatures that has been recognized at many sites for latest Miocene time and related to a strong pulse of antarctic ice formation (Hodell and Kennett, 1986). But the late Miocene ice expansion obviously caused an intensification of the oceanic circulation (Kennett, 1982), which in turn may have induced a brief ingression of warm-temperate North Atlantic Current waters into the Norwegian Sea. This explanation seems to be confirmed by the divergence of latest Miocene $\delta^{18}O$ values at Site 408 southwest of Iceland (Keigwin, et al., 1987), which can be interpreted as warm surface waters of the Irminger Current having been over cooler bottom waters.

The early Pliocene abundance drop in siliceous flagellates around 4.8 Ma may be related to a glacial input, but our data are too scarce for comparison. However, the late Pliocene disappearances of silicoflagellates, ebridians, and actiniscidians around 3.2 and 3.1 Ma are distinct and can be related to phases in the build-up of the Northern Hemisphere ice cap. Evidences are summarized in Kennett (1982) and Ruddiman, Backman et al. (1987), and include oxygen isotope data, plankton events, and records of ice-rafted material. The 2.57-Ma datum found at Site 644 corresponds to the beginning of a substantial glaciation of the Northern Hemisphere, as can be proved by oxygen isotope data from Site 606 (Keigwin, 1987) and lithologic properties from Site 609 (Ruddiman, McIntyre and Raymo et al., 1987) in the central North Atlantic. Oxygen isotope data from Sites 552 (Shackleton and Hall, 1984) and 606 (Keigwin, 1987) in the northern Atlantic indicate that the disappearance of siliceous flagellates between 2.5 and 2.1 Ma was caused by a major glaciation around 2.4 Ma.

The Pleistocene warming phases recorded at Site 644 can be only roughly compared with events outside the investigation area, as data are sparse. It is obvious, however, that the last *Mesocena* ingression at 0.76 Ma was during oxygen isotope stage 21, according to the curve of benthic foraminifers from Site 607 in the northern Atlantic (Ruddiman, McIntyre, and Raymo, 1987). The presence of *Dictyocha perlaevis* and *Mesocena quadrangula* generally indicates that during certain intervals of the Pleistocene an enhanced meridional transport of warm-temperate surface-waters existed. This is evidenced by rather strong relations to mid-Pleistocene silicoflagellate assemblages at Sites 412 (Bukry, 1979) and 606, 607, and 609 (Bukry, 1987a) in the central Atlantic, which also contain these species.

TAXONOMY

The taxonomy of silicoflagellates follows the concept outlined in Locker and Martini (1986a). Accordingly, species are treated as genetic entities or units that may comprise different phenetic subunits. These subunits are distinguished on the interpopulationary level as subspecies and on the intrapopulationary level as forms. To avoid a bulk of new names, taxonomic forms showing identical structure are given the same name in different subspecies of a species. But if members of non-type populations are present, the abbreviation nm (non-nominate morphe) is added to the form epithet without an author. From this principle only autonyms are excluded, according to the rules of the International Code of Botanical Nomenclature (ICBN).

The taxonomy of ebridians and actiniscidians does not require discussion. Both groups are treated as endosiliceous dinoflagellates (Locker and Martini, 1986b), although differences in skeletal structure are apparent.

Within the higher systematic groups all genera, species, and infraspecific taxa are described in alphabetical order. To summarize infraspecific relations, the synonymy of forms is directly attached to the species and subspecies synonymies. In general, only basionyms, different species epithets, and generic emendations are indicated. Further synonymies may be derived from Loeblich III et al. (1968) for previously described silicoflagellate and ebridian taxa, and from Locker (1974) and Locker and Martini (1986a)[4] for the silicoflagellate taxa of Ehrenberg. These publications contain also full references to the older synonymies labelled below.

Class CHRYSOPHYCEAE
Order SILICOFLAGELLATA Borgert, 1891
Genus *Cannopilus* Haeckel, 1887

Remarks: All permanently multifenestrate species are included in the genus *Cannopilus*. No generic decision is made between members with hemisphaeric or sphaeric apical apparatus (*Cannopilus* versus *Caryocha* in Bukry and Monechi, 1985) or with single or double lateral bars (*Cannopilus* vs. *Paracannopilus* in Dumitrică, 1978), as the type species *C. hemisphaericus* is considered to be the basal taxon of this monophyletic group.

[4] In recent literature, the silicoflagellate and ebridian index of Loeblich III et al. (1968) is often used as a source to determine the validity of taxa. But this overestimates the possibilities of the index. The index can indicate only the status of names, not that of taxa. With respect to names, only the legitimacy (according to article 6.3, ICBN) not the correctness (according to articles 6.5, 11.2, and 11.3) can be stated. And the status of early designated taxa can be determined, in general, only by investigating the original material, i.e., the type material in a strongest sense (holo- or lectotypes). Therefore, some of the taxonomic decisions given in Loeblich III et al. need reconsideration. In the case of the silicoflagellate species described by Ehrenberg during the 19th century a short revision was published by Locker (1974). The type fixations traced along the IRZN and ICBN (see explanations in Locker and Martini, 1986a) can be used as a base for further taxonomic procedures, such as emendations or new combinations. In this context it should be noted that the incorrect typifications of *Cannopilus* (see Locker, 1974, p. 638; Locker and Martini, 1986a, p. 901) and *Mesocena* (see Locker, 1974, p. 634; Locker and Martini, 1986a, pp. 907–908) given in Loeblich III et al. have been corrected.

Cannopilus depressus (Ehrenberg) Locker
(Plate 1, Figs. 1, 2)

Halicalyptra depressa Ehrenberg, 1854, Pl. 18, Fig. 111.
Cannopilus sphaericus Gemeinhardt, 1931, p. 105, Pl. 10, Figs. 3, 4.
Dictyocha sphaerica (Gemeinhardt), Deflandre, 1936, pp. 35–37.
Cannopilus depressus (Ehrenberg), Locker, 1974, p. 639, Pl. 4, Fig. 3.
Caryocha depressa (Ehrenberg), Bukry and Monechi, 1985, p. 378.
Cannopilus ernestinae Bachmann (Plate 1, Fig. 6).
Cannopilus ernestinae Bachmann, 1962, p. 255, Fig. 1.
Caryocha ernestinae (Bachmann), Bukry and Monechi, 1985, p. 378.

Cannopilus hemisphaericus (Ehrenberg) Haeckel
(Plate 1, Figs. 7, 8)

Dictyocha hemisphaerica Ehrenberg, 1845, pp. 266–267.
Cannopilus hemisphaericus (Ehrenberg), Haeckel, 1887, p. 1569.
Distephanus speculum subsp. *hemisphaericus* (Ehrenberg), Bukry, 1975a, p. 855, Pl. 4, Fig. 8.
Cannopilus hemisphaericus (Ehrenberg) f. *hemisphaericus*: Form represents an autonym of the species epithet.

Remarks: *Cannopilus hemisphaericus* is a polymorphic species. Variants with six radial spines are distinguished as f. *hemisphaericus*, and variants with seven spines as f. *heptagonus*.

Cannopilus hemisphaericus f. *heptagonus* n.f.
(Plate 1, Fig. 8)

Holotype: SM.B 13762; Pl. 1, Fig. 8.
Type locality: Vøring Plateau, Sample 104-642D-6X-2, 66–67 cm (lower Miocene).

Diagnosis: Basal ring heptagonal, with seven radial spines, and basal pikes at the lateral rods. Apical apparatus semiglobular, and furnished with several windows. Diameter of basal ring 35.5–43.0 μm.

Remarks: This new form is distinguished from similar taxa in other species by its large size, and the arrangement of apical windows. In *Distephanus speculum* similar forms are smaller, and in *Distephanus aculeatus* the apical windows do not fill the whole basal ring.

Occurrence: Rather continuously found from Sample 104-642C-24H-5, 70–71 cm to 104-642D-6X-2, 66–67 cm (Lower *C. triacantha* Zone, lower Miocene).

Cannopilus schulzii Deflandre in Bachmann and Ichikawa
(not illustrated)

Cannopilus schulzii Deflandre in Bachmann and Ichikawa, 1962, p. 171; refers to *Cannopilus cyrtoides* of Schulz, 1928, Fig. 65.

Remarks: Table 1 demonstrates that *C. schulzii* could be an eight-spined variant of *C. hemisphaericus*. But the taxon is separated here, as independent populations may exist.

Genus *Corbisema* Hanna, 1928

Remarks: In Tables 1 and 3, isolated occurrences of allochthoneous species are noted under "*C.* species diversae." The following taxa are included: *C. elata* (Glezer) (Sample 104-644A-24H-3, 66–67 cm), *C. globulata* (Bukry) (Sample 104-642C-13H-1, 66–67 cm), *C. lamellifera* (Glezer) (Samples 104-642C-18H-5, 60–61 cm; 104-642D-7X-2, 66–67 cm), and *Corbisema* sp. (remaining samples).

Corbisema flexuosa (Stradner) Perch-Nielsen
(not illustrated)

Corbisema triacantha var. *flexuosa* Stradner, 1961, p. 89, Figs. 1–8.
Corbisema flexuosa (Stradner), Perch-Nielsen, 1975a, p. 685, Pl. 3, Fig. 10.

Corbisema triacantha (Ehrenberg) Hanna
(Plate 1, Fig. 5)

Dictyocha triacantha Ehrenberg, 1845, p. 80.
Corbisema triacantha (Ehrenberg), Hanna, 1931, p. 198, Pl. D, Fig. 1.

Remarks: In *C. triacantha* smaller variants with rounded skeletons and larger variants with angular skeletons are included. In both groups the thickness of skeletal bars may vary arbitrarily.

Genus *Dictyocha* Ehrenberg, 1840

Remarks: In Table 1, species with the apical bar along the short axis (asperoid) and along the long axis of the skeleton (messanensoid) are distinguished. The terminus fibuloid in species with the bar parallel the length is rejected, as *D. fibula* has its bar along the short axis, according to the type revision (Locker, 1974; Locker and Martini, 1986a).

Isolated occurrences of asperoid species are summarized under "*D.* species diversae (asperoid)" in Table 1. The following taxa are included: *D. subclinata* Bukry (Sample 104-642D-10X-2, 70–71 cm), *Dictyocha* sp. 3 of Locker and Martini (1986a) (Samples 104-642C-19H-2, 50–51 cm; 104-642C-24H-2, 70–71 cm; 104-642D-8X-2, 66–67 cm), and *Dictyocha* sp. (remaining samples). Isolated occurrences of messanensoid species are cited under "*D.* species diversae (messanensoid)" in Table 1, and the following taxa are recognized: *D. fallacia* Busen and Wise (Sample 104-642C-17H-2, 60–61 cm), and *Dictyocha* sp. (remaining samples). In Table 3 only the category "D. species diversae" is used, the following taxa including: *D. curta* Ling (Sample 104-644A-30H-2, 56–57 cm), *D. rotundata* Jousé (Samples 104-644A-18H-6, 67–68 cm; 104-644A-31H-2, 66–67 cm), *D. transitoria* Deflandre (Sample 104-644A-23H-1, 55–56 cm), and *Dictyocha* sp. (remaining samples).

Dictyocha clinata (Bukry) nov. comb.
(not illustrated)

Dictyocha aspera subsp. *clinata* Bukry, 1975b, p. 687, Pl. 1, Figs. 1–5.

Dictyocha epiodon Ehrenberg
(not illustrated)

Dictyocha epiodon Ehrenberg, 1845, p. 79.

Remarks: *Dictyocha epiodon* has large skeletons with a short apical bar along the long axis. The species is diagnostic for the middle Miocene.

Dictyocha fallacia Busen and Wise
(not illustrated)

Dictyocha fallacia Busen and Wise, 1977, p. 713, Pl. 4, Figs. 2–6.

Remarks: Two specimens were found in Sample 104-642C-17H-2, 60–61 cm (upper Miocene).

Dictyocha fibula Ehrenberg
(Plate 1, Fig. 9)

Dictyocha fibula Ehrenberg, 1838, p. 132 (nomen nudum).
Dictyocha fibula Ehrenberg, 1840, p. 129.

Remarks: *Dictyocha fibula* is a polytypic species. Beside *D. fibula* s.l. only the new taxon *D. fibula* subsp. *tenuis* is noted in Table 1. The type taxon *D. fibula* subsp. *fibula* is placed in the s.l. group, as continuous transitions to other groups occur.

Dictyocha fibula Ehrenberg subsp. *fibula*
(not illustrated)

Subspecies represents an autonym of the species epithet.

Dictyocha fibula subsp. *tenuis* n. subsp.
(Plate 1, Fig. 10)

Holotype: SM.B 13763; Pl.1, Fig. 10.
Type locality: Vøring Plateau, Sample 104-642C-23H-5, 70–71 cm (middle Miocene).

Diagnosis: Basal ring strongly rhomboidal and usually without basal pikes. Apical apparatus constructed of a short and relatively thin apical bar, and appropriate struts. The apical bar is along the short axis of the skeleton. Length of basal ring 39.0–57.0 μm.

Remarks: This new subspecies is distinguished from similar taxa of the species by its strongly rhomboidal basal ring that does not show distinct indentions at the lateral rods, but slight crooking in some cases. Furthermore, the apical bar and adjoining struts are relatively thin compared with the basal rods.

Occurrence: Discontinuously found from Sample 104-642C-14H-5, 55–56 cm to 104-642C-24H-2, 70–71 cm (lower *C. triacantha* Zone to *M. diodon* Zone, lower to upper Miocene).

Dictyocha messanensis Haeckel

Dictyocha messanensis Haeckel in Peters (1861), pp. 799–800.
Dictyocha tenella Ehrenberg, 1861, p. 767; refers to *Dictyocha fibula* var. β of Ehrenberg, 1843, Pl. 2, Fig. IV 11.

Remarks: *Dictyocha messanensis* is a polytypic and polymorphic species. *Dictyocha messanensis* subsp. *aspinosa* has skeletons that are more rounded and without an apical pike, whereas *D. messanensis* subsp. *messanensis* has skeletons that are more rhomboidal and sometimes have an apical pike.

Dictyocha messanensis subsp. *aspinosa* (Bukry) Locker and Martini
(Plate 1, Fig. 4)

Dictyocha stapedia subsp. *aspinosa* Bukry, 1976a, p. 724, Pl. 2, Figs. 6–9.
Dictyocha messanensis subsp. *aspinosa* (Bukry), Locker and Martini, 1986a, p. 904, Pl. 3, Figs. 3–5, Pl. 12, Fig. 2.

Dictyocha messanensis Haeckel subsp. *messanensis*
(Plate 1, Fig. 11)

Subspecies represents an autonym of the species epithet.
Dictyocha messanensis subsp. *messanensis* f. *aspinosa* (nm): Form corresponds in shape to subsp. *aspinosa*.
Dictyocha messanensis Haeckel subsp. *messanensis* f. *messanensis*: Form represents an autonym of the species epithet.

Remarks: *Dictyocha messanensis* subsp. *messanensis* is a polymorphic taxon. Variants with an apical pike are cited as f. *messanensis* and variants without a pike as f. *aspinosa*.

Dictyocha perlaevis Frenguelli
(not illustrated)

Dictyocha perlaevis Frenguelli 1951, p. 279, Figs. 4b, 4c.
Dictyocha fibula subsp. *perlaevis* (Frenguelli), Bukry, 1975a, p. 855, Pl. 3, Fig. 5.

Dictyocha subclinata Bukry
(Plate 2, Fig. 11)

Dictyocha subclinata Bukry, 1981b, pp. 546–547, Pl. 1, Figs. 4–8; Pl. 2, Figs. 1–5, non Figs. 6–10.

Dictyocha varia Locker
(Plate 1, Fig. 3)

Dictyocha varia Locker, 1975, pp. 99–100, Figs, 1/1, 3/1, non 1/2, 1/3, 3/2, 3/3.
Dictyocha pulchella Bukry, 1975b, p. 687, Pl. 4, Figs. 1–3.

Genus *Distephanus* Stöhr, 1880

Remarks: No decision is made here between tetragonal or penta- to polygonal members of the genus (*Distephanopsis* vs. *Distephanus* in Dumitrică, 1978).

Distephanus aculeatus (Ehrenberg) Haeckel
(Plate 3, Figs. 4, 5)

Dictyocha aculeata Ehrenberg, 1841, pp. 148–149.
Distephanus aculeatus (Ehrenberg), Haeckel, 1887, p. 1565.
Dictyocha boliviensis Frenguelli, 1940, p. 44, Fig. 4a, non Figs. 4b–4d.
Distephanus boliviensis (Frenguelli), Bukry and Foster, 1973, p. 827, Pl. 4, Figs. 1–3.
Distephanus aculeatus (Ehrenberg) f. *aculeatus*: Form represents an autonym of the species epithet.
Distephanus aculeatus f. *binoculus* (Ehrenberg) Locker and Martini:
Dictyocha binoculus Ehrenberg, 1843, p. 265 (nomen nudum).
Dictyocha binoculus Ehrenberg, 1845, p. 79.
Distephanus aculeatus f. *binoculus* (Ehrenberg), Locker and Martini: 1986a, p. 905, Pl. 6, Fig. 5.

Remarks: *Distephanus aculeatus* is a polymorphic species. Variants with six radial spines and an apical ring are noted as f. *aculeatus*, and variants with six spines and several apical windows as f. *binoculus*. The name *D. boliviensis* is placed into synonymy, as this taxon is identical to *D. aculeatus* in skeletal structure and stratigraphic range.

The original diagnosis of Ehrenberg (1841) and the figures in his *Mikrogeologie* (1854) indicate that all skeletons with a hexagonal basal ring, a hexagonal apical ring, and basal but sometimes also apical pikes were summarized under the name *Dictyocha aculeata*. Similar skeletons that apparently did not possess such pikes were assigned to *Dictyocha speculum*. This species concept, however, has been recognized as wrong, as the type specimens of *D. speculum* from Oran usually show small basal pikes (Locker, 1974). Combined with the diagnosis, Ehrenberg also gave some reference localities for the taxon *D. aculeata*, among which *Griechenland*, meaning Aegina, appears. Because Ehrenberg himself cites Aegina in the species catalog of his collection, this location has been selected as type locality (Locker, 1974). The lectotype, labelled by Ehrenberg himself, and its type population circumscribe the taxon as used here.

Distephanus crux (Ehrenberg) Haeckel

Dictyocha crux Ehrenberg, 1841, pp. 207–208.
Distephanus crux (Ehrenberg), Haeckel, 1887, p. 1563.
Distephanus crux (Ehrenberg), Dumitrică, 1978, p. 213, Pl. 3, Figs. 5–12.

Remarks: *Distephanus crux* is a highly polytypic species. Beside *D. crux* s.l., several subspecies are distinguished in Table 1. Due to discrimination difficulties, the type taxon *D. crux* subsp. *crux* is included in the s.l. group.

Distephanus crux subsp. *bispinosus* Dumitrică
(not illustrated)

Distephanus crux subsp. *bispinosus* Dumitrică, 1973d, p. 850, Pl. 6, Figs. 3, 6, 7.

Remarks: One specimen of this age diagnostic subspecies was found in Sample 104-642C-15H-1, 66–67 cm (upper Miocene).

Distephanus crux (Ehrenberg) subsp. *crux*
(Plate 2, Fig. 7)

Subspecies represents an autonym of the species epithet.

Distephanus crux subsp. *darwinii* Bukry
(Plate 2, Fig. 4)

Distephanus crux subsp. *darwinii* Bukry, 1976b, p. 895, Pl. 7, Figs. 4–13.

Remarks: This subspecies is diagnostic for the late Oligocene and early Miocene.

Distephanus crux subsp. *longispinus* (Schulz) nov. comb.
(not illustrated)

Distephanus crux f. *longispinus* Schulz, 1928, p. 256, Fig. 44.
Dictyocha crux var. *longispina* (Schulz), Stradner, 1961, p. 92, Pl. 2, Figs. 56, 57.
Distephanus longispinus (Schulz), Bukry and Foster, 1973, p. 828, Pl. 4, Figs. 7, 8.

Distephanus crux subsp. *parvus* (Bachmann) Bukry
(not illustrated)

Dictyocha crux f. *parva* Bachmann in Ichikawa et al., 1967, p.156, Pl. 4, Figs. 14–31.
? *Distephanus parvus* (Bachmann), Bukry and Foster, 1973, p. 828, Pl. 5, Figs. 2, 3.
Distephanus crux subsp. *parvus* (Bachmann), Bukry, 1982, p. 433, Pl. 4, Fig. 7.

Distephanus crux subsp. *stradneri* (Jerković) nov. comb.
(Plate 2, Fig. 6)

Dictyocha schauinslandii subsp. *stradneri* Jerković, 1965, p. 3, Pl. 2, Fig. 2.
Distephanus schauinslandii subsp. *stradneri* (Jerković), Bukry, 1975a, p. 866, Pl. 4, Fig. 7.
Distephanus stradneri (Jerković), Bukry, 1978a, p. 698.

Distephanus paraspeculum n. sp.
(Plate 3, Figs. 1, 2)

Holotype: SM.B 13765; Plate 3, Fig. 1.
Type locality: Vøring Plateau, Sample 104-642D-9X-2, 66–67 cm (lower Miocene).

Diagnosis: Basal ring pentagonal, and without basal pikes. Apical apparatus constructed of a short apical bar and five struts. Diameter of basal ring 28.5–35.5 μm.

Remarks: The main forms of this species are pentagonal in outline, but besides this hexagonal forms are found also. Variants with five radial spines are distinguished as f. *paraspeculum*, and variants with six spines as f. *hexagonalis*.

The new species is similar to some variants in *Distephanus speculum*, but the latter ones are distinctly smaller. Furthermore, the solely bar-bearing variants in *D. speculum* generally co-occur with many apical ring-bearing specimens of the same size. In the present material the bar-bearing variants do not have counterparts with apical rings.

Occurrence: Restricted to an interval from Sample 104-642D-9X-2, 66–67 cm to 104-642D-10X-2, 70–71 cm (*N. lata* to *N. navicula* Zone, lower Miocene).

Distephanus paraspeculum f. *hexagonalis* n.f.
(Plate 3, Fig. 2)

Holotype: SM.B 13766; Pl. 3, Fig. 2.
Type locality: Vøring Plateau, Sample 104-642D-9H-2, 66–67 cm (lower Miocene).

Diagnosis: Basal ring hexagonal with six radial spines but without basal pikes. Apical apparatus formed by the struts that adjoin the center. Diameter of basal ring 28.5–37.5 μm.

Remarks: This new form resembles some variants of *Distephanus speculum*, but the latter ones are usually smaller. The absence of basal pikes in *D. paraspeculum* f. *hexagonalis* may be diagnostic in some cases.

Occurrence: Restricted to an interval from Sample 104-642D-8X-5, 66–67 cm to 104-642D-9X-5, 70–71 cm (*N. lata* to *N. navicula* Zone, lower Miocene).

Distephanus polyactis (Ehrenberg) Deflandre
(Plate 2, Fig. 13)

Dictyocha polyactis Ehrenberg, 1840, p. 129.
Distephanus polyactis (Ehrenberg), Deflandre, 1932, pp. 497, 501.
Paradictyocha polyactis (Ehrenberg), Frenguelli, 1940, p. 51, Figs. 7f–g, 8a, non 8b–e.

Distephanus quinarius n. sp.
(Plate 4, Figs. 1, 2)

Holotype: SM.B 13767; Pl. 4, Fig. 1.
Type locality: Vøring Plateau, Sample 104-642C-15H-1, 66–67 cm (upper Miocene).

Diagnosis: Basal ring pentagonal, with five radial spines and with basal pikes at the lateral rods. Apical apparatus highly elevated, consisting of an apical ring and five struts. Diameter of basal ring 35.5–57.0 μm.

Remarks: This species is apparently labelled as *Distephanus quinquangellus* Bukry and Foster in some publications. However, the epithet *quinquangellus* has been clearly introduced by Bukry and Foster (1973) as nomen novum or substitute name for the taxon *Distephanus speculum* var. *pentagonus* (Lemmermann) when elevating it to species rank. Thus the name *quinquangellus* cannot be applied to the large pentagonal skeletons beleaved here to represent an independent species beside the pentagonal forms of *D. speculum*.

As noted already, the new species resembles some pentagonal variants of *D. speculum*, but the latter ones are distinctly smaller and thinner. *Distephanus quinarius* cannot be related to *D. aculeatus*, as the skeletons of *D. aculeatus* are usually smaller within the same assemblages.

Occurrence: Discontinuously found from Sample 104-642C-12H-5, 65–66 cm to 104-642C-21H-1, 50–51 cm (upper *C. triacantha* Zone to *D. aculeatus* Zone, middle Miocene to lower Pliocene).

Distephanus speculum (Ehrenberg) Haeckel

Dictyocha speculum Ehrenberg, 1838, p. 132 (nomen nudum).
Dictyocha speculum Ehrenberg, 1840, p. 129, Pl. 4, Fig. X n.
Distephanus speculum (Ehrenberg), Haeckel, 1887, p. 1565.

Remarks: *Distephanus speculum* is a highly polytypic and polymorphic species. In this paper five subspecies are distinguished: *Distephanus speculum* subsp. *constrictus* is characterized by thick skeletons with a very narrow apical ring, *D. speculum* subsp. *giganteus* by large skeletons with a wide apical ring, *D. speculum* subsp. *haliomma* by the predominance of fenestrate skeletons, *D. speculum* subsp. *octonarius* by skeletons with rare seven to common eight radial spines, and *D. speculum* subsp. *speculum* by skeletons with six spines and a normal apical ring. The nominate subspecies is labelled under *D. speculum* s.l. in Tables 1 and 3, due to discrimination difficulties against other subspecies apparently present.

Within the subspecies cited, same form names are used (only autonyms are excluded), although the rules of the ICBN would require different names. As explained in Locker and Martini (1986a), identical skeletal structures in different subunits of a species may be referred to identical genetic structures, thus the same names should be permitted.

Distephanus speculum subsp. *constrictus* n. subsp.
(Plate 2, Figs. 8–10)

Holotype: SM.B 13768; Plate 2, Fig. 8.
Type locality: Vøring Plateau, Sample 104-644A-34H-5, 66–67 cm (upper Pliocene).

Diagnosis: Skeleton relatively thick. Basal ring hexagonal, with six radial spines, and with basal pikes at the lateral rods. Apical apparatus composed of a very narrow apical ring and six struts, but apical pikes usually absent. Diameter of basal ring is 25.0–32.0 μm.

Remarks: Comparable to other subspecies of *D. speculum*, this new taxon also contains several forms beside the main variant. They are generally rare and are listed under "formae diversae" in Table 1. The following forms are recognized: f. *pentagonus* (five radial spines + apical ring), f. *constrictus* (main form = six spines + ring), f. *pseudofibula* and f. *varians* (six spines + different sets of apical bars), f. *cannopileus-hexacanthus* (six spines + apical windows), and f. *septenarius* (seven spines + apical ring).

The new subspecies is distinguished from other subspecies of *D. speculum* by its thick skeleton and the very narrow apical ring without pikes. If apical pikes are present, they are small and knob-like. Radial spines are usually equal in length.

Occurrence: Continuously found from Sample 104-642C-9H-1, 64–65 cm to 104-642C-11H-5, 65–66 cm, and Sample 104-644A-34H-4, 66–67 cm to 104-644A-34H-5, 66–67 cm (both intervals *D. aculeatus* Zone, upper Pliocene).

Distephanus speculum subsp. *giganteus* Bukry
(Plate 2, Fig. 12)

Distephanus speculum subsp. *giganteus* Bukry, 1976c, pp. 848–849, Pl. 1, Fig. 19; Pl. 2, Figs. 1, 2.
Distephanus speculum subsp. *giganteus* f. *cannopileus-hexacanthus* (nm): Form corresponds in shape to subsp. *speculum* f. *cannopileus-hexacanthus*.
Distephanus speculum subsp. *giganteus* Bukry f. *giganteus*: Form represents an autonym of the subspecies epithet.

Distephanus speculum subsp. *haliomma* (Ehrenberg) Bukry
(Plate 2, Figs. 2, 3)

Dictyocha haliomma Ehrenberg, 1845, p. 80.
Distephanus speculum subsp. *haliomma* (Ehrenberg), Bukry, 1978a, p. 697, Pl. 2, Fig. 10.
Distephanus speculum subsp. *haliomma* (Ehrenberg) f. *haliomma*: Form represents an autonym of the subspecies epithet.
Distephanus speculum subsp. *haliomma* f. *speculum* (nm): Form corresponds in shape to subsp. *speculum* f. *speculum*.

Distephanus speculum subsp. *octonarius* (Ehrenberg) Busen and Wise
(not illustrated)

Dictyocha octonaria Ehrenberg, 1845, p. 201.
Distephanus octonarius (Ehrenberg), Haeckel, 1887, p. 1566.
Distephanus speculum subsp. *octonarius* (Ehrenberg), Busen and Wise, 1977, p. 714.
Distephanus floridus Bukry, 1985, p. 599, Pl. 1, Figs. 1–4.
Distephanus speculum subsp. *octonarius* (Ehrenberg) f. *octonarius*: Form represents an autonym of the subspecies epithet.
Distephanus speculum subsp. *octonarius* f. *septenarius* (nm): Form corresponds in shape to subsp. *speculum* f. *septenarius*.

Distephanus speculum (Ehrenberg) subsp. *speculum*
(Plate 2, Fig. 1)

Subspecies represents an autonym of the species epithet.
Distephanus speculum subsp. *speculum* f. *cannopileus-hexacanthus* (Frenguelli) Locker and Martini:
Dictyocha fibula f. *cannopilea-hexacantha* Frenguelli, 1935, Pl. 12, Figs. 1, 2.
Distephanus speculum subsp. *speculum* f. *cannopileus-hexacanthus* (Frenguelli), Locker and Martini, 1986a, p. 907, Pl. 17, Fig. 1.
Distephanus speculum subsp. *speculum* f. *pentagonus* (Lemmermann) Locker and Martini:
Distephanus speculum var. *pentagonus* Lemmermann, 1901, p. 264, Pl. 11, Fig. 19.
Distephanus speculum subsp. *speculum* f. *pentagonus* (Lemmermann), Locker and Martini, 1986a, p. 907, Pl. 7, Fig. 8.
Distephanus speculum subsp. *speculum* f. *septenarius* (Ehrenberg) Locker and Martini:
Dictyocha septenaria Ehrenberg, 1845, p. 80.
Distephanus speculum var. *septenarius* (Ehrenberg), Joergensen, 1899, p. 50.
Distephanus septenarius (Ehrenberg), Frenguelli, 1938, p. 121.
Dictyocha speculum var. *septenaria* (Ehrenberg), Hovasse, 1946, p. 9.
Distephanus speculum subsp. *speculum* f. *septenarius* (Ehrenberg), Locker and Martini, 1986a, p. 907, Pl. 7, Fig. 5.
Distephanus speculum (Ehrenberg) subsp. *speculum* f. *speculum*: Form represents an autonym of the species epithet.

Remarks: *Distephanus speculum* subsp. *speculum* often occurs polymorphic. Variants with six radial spines and a fenestrate apical apparatus are noted as f. *cannopileus-hexacanthus*, variants with five spines and a normal apical ring as f. *pentagonus*, variants with seven spines and an apical ring as f. *septenarius*, and variants with six spines and an apical ring as f. *speculum*. According to the rules of the ICBN, some of these forms are indicated as autonyms in other subspecies. Thus f. *cannopileus-hexacanthus* corresponds to f. *haliomma* in subsp. *haliomma*, and f. *speculum* to f. *constrictus* in subsp. *constrictus* as well as f. *giganteus* in subsp. *giganteus*. Rare variants, mainly with apical bars, are summarized under "formae diversae" in Table 1. Coronoid variants are not distinguished as special taxon, but they are labelled separately.

Distephanus stauracanthus (Ehrenberg) Haeckel
(Plate 2, Fig. 5)

Dictyocha stauracanthus Ehrenberg, 1846, p. 76.
Distephanus stauracanthus (Ehrenberg), Haeckel, 1887, p. 1564.
Distephanus crux var. *stauracanthus* (Ehrenberg), Lemmermann, 1901, p. 263.
Distephanus crux var. *octacanthus* Desikachary and Maheshwari, 1956, p. 260, Figs. 10, 12, 13.
Distephanus octacanthus (Desikachary and Maheshwari), Bukry and Foster, 1973, p. 828, Pl. 4, Fig. 12.
Distephanopsis stauracanthus (Ehrenberg), Dumitrica, 1978, p. 213, Pl. 3, Figs. 13, 15.
Distephanus stauracanthus (Ehrenberg) f. *stauracanthus*: Form represents an autonym of the species epithet.
Distephanus stauracanthus f. *octagonus* (Tsumura) Locker and Martini: *Dictyocha fibula* var. *octagona* Tsumura, 1963, pp. 55–56, Pl. 2, Fig. 4, Pl. 10, Figs. 11–13, Pl. 23, Figs. 8–10.
Dictyocha octagona (Tsumura), Martini, 1971, p. 1697, Pl. 1, Fig. 15.
Distephanus stauracanthus f. *octagonus* (Tsumura), Locker and Martini, 1986a, p. 907, Pl. 6, Fig. 8.

Remarks: *Distephanus stauracanthus* is a dimorphic species. Variants with an apical ring are distinguished as f. *stauracanthus*, and variants with an apical bar as f. *octagonus*. But only the latter one was found at Site 642. It could be shown by Bukry (1981b, 1985b) that specimens with a bar dominate in late middle Miocene populations.

Distephanus sulcatus Bukry
(Plate 3, Fig. 3; Plate 4, Fig. 6)

Distephanus sulcatus Bukry, 1979, p. 562, Pl. 4, Figs. 4–12.
Distephanus sulcatus Bukry f. *sulcatus*: Form represents an autonym of the species epithet.

Remarks: *Distephanus sulcatus* is a highly polymorphic species which includes beside predominantly multifenestrate specimens also those with an apical ring or apical bar constructions. In this paper only two taxa are used: Variants with six radial spines and several apical windows are distinguished as f. *sulcatus*, and variants with six radial spines and a single apical ring as f. *maximus*.

Distephanus sulcatus was first described from the upper Pliocene of DSDP Site 407, west of Iceland (Bukry, 1979). The species seems to be diagnostic for the early to late Pliocene time interval.

Distephanus sulcatus f. *maximus* n.f.
(Plate 3, Fig. 3)

Holotype: SM.B. 13764; Plate 3, Fig. 3.
Type locality: Vøring Plateau, Sample 104-642C-10H-4, 71–72 cm (upper Pliocene).

Diagnosis: Basal ring hexagonal, with six radial spines, and basal pikes at the lateral rods. The basal ring is distinctly indented at these rods. Apical apparatus is composed of a ring and six struts. Diameter of basal ring is 67.5–71.5 μm.

Remarks: This new form is distinguished from similar taxa in other species by its very large size, the prominent indentions at the struts and the often somewhat irregular construction of the apical ring. Occurrence: Restricted to an interval from Sample 104-642C-9H-1, 64–65 cm to 104-642C-10H-4, 71–72 cm (*D. aculeatus* Zone, lower to upper Pliocene).

Genus *Mesocena* Ehrenberg, 1841
Mesocena diodon Ehrenberg
(Plate 3, Fig. 8)

Mesocena diodon Ehrenberg, 1845, p. 84.
Bachmannocena diodon (Ehrenberg), Locker, 1974, p. 636, Pl. 2, Fig. 9.

Mesocena elliptica (Ehrenberg) Ehrenberg
(not illustrated)

Dictyocha (*Mesocena*) *elliptica* Ehrenberg, 1841, p. 208.
Mesocena elliptica (Ehrenberg), Ehrenberg, 1845, pp. 71, 84.
Mesocena elliptica var. *rhombica* Bukry, 1985b, p. 489, pl. 5, Figs. 1–6.
Bachmannocena elliptica Bukry, 1987b, p. 404.

Remarks: *Mesocena elliptica* is an exclusively early to middle Miocene species, if the taxon is restricted to populations around the type.

Mesocena quadrangula Ehrenberg ex Haeckel
(Plate 5, Fig. 6)

Mesocena quadrangula Ehrenberg, 1873, pp. 145, 273 (nomen nudum).
Mesocena quadrangula Haeckel, 1887, p. 1556.
Mesocena polymorpha var. *quadrangula* (Haeckel), Lemmermann, 1901, p. 256, Pl. 10, Figs. 5–7.

Remarks: *Mesocena quadrangula* has a distinctive acme in Pleistocene time that ranges from above the Olduvai Event to below the base of the Brunhes Epoch (Dumitrică, 1973a).

Mesocena triangula (Ehrenberg) Ehrenberg
(Plate 5, Fig. 5)

Dictyocha triangula Ehrenberg, 1840, p. 129.
Dictyocha (*Mesocena*) *triangula* Ehrenberg, Ehrenberg, 1841, p. 208.
Mesocena triangula (Ehrenberg), Ehrenberg, 1845, p. 65, 71.
Bachmannocena triangula (Ehrenberg), Locker, 1974, p. 636, Pl. 2, Fig. 10.

Remarks: *Mesocena triangula* is diagnostic for the late Miocene. However, the relations to typical *Mesocena* species having four radial spines remain unclear.

Genus *Naviculopsis* Frenguelli, 1940

Remarks: In Table 1 and 3, rare occurrences of allochthonous species are cited under "*N.* species diversae." The following taxa are included: *N. biapiculata* (Lemmermann) (Samples 104-642C-23H-5, 70–71 cm; 104-642D-8X-5, 66–67 cm; 104-644A-20H-1, 65–66 cm), *N. constricta* (Schulz) (Sample 104-642D-9X-2, 66–67 cm), *N. lata* (Deflandre) (Sample 104-644A-33H-1, 66–67 cm), *N. punctilia* Perch-Nielsen (Sample 104-642D-5X-2, 47–48 cm), *N. robusta* (Sample 104-642D-9X-5, 70–71 cm), and *Naviculopsis* sp. (remaining samples).

Naviculopsis iberica Deflandre
(Plate 4, Fig. 3)

Naviculopsis iberica Deflandre, 1950, p. 202, Figs. 231–234.

Naviculopsis lacrima Bukry
(Plate 4, Fig. 7)

Naviculopsis lacrima Bukry, 1982, p. 434, Pl. 7, Figs. 1–10, Pl. 9, Fig. 8.

Remarks: *Naviculopsis lacrima* was first found in the lower Miocene of DSDP Site 495, eastern tropical Pacific (Bukry, 1982). Thus the species seems to be diagnostic for the early Miocene.

Naviculopsis lata (Deflandre) Frenguelli
(Plate 5, Fig. 3)

Dictyocha biapiculata var. *lata* Deflandre, 1932, p. 500, Figs. 30, 31.
Naviculopsis lata (Deflandre), Frenguelli, 1940, p. 61.

Naviculopsis navicula (Ehrenberg) Deflandre

Dictyocha navicula Ehrenberg, 1838, p. 132 (nomen nudum).
Dictyocha navicula Ehrenberg, 1840, p. 129.
Naviculopsis navicula (Ehrenberg), Deflandre, 1950, p. 107.
Eunaviculopsis navicula (Ehrenberg), Ling, 1977, p. 213.

Remarks: *Naviculopsis navicula* is treated as a polytypic species. In this paper three subspecies are distinguished: *Naviculopsis navicula* subsp. *navicula* is characterized by relatively long and broad skeletons, *N. navicula* subsp. *ponticulus* by relatively small skeletons and similar proportions (compare type figures in Locker, 1974), and *N. navicula* subsp. *obtusarca* by skeletons with a broad middle part but narrow ends.

Naviculopsis navicula (Ehrenberg) subsp. *navicula*
(Plate 5, Fig. 2)

Subspecies represents an autonym of the species epithet.

Naviculopsis navicula subsp. *obtusarca* (Bukry) nov. comb.
(Plate 5, Fig. 1)

Naviculopsis obtusarca Bukry, 1978a, p. 821; refers to *Naviculopsis ponticula* in Bukry, 1978b, Pl. 3, Fig. 4.

Naviculopsis quadratum (Ehrenberg) Locker
(Plate 4, Fig. 5)

Dictyocha quadratum Ehrenberg, 1845, 267.
Dictyocha navicula var. *rectangularis* Schulz, 1928, pp. 243, 278, Figs. 17a-b.
Naviculopsis rectangularis (Schulz), Frenguelli, 1940, p. 61.
Naviculopsis quadratum (Ehrenberg), Locker, 1974, p. 635, Pl. 2, Fig. 3.

Remarks: *Naviculopsis quadratum* obviously evolved from *N. iberica*, therefore discrimination between both species may be difficult in some horizons. *Naviculopsis iberica* generally shows more acuted skeletons, whereas *N. quadratum* has more rectangular skeletons with nearly quadratic windows.

Genus *Paramesocena* Locker and Martini, 1986
Paramesocena circulus (Ehrenberg) Locker and Martini

Dictyocha (Mesocena) circulus Ehrenberg, 1841, p. 208.
Mesocena circulus (Ehrenberg), Ehrenberg, 1845, p. 65.
Paradictyocha circulus (Ehrenberg), Dumitrică, 1973d, p. 853, Pl. 9, Figs. 7–10.
Bachmannocena circulus (Ehrenberg), Locker, 1974, p. 636, Pl. 2, Fig. 11.
Paramesocena circulus (Ehrenberg), Locker and Martini, 1986a, p. 909, Pl. 9, Figs. 2–4, Pl. 12, Figs. 4, 5.

Remarks: *Paramesocena circulus* is treated as a polytypic species that includes both the taxa *P. circulus* subsp. *apiculata* and *P. circulus* subsp. *circulus*.

Paramesocena circulus subsp. *apiculata* (Lemmermann) nov. comb.
(Plate 4, Fig. 4)

Mesocena circulus var. *apiculata* Lemmermann, 1901, p. 257, Pl. 10, Figs. 9, 10.
Paradictyocha apiculata (Lemmermann), Frenguelli, 1940, p. 52, Pl. 4, Fig. 4.
Paramesocena apiculata (Lemmermann), Locker and Martini, 1986a, p. 909, Pl. 9, Figs. 1, 5, Pl. 12, Fig. 3.

Paramesocena circulus (Ehrenberg) subsp. *circulus*
(Plate 3, Fig. 6)

Subspecies represents an autonym of the species epithet.

Genus *Septamesocena* Bachmann, 1970
Septamesocena apiculata (Schulz) Bachmann
(Plate 5, Fig. 4)

Mesocena oamaruensis var. *apiculata* Schulz, 1928, p. 240, Fig. 11.
Mesocena apiculata (Schulz), Hanna, 1931, p. 198, Pl. D, Fig. 3.
Septamesocena apiculata (Schulz), Bachmann, 1970, p. 13–14.
Bachmannocena apiculata (Schulz) subsp. *apiculata*, Bukry, 1987b, p. 403, Pl. 1, Fig. 1.
Septamesocena apiculata (Schulz) f. *apiculata.*: Form represents an autonym of the species epithet.
Septamesocena apiculata f. *curvata* (Bukry) nov. comb.:
Mesocena apiculata subsp. *curvata* Bukry, 1976c, p. 849, Pl. 2, Figs. 15, 16.
Bachmannocena apiculata subsp. *curvata* (Bukry), Bukry, 1987b, p. 403.

Remarks: *Septamesocena apiculata* is a polymorphic and probably also polytypic species. In this paper only two intrapopulationary variants are distinguished: f. *apiculata* with all basal bars convex, and f. *curvata* with one bar concave.

Class CHRYSOPHYCEAE
Order CHRYSOMONADALES Engler, 1898
Family SYNURACEAE Lemmermann, 1899
Genus *Macrora* Hanna, 1932
Macrora stella (Azpeitia) Hanna
(Plate 3, Fig. 7)

Pyxidicula? stella Azpeitia, 1911, p. 150, Pl. 1, Fig. 1.
Macrora stella (Azpeitia), Hanna, 1932, p. 196, Pl. 12, Fig. 7.
Pseudorocella corona Deflandre, 1947, p. 337, Fig. 4.

Class DINOPHYCEAE
Order EBRIALES Fott, 1959

Fossil ebridians show two curious features which need brief discussion. First, in some species double skeletons are formed, and, second, in same species cysts occur. Double skeletons are constructed of two normal skeletons that are united by siliceous bridges. The causes of duplet formation were hitherto unknown (Tappan, 1980). The stratigraphic distribution of double skeletons at Site 642 (Fig. 8) indicates, however, that they were formed under unfavorable ecological conditions. In the present material, double skeletons were found in *Ammodochium pyramidale, A. serotinum, Ditripodium latum, Ebriopsis cornuta, Falsebria* cf. *arborea, Haplohermesinum hovassei, Hermesinella conata, H. fenestrata, H. primitiva, H. schulzii, Parathranium bispinum, P.* cf. *californicum, P. clathratum, P.* cf. *clathratum, Thranium crassipes*, and *Pseudammodochium robustum*. Double skeletons of *A. serotinum, F.* cf. *arborea, P. bispinum, P.* cf. *clathratum* and *P. robustum* may be rather common in some stratigraphic intervals.

Cysts or loricae are globular, hollow, siliceous bodies that are firmly attached to normal skeletons. They posess an aperture that probably functioned as an extrusion opening. Loricae are recognized to be formed under deteriorated ecological conditions (Tappan, 1980). In the present material, loricae were found in *Ammodochium serotinum, Ebriopsis cornuta, Haplohermesinum hovassei Paruthennium bispinum, P.* cf. *califonicum, P.* cf. *clathratum* and *Podamphora elgeri*. Loricae are common only in *E. cornuta* and *P. elgeri*.

Genus *Ammodochium* Hovasse, 1932

Remarks: In Table 2, rare occurrences of allochthonous species are summarized under "*A.* species diversae." The following taxa are included: *A. complexum* Dumitrică and Perch-Nielsen (Sample 104-642C-11H-5, 65–66 cm), *A. rectangulare* (Schulz) (Sample 104-642C-22H-1, 66–67 cm; 104-642C-23H-2, 54–55 cm), and *Ammodochium* sp. (remaining samples).

Ammodochium pyramidale Hovasse
(Plate 16, Figs. 1, 2)

Ammodochium pyramidale Hovasse, 1943, p. 288, Fig. 12.
Ammodochium serotinum Locker and Martini
(Plate 6, Figs. 3–5)
Ammodochium serotinum Locker and Martini, 1986b, p. 943, Pl. 2, Figs. 1, 2.

Genus *Craniopsis* Hovasse ex Frenguelli, 1940
Craniopsis sp.

Remarks: In Table 2, some isolated occurrences of *Craniopsis* skeletons are indicated. As the specimens are allochthonous, no attempt was made for specific distinction.

Genus *Ditripodium* Hovasse, 1932
Ditripodium amphora Hovasse
(Plate 6, Fig. 13)

Ditripodium amphora Hovasse, 1943, p. 289, Fig. 15.

Remarks: Only typical skeletons having mesoclades are cited as *D. amphora*. Specimens without mesoclades or the mesoclades probably broken off are placed in *D.* cf. *amphora*.

Ditripodium elephantinum Hovasse
(Plate 6, Fig. 14)

Ditripodium elephantinum Hovasse, 1932, p. 125, Figs. 8a, b.

Remarks: Only typical skeletons with a narrow angle between the proclades are listed as *D. elephantinum*. Other specimens showing a rather large angle are cited as *D.* cf. *elephantinum*.

Ditripodium japonicum Deflandre
(Plate 6, Fig. 15)

Ditripodium japonicum Deflandre, 1951, pp. 51–52, 76, Figs. 177–179, 182.

Remarks: *Ditripodium japonicum* was first described from the upper Miocene of Sendai, Japan (Deflandre, 1951). Its appearance in Sample 104-642C-11H-5, 65–66 cm (upper Pliocene) coincides with a mass occurrence of *Pseudammodochium robustum* at Site 642.

Ditripodium latum Hovasse
(Plate 6, Figs. 11, 12)

Ditripodium latum Hovasse, 1932, p. 282, Fig. 6.

Genus *Ebria* Borgert, 1891
Ebria inornata (Hovasse) Deflandre
(not illustrated)

Proebria inornata Hovasse, 1943, p. 281, Fig. 6.
Ebria inornata (Hovasse), Deflandre, 1951, p. 59, 81, Figs. 235–238.

Genus *Ebriopsis* Hovasse, 1932

Remarks: In Tables 2 and 3, some isolated occurrences of *Ebriopsis crenulata* Hovasse are listed. As these occurrences are allochthonous, synonymies are not given below.

Ebriopsis cornuta (Ling) Locker and Martini
(Plate 7, Fig. 15; Plate 8, Figs. 1, 5)

non-*Ebriopsis cornuta* Dumitrică and Perch-Nielsen in Perch-Nielsen, 1975b, p. 880, text-fig. 2, Pl. 7, Figs. 8, 9.
Ebriopsis antiqua subsp. *cornuta* Ling, 1977, p. 215–216, pl. 3, Figs. 19–22.
Ebriopsis cornuta (Ling). Locker and Martini, 1986b, pp. 943–944, Pl. 2, Figs. 14, 15.

Remarks: *Ebriopsis cornuta* is regarded as a polymorphic species that contains variants with and without a pike.

Genus *Falsebria* Deflandre, 1951
Falsebria ambigua Deflandre
(not illustrated)

Falsebria ambigua Deflandre, 1950, p. 159, Fig. 3 (invalid).
Falsebria ambigua Deflandre, 1951, pp. 33, 73, Figs. 88, 89, 100, 101.

Remarks: The thick skeletons indicated as *Falsebria ambigua* s.l. are possibly allochthonous.

Falsebria arborea n. sp.
(Plate 8, Fig. 16; Plate 9, Fig. 1)

Holotype: SM.B 13769; Plate 8, Fig. 16.
Type locality: Vøring Plateau, Sample 104-642C-11H-2, 52–53 cm (upper Pliocene).

Diagnosis: Rhabde and actines equally developed, with highly branched terminations. Diameter 46.5–57.0 μm.

Remarks: The skeletons have four thick arms that are manifold branched after their first and distinct furcation. The terminations may be united sometimes to an irregular ring, thus providing a more plane skeleton.

The new species appears unique with respect to its excessive branching. However, it remains unclear whether the skeletons represent single units or deviated double skeletons.

Occurrence: Continuously found from Sample 104-642C-9H-1, 64–65 cm to 104-642C-11H-2, 52–53 cm and Sample 104-644A-30H-2, 56–57 cm to 104-644A-34H-5, 66–67 cm (both intervals *E. cornuta* Zone, upper Pliocene).

Falsebria sp.

Remarks: In *Falsebria* sp. different types of skeletons are placed together, which need further investigation.

Genus *Haplohermesinum* Hovasse, 1943 emend.

Type species: *Haplohermesinum simplex* (Schulz, 1928) sensu Hovasse, 1943 = *Haplohermesinum hovassei* Locker and Martini n. sp.

Remarks: Hovasse (1943) introduced the genus *Haplohermesinum* with a description and some figures which he named *Haplohermesinum simplex*. Both description and figure caption indicate that *Ebria tripartita* var. *simplex* Schulz was used as basionym. But it is obvious now that the var. *simplex* of Schulz really includes variants of *Ebria*, which would require to placing *Haplohermesinum* into synonymy of *Ebria*. However, the figures presented by Hovasse permit recognizing the unique features of the taxon *Haplohermesinum*. Therefore, the new species *Haplohermesinum hovassei* is introduced here to retain the genus *Haplohermesinum* in its original sense, and to fulfill the requirements of the ICBN.

According to the figures of Hovasse (1943), the genus *Haplohermesinum* includes all species that have one cladian triplet (two synclades + one proclade + one opisthoclade) of the triaenic skeleton flattened. The flat and thin procladian-opisthocladian combination of the triplet is generally aligned with the rhabde of the triaene. The differences to other genera are as follows: *Ebriopsis* shows one cladian triplet distorted against the other one. *Parebria* has a skeleton with an asymmetric opisthoclade. In *Hermesinella* the skeleton is unflattened. The very similar skeleton of *Ebria* does not have a triaene but a triode.

Haplohermesinum hovassei n. sp.
(Plate 7, Figs. 11, 12)

Haplohermesinum simplex (Schulz), Hovasse, 1943, p. 286, Figs. 11a, b.

Holotype: SM.B 13770; Plate 7, Fig. 11.
Type locality: Vøring Plateau, Sample 104-642D-8X-2, 66–67 cm (lower Miocene).

Diagnosis: Proclades short, connected by two straight synclades and a highly arched one. Opisthocladian basket fully developed, and usually with indentions where actines adjoin the outer skeletal elements. Length 21.5–29.0 μm.

Remarks: The species is sometimes cited as *Haplohermesinum simplex*. But as the basionym *Ebria tripartita* var. *simplex* Schulz (1928) refers to true variants of *E. tripartita*, the new name *hovassei* is introduced for this taxon.

The new species resembles *Haplohermesinum narbonensis*, but its non- arched upper syncladians are generally straight.

Occurrence: Continuously found from Sample 104-642C-22H-4, 60–61 cm to 104-642D-11X-1, 55–56 cm, but after that only discontinuously up to Sample 104-642C-17H-5, 50–51 cm (*F. atlanticus* Zone to *H. schulzii* Zone, lower to upper Miocene).

Haplohermesinum narbonensis (Deflandre and Gageonnet) nov. comb.
(Plate 7, Figs. 13, 14)

Ebriopsis narbonensis Deflandre and Gageonnet, 1950, p. 204, Figs. 1–6.

Remarks: *Haplohermesinum narbonensis* exhibits the typical structure of the genus with one opisthoclade parallel the triaene.

Genus *Hermesinella* Deflandre, 1934
Hermesinella conata (Deflandre) Locker and Martini
(Plate 7, Fig. 6)

Hermesinum conatum Deflandre, 1951, pp. 44, 46, 68, Fig. 141.
Hermesinella conata (Deflandre), Locker and Martini, 1986b, p. 944, Pl. 2, Figs. 9, 10.

Hermesinella fenestrata Frenguelli
(PIate 7, Fig. 7)

Hermesinella fenestrata Frenguelli, 1951, p. 279, fig. 5a.

Hermesinella primitiva n. sp.
(Plate 7, Figs. 9, 10)

Holotype: SM.B 13771; Plate 7, Fig. 9.
Type locality: Vøring Plateau, Sample 104-642D-10X-2,70-71 cm (lower Miocene).

Diagnosis: Proclades short and without windows, connected by slightly arched synclades. Triaene massive. Opisthocladian basket fully developed and with broadly arched clades. Length 23.0–25.0 μm.

Remarks: This new species superficially resembles other *Hermesinella* species, but it is distinguished by its strongly rounded skeleton, the massive triaene and the lack of procladian windows.
Occurrence: Rather continously found from Sample 104-642D-6X-2, 66–67 cm, to 104-642D-10X-6, 70–71 cm (*F. folia* Zone to *H. adriaticum* Zone, lower Miocene).

Hermesinella schulzii (Hovasse) nov. comb.
(Plate 7, Fig. 8)

Hermesinum schulzii Hovasse, 1932, p. 125; refers to *Ebria antiqua* in Gemeinhardt, 1931, Pl. 10, Figs. 21, 22.

Remarks: *Hermesinella schulzii* is distinguished from *H. fenestrata* by its rather wide syncladian ring, and the indented junction between the rhabde and opisthoclades.

Genus *Hermesinum* Zacharias, 1906
Hermesinum adriaticum Zacharias
(Plate 7, Fig. 3)

Hermesinum adriaticum Zacharias, 1906, p. 94, Figs. a–d.
Bosporella triaenoides Hovasse, 1931, p. 781, Figs. A–E.

Hermesinum mirabile Deflandre
(not illustrated)

Hermesinum mirabile Deflandre, 1951, pp. 47, 69, Fig. 159.

Remarks: *Hermesinum mirabile* was first described from the middle Miocene of Nyermegy, Hungary (Deflandre, 1951).

Hermesinum obliquum Locker and Martini
(Plate 7, Figs. 4, 5)

Hermesinum obliquum Locker and Martini, 1986b, p. 944, Pl. 1, Figs. 1–4.

Genus *Parathranium* Hovasse, 1932

Remarks: Discrimination between the different species of *Parathranium* may be difficult. *Parathranium bispinum* usually has short opisthoclades which are bent outward, and knobs at the proclades. *Parathranium californicum* possesses short opisthoclades, narrow procladian openings, and a small syncladian pike. *Parathranium clathratum* usually shows long opisthoclades which are curved inward. *Parathranium curvipes* displays short sigmoidal opisthoclades.

Parathranium bispinum Deflandre
(Plate 6, Figs. 19, 20)

Parathranium bispinum Deflandre, 1951, p. 51, 78, Fig. 174.

Parathranium cf. *californicum* Deflandre
(Plate 6, Fig. 18)

cf. *Parathranium californicum* Deflandre, 1951, p. 49–51, 77, Figs. 168–171.

Remarks: As the skeletons found do not have furcated opisthoclades, they are listed as *P.* cf. *californicum*.

Parathranium clathratum (Ehrenberg) Deflandre
(Plate 7, Fig. 2)

Dicladia? *clathrata* Ehrenberg, 1845, p. 79.
Thranium tenuipes Hovasse, 1932, p. 123, Fig. 5 (invalid).
Parathranium tenuipes Hovasse, 1932, pp. 464–465.
Parathranium clathratum (Ehrenberg), Deflandre, 1944, p. 67.

Remarks: Beside true *P. clathratum* specimens with long opisthoclades, skeletons having short opisthoclades are labelled as *P.* cf. *clathratum*.

Parathranium curvipes Hovasse
(Plate 7, Fig. 1)

Parathranium curvipes Hovasse, 1943, p. 288, Fig. 13.

Remarks: *Parathranium curvipes* was first described from the lower Miocene of Saint-Laurent-la-Vernède, France (Hovasse, 1943).

Genus *Podamphora* Gemeinhardt, 1931
Podamphora elgeri Gemeinhardt
(Plate 7, Figs. 16, 17)

Podamphora elgeri Gemeinhardt, 1931, p. 107, Pl. 10, Fig. 19.

Remarks: *Podamphora elgeri* usually shows large loricae, as mentioned previously by Gemeinhardt (1931) and Deflandre (1951).

Genus *Pseudammodochium* Hovasse, 1932

Remarks: In Tables 2 and 3, rare occurrences of allochthonous species are registered under "*P. species diversae*." The following taxa are included: *P. doliolum* (Hovasse) (Sample 104-644A-31H-3, 66–67 cm), and *Pseudammodochium* sp. (remaining samples).

Pseudammodochium fenestratum n. sp.
(Plate 6, Figs. 9, 10)

Holotype: SM.B 13772; Plate 6, Fig. 10.
Type locality: Vøring Plateau, Sample 104-644A-16H-1, 66–67 cm (Pleistocene, allochthonous?).

Diagnosis: Skeleton ovoid, with three larger openings in the center and six smaller ones in each bandlike portion in between. Length 19.5–25.0 μm.

Remarks: The skeletons are very characteristically constructed. If one of the larger central openings is in front, two smaller openings may be seen above and two below, whereas two other ones appear as a half at both sides. If one bandlike portion is in front, two small openings lie above and two below, whereas two single openings are in the middle part; the larger central openings may be observed as a half at each side of the band. Through the central opening the triode can be distinctly recognized.

This new species resembles some *Ammodochium* and *Pseudammodochium* species, especially *A. complexum*, *A. novum*, *P. dictyodes* and *P. doliolum*. But the *Ammodochium* species have larger central openings and additional pores in their bands, and the *Pseudammodochium* species possess small and indistinct openings or pores in their bandlike portions.

Occurrence: Discontinously found from Sample 104-644A-15H-5, 66–67 cm to 104-644A-31H-4, 66–67 cm (*E. cornuta* Zone to *A. pentasterias* Zone, upper Pliocene to Pleistocene), and possibly allochthonous.

Pseudammodochium robustum Deflandre
(Plate 6, Figs. 6–8)

Pseudammodochium robustum Deflandre, 1934, p. 94, Figs. 39–42.

Remarks: *Pseudammodochium robustum* was first cited from the middle Miocene of Abashiri, Japan (Deflandre, 1934).

Genus *Spongebria* Deflandre, 1950

Remarks: The skeletons of *Spongebria* species are strongly reduced. The primarily triaenic skeleton shows a pseudotriode consisting of the rhabde and two actines, whereas one actine is atrophied to a central knob.

Spongebria curta n. sp.
(Plate 9, Figs. 6–8)

Holotype: SM.B 13773; Plate 9, Fig. 7.
Type locality: Vøring Plateau, Sample 104-642C-24H-2, 70–71 cm (lower Miocene).

Diagnosis: Pseudotriode massive, with very short arms that are usually branched toward the distal end. Ends of the arms free and covered by many small crests which leave pits in between. Diameter 50.0–68.0 μm.

Remarks: The new species is distinguished from other *Spongebria* taxa by its very massive skeleton and the free arms. The massiveness may be forced sometimes by the disappearance of the distal furcation of arms.

Occurrence: Restricted to an interval from Sample 104-642C-23H-5, 70–71 cm to 104-642C-24H-5, 70–71 cm (*S. miocenica* Zone, lower to middle Miocene).

Spongebria miocenica n. sp.
(Plate 9, Figs. 2–5)

Holotype: SM.B 13774; Plate 2, Fig. 5.
Type locality: Vøring Plateau, Sample 104-642C-23H-2, 54–55 cm (middle Miocene).

Diagnosis: Pseudotriode massive, with arms that are branched toward the outer margin. Outer margin thick and ring-shaped, covered by many small crests which leave pits in between. Diameter 64.0–82.0 μm.

Remarks: This new species is distinguished from other *Spongebria* taxa by its nearly circular outline and the thick dimpled margin.

Occurrence: Continuously found from Sample 104-642C-22H-1, 66–67 cm to 104-642C-24H-5, 70–71 cm (*S. miocenica* Zone, lower to middle Miocene).

Genus *Thranium* Hovasse, 1932
Thranium crassipes Hovasse
(Plate 6, Figs. 16, 17)

Thranium crassipes Hovasse, 1932, p. 122, Figs. 4a–4c (invalid).
Thranium crassipes Hovasse, 1932, p. 464.

Remarks: Above the first occurrence in Sample 104-642C-24H-2, 70–71 cm (lower Miocene) the skeletons of *T. crassipes* have rather long procladian pikes, which indicate derivation from true mesoclades. In the upper Miocene a special group of variants is distinguished as *T.* cf. *crassipes*, because they posses highly arched and crooked synclades.

Thranium patulum Deflandre
(not illustrated)

Thranium patulum Deflandre, 1951, pp. 52–53, 77, Figs. 184, 185.

Class DINOPHYCEAE
Order PERIDINIALES Ehrenberg, 1830
Family ACTINISCACEAE Kützing, 1849
Genus *Actiniscus* Ehrenberg, 1841

Remarks: The star-shaped skeletons of most *Actiniscus* species usually have five arms, but in some stratigraphic intervals specimens with six arms are rather common. Skeletons with four or seven arms are rare in species that normally bear five arms.

Actiniscus elongatus Dumitrică
(not illustrated)

Actiniscus elongatus Dumitrică, 1968, p. 240, Pl. 4, Figs. 22, 26.

Actiniscus flosculus Locker and Martini
(Plate 8, Fig. 9)

Actiniscus flosculus Locker and Martini, 1986, p. 945, Pl. 3, Fig. 15; Pl. 4, Figs. 4–7.

Actiniscus laciniatus Locker and Martini
(not illustrated)
Actiniscus laciniatus Locker and Martini, 1986, p. 945, Pl. 3, Fig. 9.

Actiniscus pentasterias (Ehrenberg) Ehrenberg
(Plate 8, Figs. 6, 7)

Dictyocha (Actiniscus) pentasterias Ehrenberg, 1841, pp. 149–150.
Actiniscus pentasterias (Ehrenberg), Ehrenberg, 1854, Pl. 18, Fig. 61, and other plate-figures.
Gymnaster pentasterias (Ehrenberg), Schütt, 1895, pp. 31–35, Pl. 27, Figs. 100/1–4.

Actiniscus planatus n. sp.
(Plate 8, Figs. 2–4)

Holotype: SM.B 13775; Plate 8, Fig. 2.
Type locality: Vøring Plateau, Sample 104-642C-22H-1, 66–67 cm (middle Miocene).

Diagnosis: Central field entirely occupied by the enlarged central knob. Arms not developed. With sharp terrace lines between the pointed rays of the central star. Diameter 25.0- to 34.0 μm.

Remarks: This new species is distinguished from other *Actiniscus* taxa by its large flat central field and the absence of distinct arms. Beside the pentaradiate forms, hexaradiate were found rarely.

Occurrence: Found in Samples 104-642C-21H-4, 60–61 cm and 104-642C-22H-1, 66–67 cm (*S. miocenica* Zone/*H. schulzii* Zone, middle Miocene).

Actiniscus tetrasterias Ehrenberg
(Plate 8, Fig. 8)

Actiniscus tetrasterias Ehrenberg, 1845, p. 76.
Actiniscus sp.

Remarks: Under *Actiniscus* sp. undetermined skeletons are listed, including juvenile, slightly or highly silicified ones.

Genus *Foliactiniscus* Dumitrică, 1973
Foliactiniscus atlanticus Perch-Nielsen
(Plate 8, Fig. 15)

Foliactiniscus atlanticus Perch-Nielsen, 1978, p. 154, Pl. 6, Figs. 1–8.

Foliactiniscus folia (Hovasse) Dumitrică
(Plate 8, Fig. 14)

Gymnaster? folia Hovasse, 1943, p. 278, Fig. 1.
Foliactiniscus folia (Hovasse), Dumitrică, 1973c, p. 823, Pl. 1, Fig. 11.
Actiniscus folia (Hovasse), Bachmann, 1973, p. 285, Pl. 3, Figs. 7, 8.

Foliactiniscus mirabilis Dumitrică
(not illustrated)

Foliactiniscus mirabilis Dumitrică, 1973c, p. 823, Pl. 1, Figs. 12, 13, 20, Pl. 20, Figs. 4, 12, 13.

Foliactiniscus pulvinus n. sp.
(Plate 8, Figs. 11–13)

Holotype: SM.B 13776; Plate 8, Fig. 11.
Type locality: Vøring Plateau, Sample 104-642D-7X-5, 66–67 cm (lower Miocene).

Diagnosis: Central field large, with irregular concentric wrinkles. Arms indistinctly developed, with thin crests that adjoin the small and crooked central crest. Diameter 28.5- to 39.5 μm.

Remarks: This new species is distinguished from other *Foliactiniscus* taxa by the insignificant differentiation between central field and arms. In proximal view the skeletons resemble, therefore, a small glass shard.

Occurrence: Found only in Sample 104-642D-7X-5, 66–67 cm (*F. folia* Zone, lower Miocene).

ACKNOWLEDGMENTS

Thanks are due the Deutsche Forschungsgemeinschaft, Bonn, for supporting the present study. The Geologisch-Paläontologisches Institut der Universität, Kiel, generously provided space for laboratory work, and computer facilities (S.L.). We gratefully acknowledge various discussions with D. Spiegler, G. Bohrmann, R. Henrich, and T. Wolf, all members of the Kiel working group. Our thanks go also to Dr. David Murray for reviewing this paper. The type specimens of new taxa are deposited in the Naturmuseum und Forschungsinstitut Senckenberg, Frankfurt am Main, Germany, under Catalog Nos. SM.B 13762 to - 13776.

REFERENCES

Bachmann, A., 1970. Flagellata (Silicoflagellata). *Catalogus Fossilium Austriae*, 1b: 1-28.

_____, 1973. Die Silicoflagellaten aus dem Stratotypus des Ottnangien. *Chronostratotypen und Neostratotypen, Miozän der Zentralen Paratethys*, 3, M_2, Ottnanyien: Bratislava (Slowak. Acad. Wiss.), 275-295.

Barron, J. A., 1980. Lower Miocene to Quaternary diatom biostratigraphy of Leg 57 off northeastern Japan, Deep Sea Drilling Project. *In* Scientific Party, *Init. Repts. DSDP*, 56/57, Pt. 2: Washington (U.S. Govt. Printing Office), 641-685.

Barton, C. E., and Bloemendal, J., 1986. Paleomagnetism of sediments collected during Leg 90, Southwest Pacific. *In* Kennett, J. P., von der Borch, C. C., et al., *Init. Repts. DSDP*, 90: Washington (U.S. Govt. Printing Office), 1273-1316.

Berggren, W. A., Kent, D. V., Flynn, J. J., and van Couvering, J. A., 1985. Cenozoic geochronology. *Geol. Soc. Am. Bull.*, 96: 1407-1418.

Bleil, U., 1985. The magnetostratigraphy of Northwest Pacific sediments, Deep Sea Drilling Project Leg 86. *In* Heath, G. R., Burckle, L. H., et al., *Init. Repts. DSDP*, 86: Washington (U.S. Govt. Printing Office), 441-458.

Bukry, D., 1973. Coccolith stratigraphy, eastern equatorial Pacific, Leg 16 Deep Sea Drilling Project. *In* van Andel, T. H., Heath, G. R., et al., *Init. Repts. DSDP*, 16: Washington (U.S. Govt. Printing Office), 653-711.

_____, 1975a. Silicoflagellate and coccolith stratigraphy, Deep Sea Drilling Project Leg 29. *In* Kennett, J. P., Houtz, R. E., et al., *Init. Repts. DSDP*, 29: Washington (U.S. Govt. Printing Office), 845-872.

_____, 1975b. Coccolith and silicoflagellate stratigraphy, northwestern Pacific Ocean, Deep Sea Drilling Project Leg 32. *In* Larson, R. L., Moberly, R., et al., *Init. Repts. DSDP*, 32: Washington (U.S. Govt. Printing Office), 677-701.

_____, 1976a. Silicoflagellate and coccolith stratigraphy, southeastern Pacific Ocean, Deep Sea Drilling Project Leg 34. *In* Yeats, R. S., Hart, S. R., et al., *Init. Repts. DSDP*, 34: Washington (U.S. Govt. Printing Office), 715-735.

_____, 1976b. Cenozoic silicoflagellate and coccolith stratigraphy, South Atlantic Ocean, Deep Sea Drilling Project Leg 36. *In* Hollister, C. D., Craddock, C., et al., *Init. Repts. DSDP*, 35: Washington (U.S. Govt. Printing Office), 885-917.

_____, 1976c. Silicoflagellate and coccolith stratigraphy, Norwegian-Greenland Sea, Deep Sea Drilling Project Leg 38. *In* Talwani, M., Udintsev, G., et al., *Init. Repts. DSDP*, 38: Washington (U.S. Govt. Printing Office), 843-855.

_____, 1978a. Cenozoic coccolith and silicoflagellate stratigraphy, offshore Northwest Africa, Deep Sea Drilling Project Leg 41. *In* Lancelot Y., Seibold, E., et al., *Init. Repts. DSDP*, 41: Washington (U.S. Govt. Printing Office), 689-707.

_____, 1978b. Cenozoic coccolith, silicoflagellate, and diatom stratigraphy, Deep Sea Drilling Project Leg 44. *In* Benson, W. E., Sheridan, R. E., et al., *Init. Repts. DSDP*, 44: Washington (U.S. Govt. Printing Office), 807-863.

_____, 1979. Coccolith and silicoflagellate stratigraphy, northern Mid-Atlantic Ridge and Reykjanes Ridge, Deep Sea Drilling Project Leg 49. *In* Luyendyk, B. P., Cann, J. R., et al., *Init. Repts. DSDP*, 49: Washington (U.S. Govt. Printing Office), 551-581.

_____, 1980. Miocene *Corbisema triacantha* Zone phytoplankton from Deep Sea Drilling Project Sites 415 and 416, off Northwest Africa. *In* Lancelot, Y, Winterer, E. L., et al., *Init. Repts. DSDP*, 50: Washington (U.S. Govt. Printing Office), 507-523.

_____, 1981a. Synthesis of silicoflagellate stratigraphy for Maestrichtian to Quaternary marine sediment. *Spec. Publ. Soc. Econ. Paleontol. Mineral.*, 32: 433-444.

_____, 1981b. Silicoflagellate stratigraphy of offshore California and Baja California, Deep Sea Drilling Project Leg 63. *In* Yeats, R. S., Haq, B. U., et al., *Init. Repts. DSDP*, 63: Washington (U.S. Govt. Printing Office), 539-557.

_____, 1982. Cenozoic silicoflagellates from offshore Guatemala, Deep Sea Drilling Project Site 495. *In* Aubouin, J., von Huene, R., et al., *Init. Repts. DSDP*, 67: Washington (U.S. Govt. Printing Office), 425-445.

_____, 1985a. Mid-Atlantic Ridge coccolith and silicoflagellate biostratigraphy, Deep Sea Drilling Project Sites 558 and 563. *In* Bougault, H., Cande, S. C., et al., *Init. Repts. DSDP*, 82: Washington (U.S. Govt. Printing Office), 591-603.

_____, 1985b. Tropical Pacific silicoflagellate zonation and paleotemperature trends of the late Cenozoic. *In* Mayer, L., Theyer, F., et al., *Init. Repts. DSDP*, 85: Washington (U.S. Govt. Printing Office), 477-497.

_____, 1987a. North Atlantic Quaternary silicoflagellates , Deep Sea Drilling Project Leg 94. *In* Ruddiman, W. F., Kidd, R. B., et al., *Init. Repts. DSDP*, 94: Washington (U.S. Govt. Printing Office), 779-783.

_____, 1987b. Eocene siliceous and calcareous phytoplankton, Deep Sea Drilling Project Leg 95. *In* Poag, C. W., Watts, A. B., et al., *Init. Repts. DSDP*, 95: Washington (U.S. Govt. Printing Office), 395-415.

Bukry, D., and Foster J. J., 1973. Silicoflagellate and diatom stratigraphy, Leg 16, Deep Sea Drilling Project. *In* van Andel, T. H., Heath, G. R., et al., *Init. Repts. DSDP*, 16: Washington (U.S. Govt. Printing Office), 815-871.

Bukry, D., and Monechi, S., 1985. Late Cenozoic silicoflagellates from the Northwest Pacific, Deep Sea Drilling Project Leg 86: paleotemperature trends and texture classification. *In* Heath, G. R., Burckle, L. H., et al., *Init. Repts. DSDP*, 86: Washington (U.S. Govt. Printing Office), 367-397.

Burns, D. A., 1975. Nannofossil biostratigraphy for Antarctic sediments, Leg 28, Deep Sea Drilling Project. *In* Hayes, D. E., Frakes, L. A., et al., *Init. Repts. DSDP*, 28: Washington (U.S. Govt. Printing Office), 589-598.

Busen, K. E., and Wise, S. W., 1977. Silicoflagellate stratigraphy, Deep Sea Drilling Project Leg 36. *In* Barker, P. F., Dalziel, I.W.D., et al., *Init. Repts. DSDP*, 36: Washington (U.S. Govt. Printing Office), 697-743.

Ciesielski, P. F., 1975. Biostratigraphy and paleoecology of Neogene and Oligocene silicoflagellates from cores recovered during Antarctic Leg 28, Deep Sea Drilling Project . In Hayes, D. E., Frankes, L. A., et al., Init. Repts. DSDP, 28: Washington (U.S. Govt. Printing Office), 625-691.

_____, 1983. The Neogene and Quaternary diatom biostratigraphy of Subantarctic sediments , Deep Sea Drilling Project Leg 71. In Ludwig, W. J., Krasheninnikov, V. A., et al., Init. Repts. DSDP, 71: Washington (U.S. Govt. Printing Office), 635-665.

Deflandre, G., 1934. Nomenclature du squelette des Ebriacées et description de quelques formes nouvelles. Ann. Protist., 4: 75-96.

_____, 1951. Recherches sur les Ebriédiens: paléobiologie, évolution, systématique. *Bull. Biol. France Belg.*, 85:1-84.

Dumitrică, P., 1968. Consideratii micropaleontologice asupra orizontului argilos cu radiolari din Tortonianul regiunii carpatice. *Stud. Cerc. Geol. Geofiz. Geogr.*, 13:227-241.

_____, 1973a. Miocene and Quaternary silicoflagellates in sediments from the Mediterranean Sea. In Ryan, W.B.F., Hsü, K. J., et al., *Init. Repts. DSDP*, 13: Washington (U.S. Govt. Printing Office), 902-933.

_____, 1973b. Miocene and Quaternary ebridians from the Mediterranean Sea, Deep Sea Drilling Project Leg 13. *In* Ryan, W.B.F., Hsü, K. J., et al., *Init. Repts. DSDP*, 13: Washington (U.S. Govt. Printing Office), 934-939.

Dumitrică, P., 1973c. Cenozoic endoskeletal dinoflagellates in southwestern Pacific sediments cored during Leg 21 of the DSDP. *In* Burns, R. E., Andrews, J. E., et al., *Init. Repts. DSDP*, 21: Washington (U.S. Govt. Printing Office), 819-835.

_____, 1973d. Paleocene, late Oligocene and post-Oligocene silicoflagellates in southwestern Pacific sediments cored on DSDP Leg 21. *In* Burns, R. E., Andrews, J. E., et al., *Init. Repts. DSDP*, 21: Washington (U.S. Govt. Printing Office), 837–883.

_____, 1978. Badenian Silicoflagellates from Central Paratethys. *In* Papp, A., Cicha, I., et al. (Eds.), *Chronostratigraphie und Neostratotypen, Miozän der Zentralen Paratethys*, 6, M_4, Badenien, Bratislava (Slowak. Acad. Wiss.), 207–229.

Edwards, A. R., 1973. Calcareous nannofossils from the Southwest Pacific, Deep Sea Drilling Project Leg 21. *In* Burns, R. E., Andrews, J. E., et al., *Init. Repts. DSDP*, 21: Washington (U.S. Govt. Printing Office), 641–691.

Edwards, A. R., and Perch-Nielsen, K., 1975. Calcareous nannofossils from the southern Southwest Pacific, Deep Sea Drilling Project, Leg 29. *In* Kennett, J. P., Houtz, R. E., et al., *Init. Repts. DSDP*, 29: Washington (U.S. Govt. Printing Office), 469–539.

Eldholm, O., Thiede, J., and Taylor, E., 1987. Evolution of the Norwegian continental margin: background and objectives. *In* Eldholm, O., Thiede, J., Taylor, E., et al., *Proc. ODP, Init. Repts.*, 104: College Station, TX (Ocean Drilling Program), 5–25.

Eldholm, O., Thiede, J., Taylor, E., et al., 1987. *Proc. ODP, Init. Repts.*, 104: College Station, TX (Ocean Drilling Program).

Gemeinhardt, K., 1931. Organismenformen an der Grenze zwischen Radiolarien und Flagellaten. *Ber. Dtsch. Bot. Ges.*, 49:103–110.

Hodell, D. A., and Kennett, J. P., 1986. Late Miocene—early Pliocene stratigraphy and paleoceanography of the South Atlantic and Southwest Pacific Oceans: a synthesis *Paleoceanography*, 1: 285–311.

Hovasse, R., 1943. Nouvelles recherches sur les flagellés á squelette silicieux: Ebriidés et Silicoflagellés fossiles de la diatomite de Saint-Laurent-la-Vernède (Gard). *Bull. Biol. France Belg.*, 77:271–294.

ICBN. See Stafleu, F. A. (Ed.).

Kanaya, T., and Koizumi, I., 1966. Interpretation of diatom thanatocoenoses from the North Pacific applied to a study of Core V20-130. *Sci. Rep., Tohoku Univ. Sendai*, 2nd Ser, 37:89–130.

Kaneps, A., 1973. Carbonate chronology for Pliocene deep-sea sediments. *In* van Andel, T. H., Heath, G. R., et al., *Init. Repts. DSDP*, 16: Washington (U.S. Govt. Printing Office), 873–881.

Keigwin, L. D., 1987. Pliocene stable-isotope record of Deep Sea Drilling Project Site 606: sequential events of $^{18}0$ enrichment beginning at 3.1 Ma. *In* Ruddiman, W. F., Kidd., R. B., et al., *Init. Repts. DSDP*, 94: Washington (U.S. Govt. Printing Office), 911–920.

Keigwin, L. D., Aubry, M.-P., and Kent, D.-V., 1987. North Atlantic late Miocene stable-isotope stratigraphy, biostratigraphy, and magnetostratigraphy. *In* Ruddiman, W. F., Kidd, R. B., et al., *Init. Repts. DSDP*, 94: Washington (U.S. Govt. Printing Office), 935–963.

Kennett, J. P., 1982. *Marine Geology*: Englewood Cliffs N. J. (Prentice-Hall Inc.).

Koizumi, I., 1973. The late Cenozoic diatoms of Sites 183-193, Leg 19, Deep Sea Drilling Project. *In* Creager, J. S., Scholl, D. W., et al., *Init. Repts. DSDP*, 19: Washington (U.S. Govt. Printing Office), 805–855.

Ling, H. Y., 1970. Silicoflagellates from central North Pacific core sediments. *Bull. Am. Paleontol.*, 58: 85–129.

_____, 1972. Upper Cretaceous and Cenozoic silicoflagellates and ebridians. *Bull. Am. Paleontol.*, 62: 135–229.

_____, 1973. Silicoflagellates and ebridians from Leg 119. *In* Creager, J. S., Scholl, D. W., et al., *Init. Repts. DSDP*, 19: Washington (U.S. Govt. Printing Office), 751–775.

_____, 1976. Distribution and biostratigraphic siginificance of *Dictyocha subarctios* (silicoflagellate) in the North Pacific. *Trans. Proc. Paleontol. Soc. Japan*, N.S., 101:264–270.

_____, 1977. Late Cenozoic Silicoflagellates and Ebridians from the eastern North Pacific region. *Proc. Intern. Congr. Pacific Neogene Stratigr., Ist*, Tokyo, Japan, 1976:205–233.

Loeblich III, A. R., Loeblich, L. A., Tappan, H., and Loeblich, A. R. Jr., 1968. Annotated Index of Fossil and Recent Silicoflagellates and Ebridians. *Mem. Geol. Soc. Am.*, 106.

Locker, S., 1974. Revision der Silicoflagellaten aus der Mikrogeologischen Sammlung von C. G. Ehrenberg. *Ecl. Geol. Helv.*, 67: 631–646.

_____, 1975. *Dictyocha varia* sp. n., eine miozäne Silicoflagellaten-Art mit kompliziertem Variationsmodus. *Z. Geol. Wiss.*, 3: 99–103.

Locker, S., and Martini, E., 1986a. Silicoflagellates and some sponge spicules from the Southwest Pacific, Deep Sea Drilling Project Leg 90. *In* Kennett, J. P., von der Borch, C. C., et al., *Init. Repts. DSDP*, 90: Washington (U.S. Govt. Printing Office), 887–924.

_____, 1986b. Ebridians and actiniscidians from the southwest Pacific. *In* Kennett, J. P., von der Borch, C. C., et al., *Init. Repts. DSDP*, 90: Washington (U.S. Govt. Printing Office), 939–951.

Lohmann, W. H., 1986. Calcareous nannoplankton biostratigraphy of the southern Coral Sea, Tasman Sea, and southwestern Pacific Ocean, Deep Sea Drilling Project Leg 90: Neogene and Quaternary. *In* Kennett, J. P., von der Borch, C. C., et al., *Init. Repts. DSDP*, 90: Washington (U.S. Govt. Printing Office), 763–793.

Martini, E., 1971. Neogene silicoflagellates from the equatorial Pacific. *In* Winterer, E. L., Riedel, W. R., et al., *Init. Repts. DSDP*, 7: Washington (U.S. Govt. Printing Office), 1695–1708.

_____, 1972. Silicoflagellate zones in the late Oligocene and early Miocene of Europe. *Senck. Leth.*, 53: 119–122.

_____, 1979. Calcareous nannoplankton and silicoflagellate biostratigraphy at Reykjanes Ridge, northeastern North Atlantic (DSDP Leg 49, Sites 407 and 409). *In* Luyendyk, B. P., Cann, J. R., et al., *Init. Repts. DSDP*, 49: Washington (U.S. Govt. Printing Office), 533–549.

Martini, E., and Müller, C., 1976. Eocene to Pleistocene silicoflagellates from the Norwegian-Greenland Sea (DSDP Leg 38). *In* Talwani, M., Udintsev, G., et al., *Init. Repts. DSDP*, 38: Washington (U.S. Govt. Printing Office), 857–895.

_____, 1986. Current Tertiary and Quaternary calcareous nannoplankton stratigraphy and correlations. *Newsl. Strat.*, 16:99–112.

Müller, C., 1976. Tertiary and Quaternary calcareous nannoplankton in the Norwegian-Greenland Sea, DSDP Leg 38. *In* Talwani, M., Udintsev, G., et al., *Init. Repts*. DSDP, 38: Washington (U.S. Govt. Printing Office), 823–841.

Perch-Nielsen, K., 1975a. Late Cretaceous to Pleistocene silicoflagellates from the southern Southwest Pacific, DSDP Leg 29. *In* Kennett, J. P., Houtz, R. E., et al., *Init. Repts. DSDP*, 29: Washington (U.S. Govt. Printing Office), 677–721.

_____, 1975b. Late Cretaceous to Pleistocene archaeomonads, ebridians, endoskeletal dinoflagellates, and other siliceous microfossils from the subantarctic southwest Pacific, DSDP Leg 29. *In* Kennett, J. P., Houtz, R. E., et al., *Init. Repts. DSDP*, 29: Washington (U.S. Govt. Printing Office), 873–907.

_____, 1978. Eocene to Pliocene archaeomonads, ebridians, and endoskeletal dinoflagellates from the Norwegian Sea, DSDP Leg 38. *In* Talwani, M., Udintsev, G., et al., *Init. Repts. DSDP*, Suppl. 38–41: Washington (U.S. Govt. Printing Office), 147–175.

_____, 1985. Silicoflagellates. *In* Bolli, H. M., Saunders, J. B., and Perch-Nielsen, K. (Eds.), *Plankton Stratigraphy*: Cambridge, U.K. (Cambridge Univ. Press) 811–846.

Poelchau, H. S., 1976. Distribution of Holocene silicoflagellates in North Pacific sediments. *Micropaleontology*, 22:164–193.

Pujot, A., 1985. Cenozoic nannofossils, central equatorial Pacific, Deep Sea Drilling Project Leg 85. *In* Mayer, L., Theyer, F., et al., *Init. Repts. DSDP*, 85: Washington (U.S. Govt. Printing Office), 581–607.

Ruddiman, W. F., Backman, J., Baldauf, J., Hooper, P., Keigwin, L., Miller, K., Raymo, M., and Thomas, E., 1987. Leg 94 paleoenvironmental synthesis. *In* Ruddiman, W. F., Kidd, R. B., et al., *Init. Repts. DSDP*, 94: Washington (U.S. Govt. Printing Office), 1207–1215.

Ruddiman, W. F., McIntyre, A., and Raymo, M., 1987. Paleoenvironmental results from North Atlantic Sites 607 and 609. *In* Ruddiman, W. F., Kidd, R. B., et al., *Init. Repts.* DSDP, 94: Washington (U.S. Govt. Printing Office), 855–878.

Schulz, P., 1928. Beiträge zur Kenntnis fossiler und rezenter Silicoflagellaten. *Bot. Arch.*, 21:225–292.

Schwerdtfeger, F., 1975. *Ökologie der Tiere*. Band 3: *Synökologie*. Hamburg—Berlin (Parey).

Shackleton, N. J., and Hall, M. A., 1984. Oxygen and carbon isotope stratigraphy of Deep Sea Drilling Project Hole 552A: Plio-Pleistocene glacial history. *In* Roberts, D. G., Schnitker, D., et al., *Init. Repts. DSDP*, 81: Washington (U.S. Govt. Printing Office), 599–609.

Shackleton, N. J., Hall, M. A., and Boersma, A., 1984. Oxygen and carbon isotope data from Leg 74 foraminifers. *In* Moore, T. C., Jr., Rabinowitz, P. D., et al., *Init. Repts. DSDP*, 74: Washington (U.S. Govt. Printing Office), 599–612.

Shackleton, N. J., and Kennett, J. P., 1975. Paleotemperature history of the Cenozoic and the initiation of antarctic glaciation: oxygen and carbon isotope analyses in DSDP Sites 277, 279, and 281. *In* Kennett, J. P., Houtz, R. E., et al., *Init. Repts. DSDP*, 29: Washington (U.S. Govt. Printing Office), 743–755.

Shaw, C. A., and Ciesielski, P. F., 1983. Silicoflagellate biostratigraphy of middle Eocene to Holocene subantarctic sediments recovered by Deep Sea Drilling Project Leg 71. *In* Ludwig, W. J., Krasheninnikov, V. A., et al., *Init. Repts. DSDP*, 71: Washington (U.S. Govt. Printing Office), 687–737.

Stafleu, F. A. (Ed.), 1978. *International Code of Botanical Nomenclature, Adopted by the Twelfth International Botanical Congress, Leningrad, July 1975*. Utrecht (Bohn, Scheltema and Holkema).

Tappan, H., 1980. *The Paleobiology of Plant Protists*: San Francisco (Freemann and Co.).

Weinreich, N., and Theyer, F., 1985. Paleomagnetism of Deep Sea Drilling Project Leg 85 sediments: Neogene magnetostratigraphy and tectonic history of the central equatorial Pacific. *In* Mayer, L., Theyer, F., et al., *Init. Repts. DSDP*, 85: Washington (U.S. Govt. Printing Office), 849–901.

Wise, S. W., 1973. Calcareous nannofossils from cores recovered during Leg 18, Deep Sea Drilling Project: biostratigraphy and observations of diagenesis. *In* Kulm, L. D., von Huene, R., et. al., *Init. Repts. DSDP*, 18: Washington (U.S. Govt. Printing Office), 569–615.

Yanagisawa, T., 1943. Klishitsu benmochu nitsuite (Silicoflagellatae). *Umi to Sora*, 23.

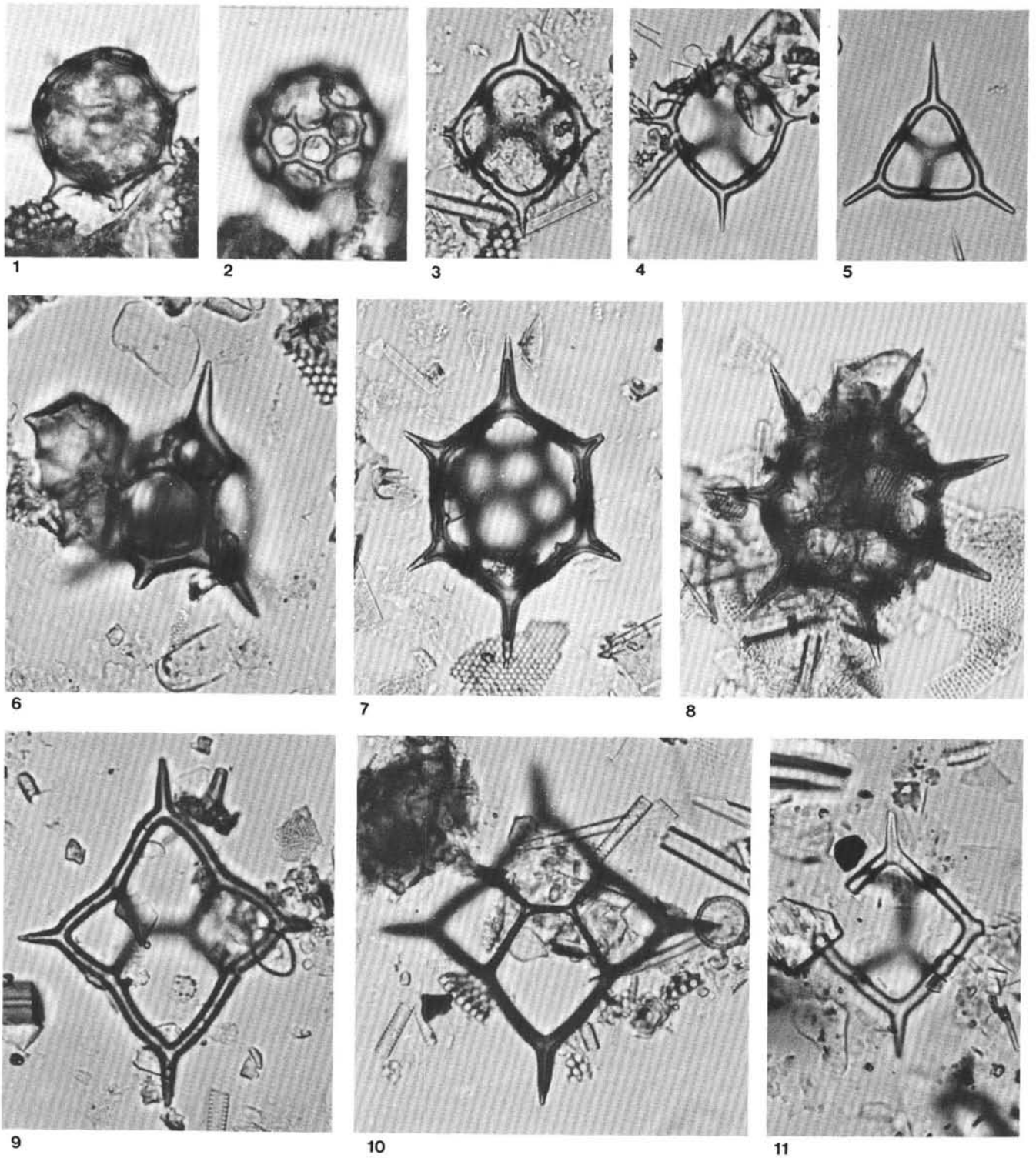

Plate 1. Lower Miocene to upper Pliocene silicoflagellates. All specimens magnified ×800, bar = 10 μm. **1, 2.** *Cannopilus depressus* (Ehrenberg), low and high focus, Sample 104-642C-23H-5, 70–71 cm, middle Miocene. **3.** *Dictyocha varia* Locker, Sample 104-642C-19H-5, 50–51 cm, middle Miocene. **4.** *Dictyocha messanensis* subsp. *aspinosa* (Bukry), Sample 104-642D-10X-4, 70–71 cm, lower Miocene. **5.** *Corbisema triacantha* (Ehrenberg), Sample 104-642D-10X-2, 70–71 cm, lower Miocene. **6.** *Cannopilus ernestinae* Bachmann, Sample 104-642C-20H-4, 55–56 cm, middle Miocene. **7.** *Cannopilus hemisphaericus* (Ehrenberg) f. *hemisphaericus*, Sample 104-642D-7X-5, 66–67 cm, lower Miocene. **8.** *Cannopilus hemisphaericus* f. *heptagonus* n.f., holotype, Sample 104-642D-6X-2, 66–67 cm, lower Miocene. **9.** *Dictyocha fibula* Ehrenberg s.l., Sample 104-642C-15H-4, 66–67 cm, upper Miocene. **10.** *Dictyocha fibula* subsp. *tenuis* n. subsp., holotype, Sample 104-642C-23H-5, 70–71 cm, middle Miocene. **11.** *Dictyocha messanensis* Haeckel subsp. *messanensis*, Sample 104-644A-20H-4, 66–67 cm, upper Pliocene.

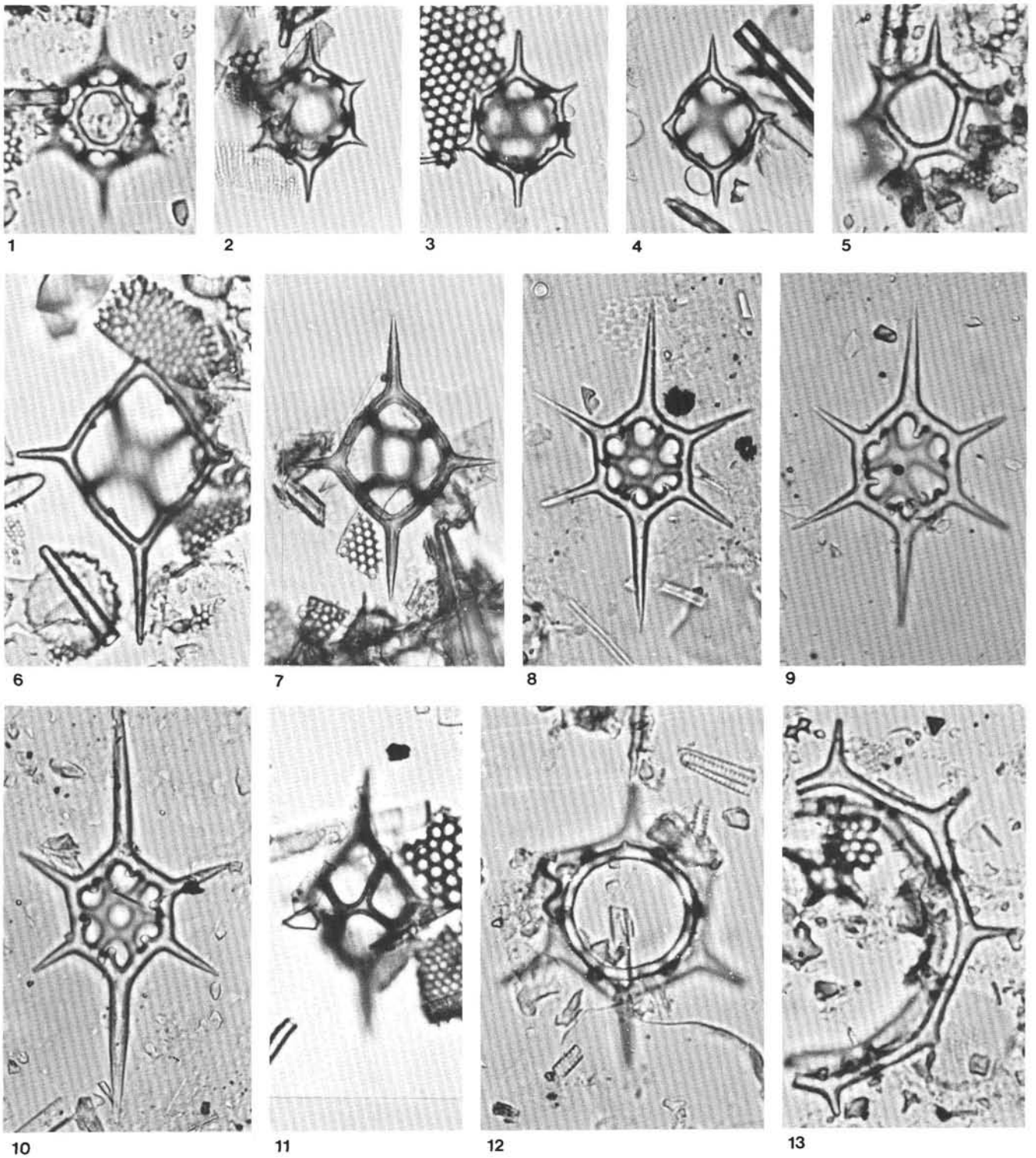

Plate 2. Lower Miocene to upper Pliocene silicoflagellates. All specimens magnified ×800, bar = 10 μm. **1.** *Distephanus speculum* (Ehrenberg) s.l. f. *speculum*, coronoid variant, Sample 104-642C-9H-1, 64–65 cm, upper Pliocene. **2.** *Distephanus speculum* subsp. *haliomma* (Ehrenberg) f. *speculum*, Sample 104-642D-6X-2, 66–67 cm, lower Miocene. **3.** *Distephanus speculum* subsp. *haliomma* (Ehrenberg) f. *haliomma*, Sample 104-642D-9X-2, 66–67 cm, lower Miocene. **4.** *Distephanus crux* subsp. *darwinii* Bukry, Sample 104-642D-10X-2, 70–71 cm, lower Miocene. **5.** *Distephanus stauracanthus* f. *octagonus* (Tsumura), Sample 104-642C-19H-5, 50–51 cm, middle Miocene. **6.** *Distephanus crux* subsp. *stradneri* (Jerković), Sample 104-642D-10X-4, 70–71 cm, lower Miocene. **7.** *Distephanus crux* (Ehrenberg) subsp. *crux*, Sample 104-642C-24H-5, 70–71 cm, lower Miocene. **8, 10.** *Distephanus speculum* subsp. *constrictus* f. *constrictus* n. subsp.; **8.** Holotype, Sample 104-644A-34H-5, 66–67 cm, upper Pliocene; **10.** Syntype, Sample 104-642C-11H-2, 52–53 cm, upper Pliocene. **9.** *Distephanus speculum* subsp. *constrictus* f. *varians* Gran and Braarud, Sample 104-642C-11H-2, 52–53 cm, upper Pliocene. **11.** *Dictyocha subclinata* Bukry, Sample 104-642D-10X-2, 70–71 cm, lower Miocene. **12.** *Distephanus speculum* subsp. *giganteus* Bukry, Sample 104-642C-13H-1, 66–67 cm, lower Pliocene. **13.** *Distephanus polyactis* (Ehrenberg), Sample 104-642C-11H-5, 65–66 cm, upper Pliocene.

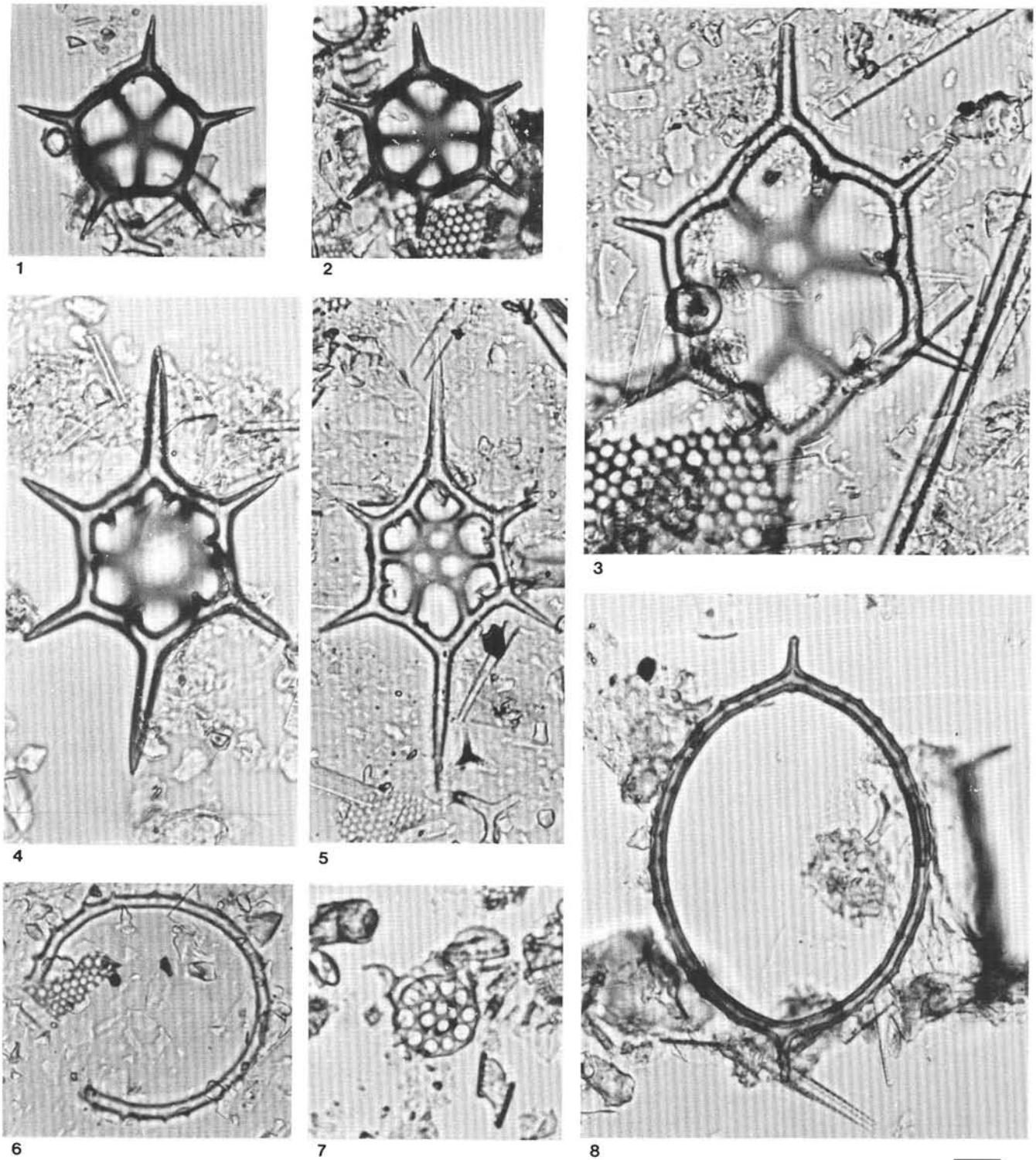

Plate 3. Lower Miocene to upper Pliocene silicoflagellates. All specimens magnified ×800, bar = 10 μm. **1.** *Distephanus paraspeculum* f. *paraspeculum* n. subsp., holotype, Sample 104-642D-9X-2, 66–67 cm, lower Miocene. **2.** *Distephanus paraspeculum* f. *hexagonalis* n.f., holotype, Sample 104-642D-9X-2, 66–67 cm, lower Miocene. **3.** *Distephanus sulcatus* f. *maximus* n.f., holotype, Sample 104-642C-10H-4, 71–72 cm, upper Pliocene. **4.** *Distephanus aculeatus* (Ehrenberg) f. *aculeatus*, Sample 104-642C-13H-1, 66–67 cm, lower Pliocene. **5.** *Distephanus aculeatus* f. *binoculus* (Ehrenberg), Sample 104-642C-10H-4, 71–72 cm, upper Pliocene. **6.** *Paramesocena circulus* subsp. *circulus* (Ehrenberg), Sample 104-642C-11H-2, 52–53 cm, upper Pliocene. **7.** *Macrora stella* (Azpeitia), synuracean species, Sample 104-642D-8X-5, 66–67 cm, lower Miocene. **8.** *Mesocena diodon* Ehrenberg, Sample 104-642C-14H-2, 66–67 cm, upper Miocene.

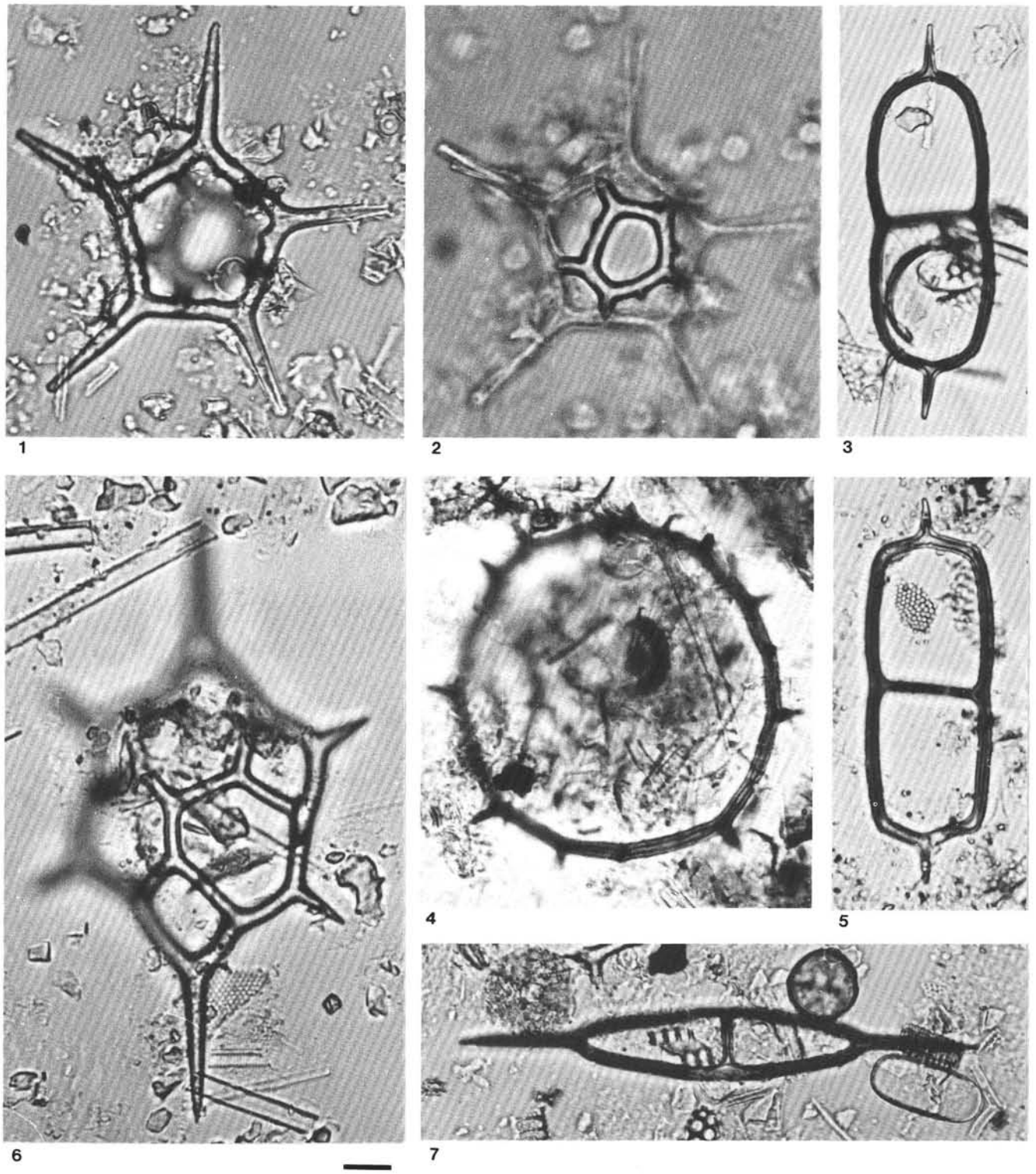

Plate 4. Lower Miocene to upper Pliocene silicoflagellates. All specimens magnified ×800, bar = 10 μm. **1, 2.** *Distephanus quinarius* n. sp.; **1.** Holotype, **2.** syntype; both, Sample 104-642C-15H-1, 66–67 cm, upper Miocene. **3.** *Naviculopsis iberica* Deflandre, Sample 104-642D-6X-4, 66–67 cm, lower Miocene. **4.** *Paramesocena circulus* subsp. *apiculata* (Lemmermann), Sample 104-642C-17H-5, 50–51 cm, upper Miocene. **5.** *Naviculopsis quadratum* (Ehrenberg), Sample 104-642D-8X-2, 66–67 cm, lower Miocene. **6.** *Distephanus sulcatus* Bukry, variant with apical bars, Sample 104-642C-10H-4, 71–72 cm, upper Pliocene. **7.** *Naviculopsis lacrima* Bukry, Sample 104-642C-19H-5, 50–51 cm, middle Miocene.

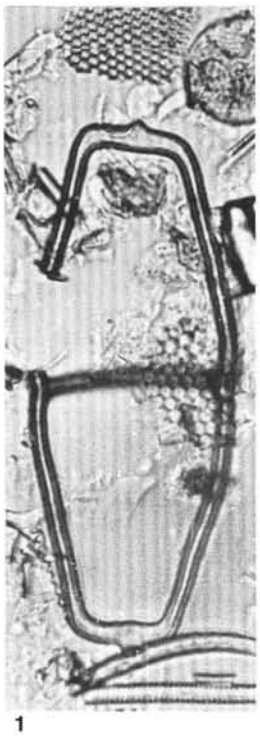

1

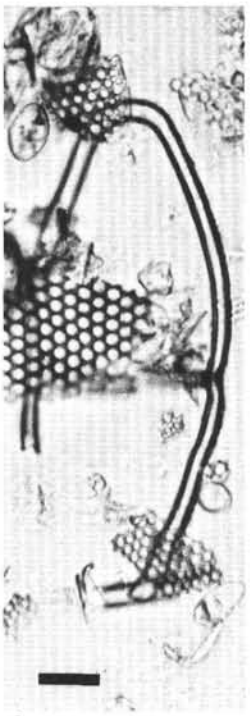

2

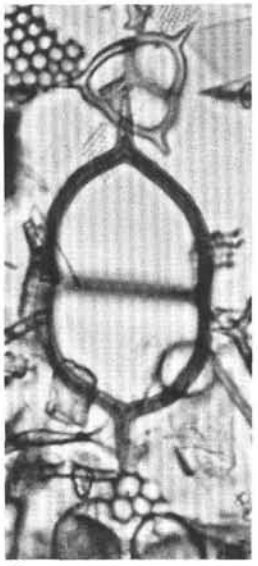

3

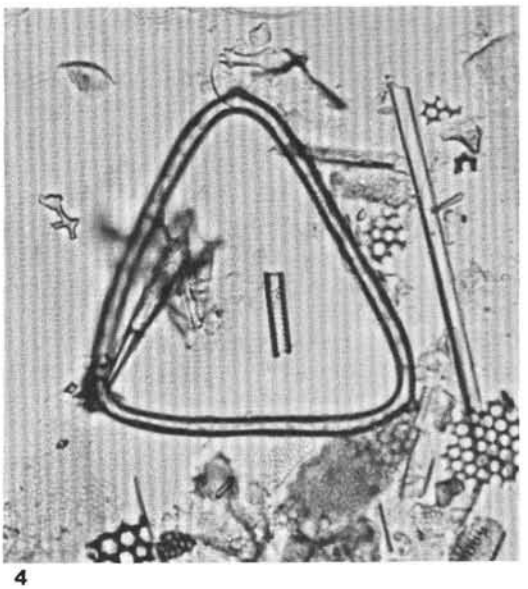

4

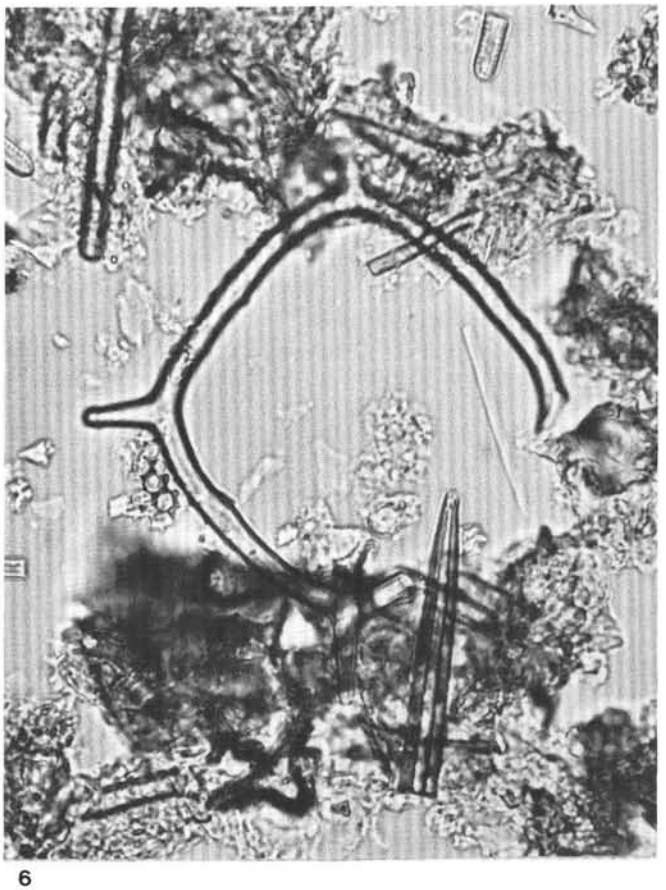

6

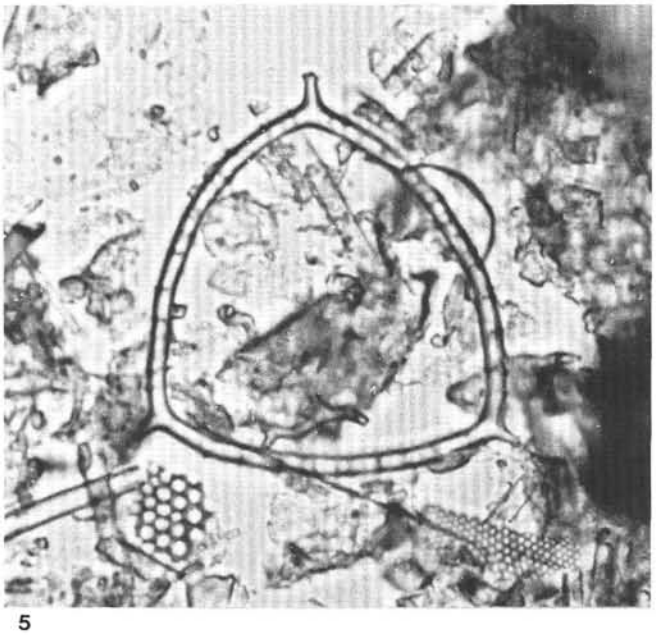

5

Plate 5. Lower to upper Miocene silicoflagellates. All specimens magnified ×800, bar = 10 μm. **1.** *Naviculopsis navicula* subsp. *obtusarca* (Bukry), Sample 104-642D-8X-5, 66–67 cm, lower Miocene. **2.** *Naviculopsis navicula* (Ehrenberg) subsp. *navicula*, Sample 104-642D-8X- 5, 66–67 cm, lower Miocene. **3.** *Naviculopsis lata* (Deflandre), Sample 104-642D-10X-2, 70–71 cm, lower Miocene. **4.** *Septamesocena apiculata* (Lemmermann) f. *apiculata*, Sample 104-642D-6X-2, 66–67 cm, lower Miocene. **5.** *Mesocena triangula* (Ehrenberg), Sample 104-642C-14H-2, 66–67 cm, upper Miocene. **6.** *Mesocena quadrangula* Ehrenberg ex Haeckel, Sample 104-642C-14H-2, 66–67 cm, upper Miocene.

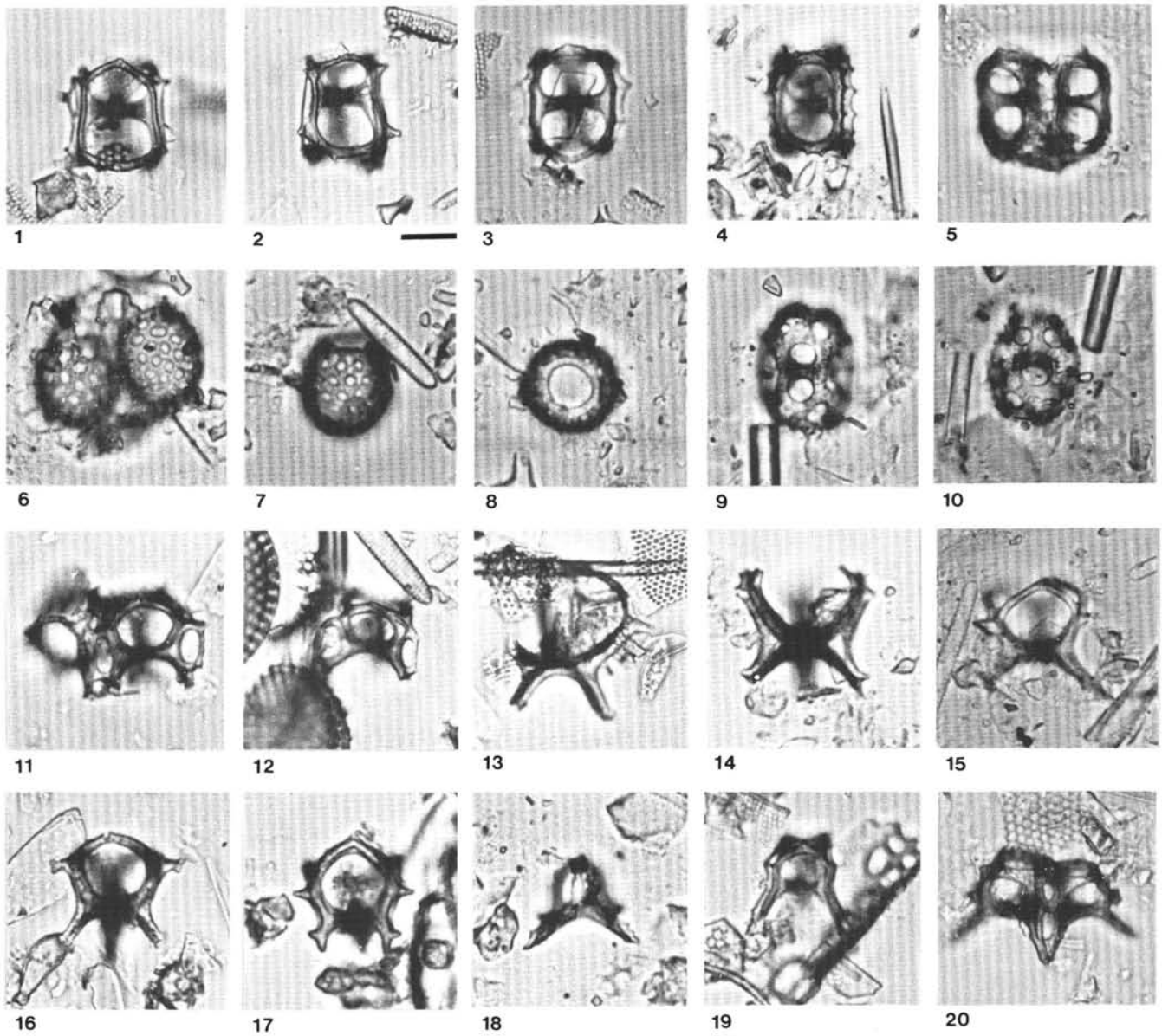

Plate 6. Lower Miocene to Pleistocene ebridians. All specimens magnified ×800, bar = 10 μm. **1, 2.** *Ammodochium pyramidale* Hovasse; **1.** Sample 104-642D-6X-2, 66–67 cm, lower Miocene; **2.** Sample 104-642D-10X-4, 70–71 cm, lower Miocene. 3–5. *Ammodochium serotinum* Locker and Martini; **3.** Sample 104-642C-20H-4, 55–56 cm, middle Miocene; **4.** Sample 104-642C-17H-5, 50–51 cm, upper Miocene; **5.** double skeleton, Sample 104-642C-16H-1, 50–51 cm, upper Miocene. **6–8.** *Pseudammodochium robustum* Deflandre; **6.** Double skeleton, Sample 104-642C-llH-5, 65–66 cm, upper Pliocene; **7.** Sample 104-642C-9H-1, 64–65 cm, upper Pliocene; **8.** Apical view, Sample 104-642C-10H-4, 71–72 cm, upper Pliocene. **9, 10.** *Pseudammodochium fenestratum* n. sp.; **9.** Syntype, Sample 104-644A-26H-2, 48–49 cm, upper Pliocene; **10.** Holotype, Sample 104-644A-16H-1, 66–67 cm, Pleistocene. **11, 12.** *Ditripodium latum* Hovasse; **11.** Double skeleton, Sample 104-642C-23H-5, 70–71 cm, middle Miocene; **12.** Sample 104-642C-22H-4, 60–61 cm, middle Miocene. **13.** *Ditripodium amphora* Hovasse, Sample 104-642D-4X-5, 62–63 cm, lower Miocene. **14.** *Ditripodium elephantinum* Hovasse, Sample 104-642C-17H-5, 50–51 cm, upper Miocene. **15.** *Ditripodium japonicum* Deflandre, Sample 104-642C-11H,65–66 cm, upper Pliocene. **16.** *Thranium crassipes* Hovasse, Sample 104-642C-22H-1, 66–67 cm, middle Miocene. **17.** *Thranium* cf. *crassipes* Hovasse, Sample 104-64 2C-14H-5, 55–56 cm, upper Miocene. **18.** *Parathranium* cf. *californicum* Deflandre, Sample 104-642C-16H-4, 50–51 cm, upper Miocene. **19, 20.** *Parathranium bispinum* Deflandre; **19.** Sample 104-642D-6X-2, 66–67 cm, lower Miocene; **20.** Double skeleton, Sample 104-642C-12H-5, 65–66 cm, lower Pliocene.

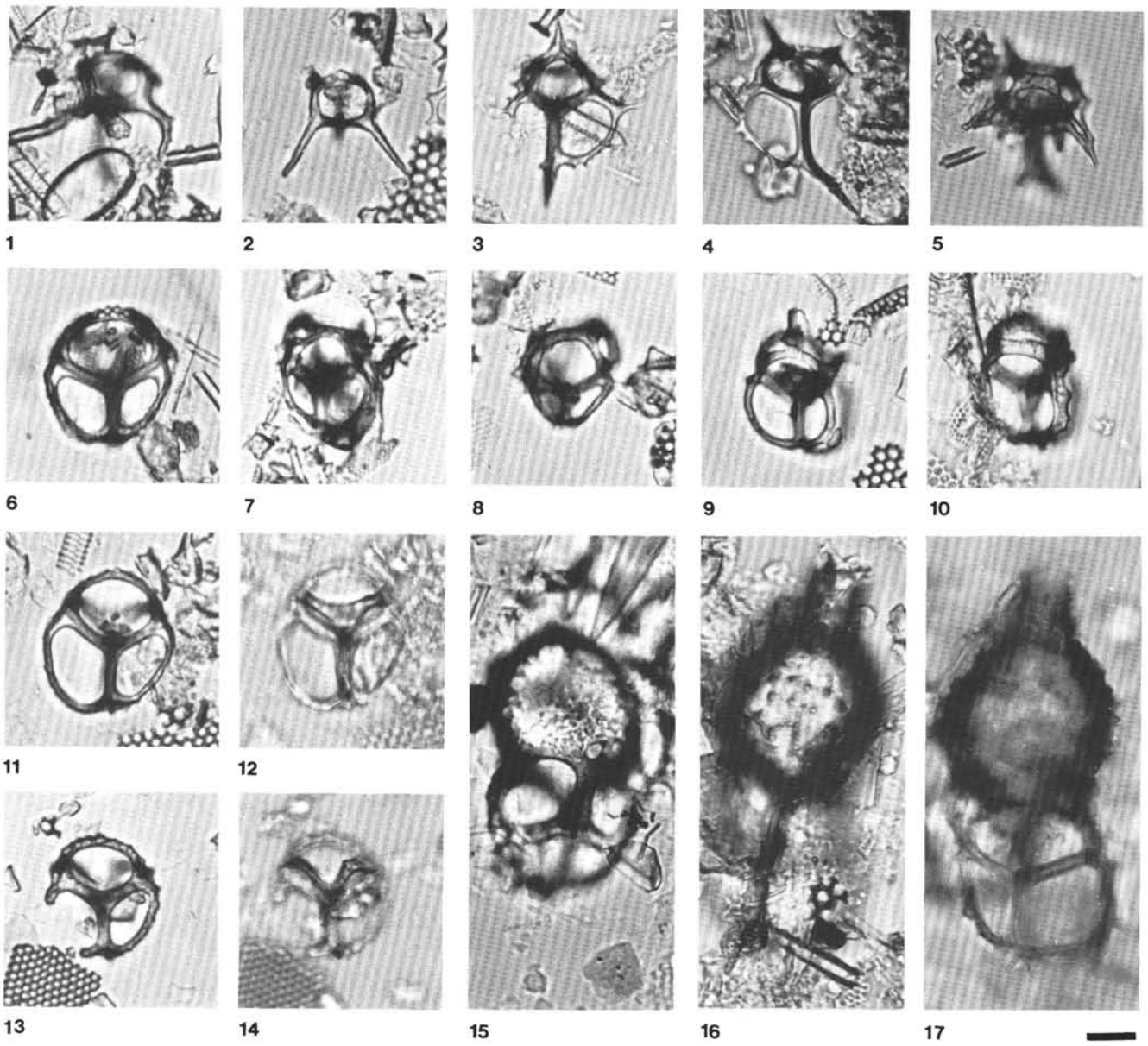

Plate 7. Lower Miocene to upper Pliocene ebridians. All specimens magnified ×800, bar = 10 μm. **1.** *Parathranium curvipes* Hovasse, Sample 104-642D-4X-5, 62–63 cm, lower Miocene. **2.** *Parathranium clathratum* (Ehrenberg), Sample 104-642C-21H-1, 50–51 cm, middle Miocene. **3.** *Hermesinum adriaticum* Zacharias, Sample 104-642C-23H-5, 70–71 cm, middle Miocene. **4, 5.** *Hermesinum obliquum* Locker and Martini; **4.** Sample 104-642C-21H-4, 60–61 cm, middle Miocene; **5.** Sample 104-642C-19H-2, 50–51 cm, upper Miocene. **6.** *Hermesinella* conata (Deflandre), Sample 104-642D-10X-4, 70-71 cm, lower Miocene. **7.** *Hermesinella fenestrata* Frenguelli, Sample 104-642D-7X-2, 66–67 cm, lower Miocene. **8.** *Hermesinella schulzii* (Hovasse), Sample 104-642D-10X-4, 70–71 cm, lower Miocene. **9, 10.** *Hermesinella primitiva* n. sp.; **9.** Holotype, Sample 104-642D-10X-2, 70–71 cm; **10.** Syntype, Sample 104-642D-6X-2, 66–67 cm, lower Miocene. **11, 12.** *Haplohermesinum hovassei* n. sp., holotype, high and low focus, Sample 104-642D-8X-2, 66–67 cm, lower Miocene. **13, 14.** *Haplohermesinum narbonensis* (Deflandre and Gageonnet), high and low focus, Sample 104-642D-10X-2, 70–71 cm, lower Miocene. **15.** *Ebriopsis cornuta* (Ling), skeleton with lorica, Sample 104-644A-34H-5, 66–67 cm, upper Pliocene. **16, 17.** *Podamphora elgeri* Gemeinhardt, skeleton with lorica, high and low focus, Sample 104-642C-19H-5, 50–52 cm, middle Miocene.

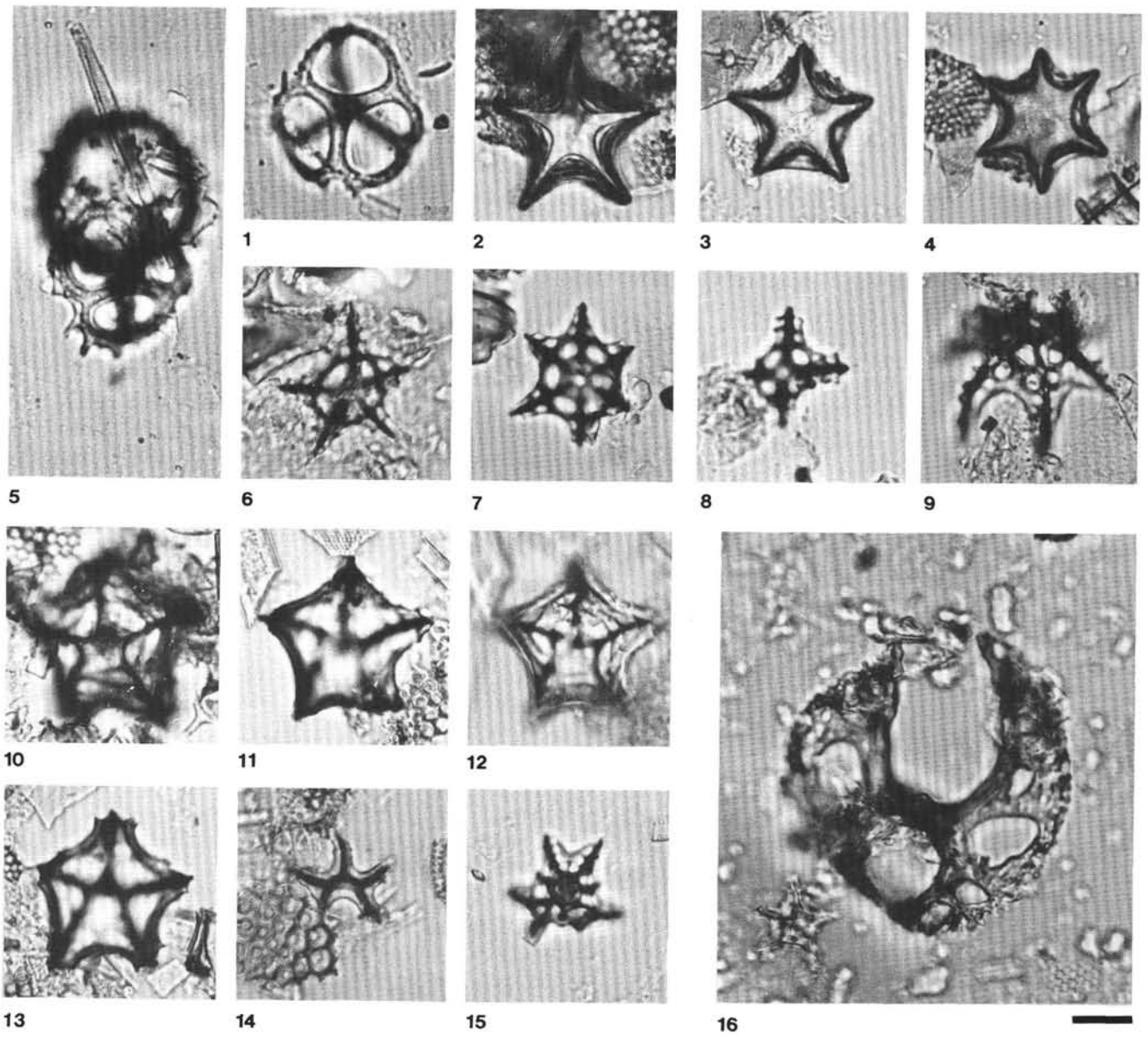

Plate 8. Lower Miocene to upper Pliocene ebridians and actiniscidians. All specimens magnified ×800, bar = 10 μm. **1.** *Ebriopsis cornuta* (Ling), Sample 104-644A-34H-2, 68–69 cm, upper Pliocene. **2–4.** *Actiniscus planatus* n. sp.; **2.** Holotype, **3.** Syntype, **4.** Six-rayed skeleton; all Sample 104-642C-22H-1, 66–67 cm, middle Miocene. **5.** *Ebriopsis cornuta* (Ling), skeleton with lorica, Sample 104-642C-10H-4, 71–72 cm, upper Pliocene. **6, 7.** *Actiniscus pentasterias* (Ehrenberg); **6.** Five-rayed skeleton, **7.** Six-rayed skeleton; both Sample 104-642C-16H-1, 50–51 cm, upper Miocene. **8.** *Actiniscus tetrasterias* Ehrenberg, Sample 104-642C-16H-1, 50–51 cm, upper Miocene. **9.** *Actiniscus flosculus* Locker and Martini, Sample 104-642C-16H-1, 50–51 cm, upper Miocene. **10–13.** *Foliactiniscus pulvinus* n. sp.; **10, 13.** Syntypes, **11, 12.** Holotype, high and low focus; all Sample 104-642D-7X-5, 66–67 cm, lower Miocene. **14.** *Foliactiniscus folia* (Hovasse), Sample 104-642C-24H-2, 70–71 cm, lower Miocene. **15.** *Foliactiniscus atlanticus* Perch-Nielsen, Sample 104-642D-3X-2, 60–61 cm, lower Miocene. **16.** *Falsebria arborea* n. sp., holotype, Sample 104- 642C-11H-2, 52–53 cm, upper Pliocene.

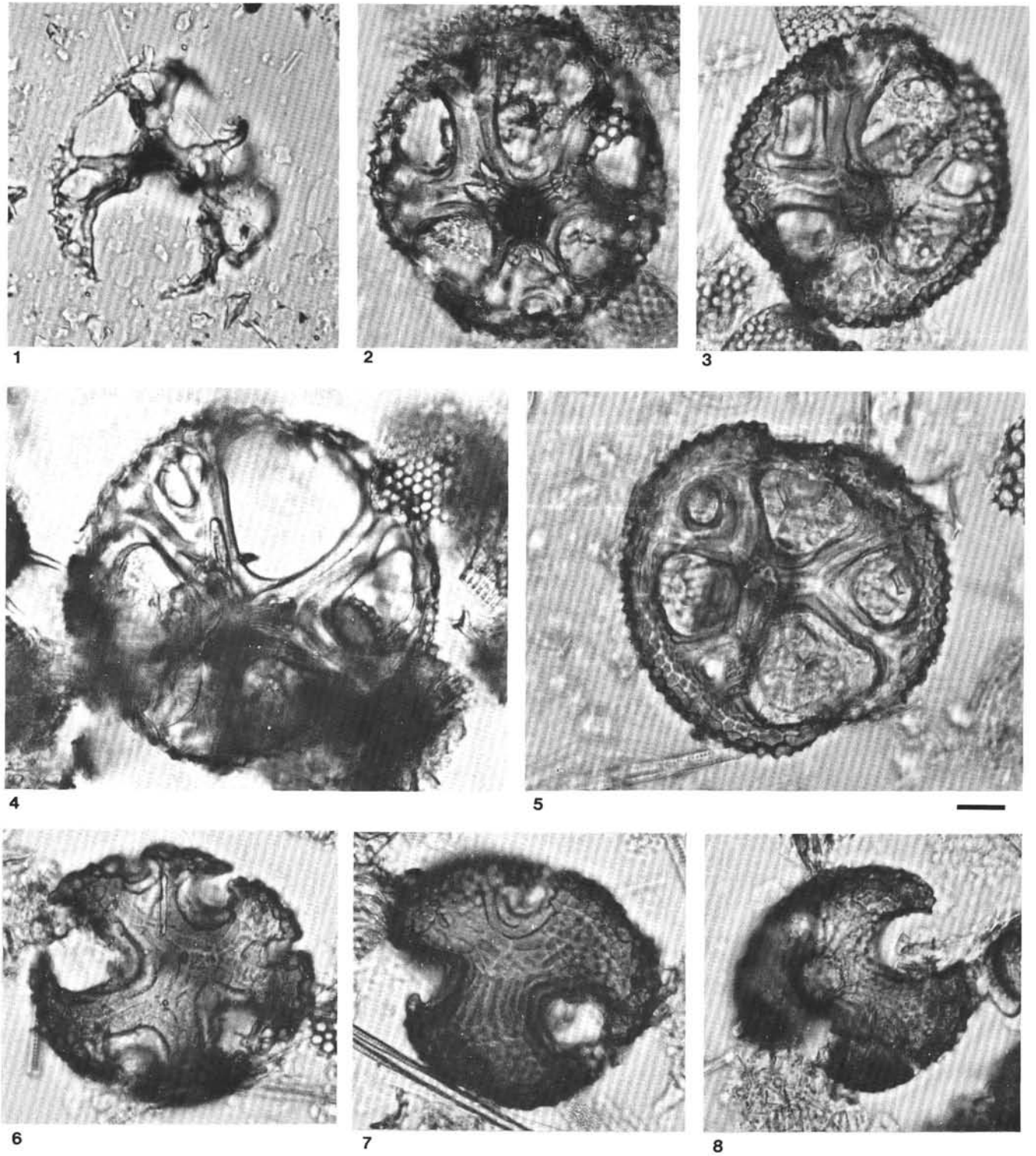

Plate 9. Lower Miocene to upper Pliocene ebridians. All specimens magnified ×800, bar = 10 μm. **1.** *Falsebria arborea* n. sp., syntype, Sample 104-642C-llH-2, 52–53 cm, upper Pliocene. **2–5.** *Spongebria miocenica* n. sp.; **2, 4.** Syntypes, Sample 104-642C-22H-4, 60–61 cm, middle Miocene; **3.** Syntype, Sample 104-642C-23H-2, 54–55 cm, middle Miocene; **5.** Holotype, Sample 104-642C-23H-2, 54–55 cm, middle Miocene. 6–8. n. sp.; **6.** Syntype, Sample 104-642C-24H-2, 70–71 cm, lower Miocene; **7.** Holotype, Sample 104-642C-24H-2, 70–71 cm, lower Miocene; **8.** Syntype, Sample 104-642C-23H-5, 70–71 cm, middle Miocene.